DELFT UNIVERSITY OF TECHNOLOGY

Faculty of Electrical Engineering

Department of Telecommunication and Traffic-Control Systems

UNIVERSITAT POLITÈCNICA DE CATALUNYA

Escola Tècnica Superior d'Enginyers Industrials de Barcelona

Title : Effect of Pulse Shaping on the Performance of **DS-CDMA** in a Multipath Fading Channel

Author : R. Munné

Type : Graduation thesis

Size : 164 + xiii

Date : October 1996

Professor : Prof. dr. R. Prasad

Mentor : Dr. H. Nikookar

Period : March 1996 - October 1996

Abstract:

This report gives first an overview of the main modulation methods and of the multipath propagation effects. A model is described to simulate BPSK, QPSK and OK-QPSK in some measured indoor channels. Several pulse shapes are analysed and their effects discussed on single-user systems and on DS-CDMA. The main performance parameter is the bit error rate for different noise levels. Finally, some conclusions on the possible increase of a DS-CDMA system capacity are exposed, based on the different interference reductions achieved by pulse shaping.

Indexing terms:

Wireless communications, pulse shaping, Code Division Multiple Access, Direct Sequence, Spread Spectrum systems, frequency selective channels, modulation methods, BPSK, QPSK, OK-QPSK.

SUMMARY

This report has two purposes. The first one is to introduce the reader to the advantages of digital communications and the current limitations of mobile systems that should be overcome. On this context, an overview about modulation methods and multipath propagation is given in the first chapters.

The second purpose of this report is to describe the research that has been carried out to determine the effect of pulse shaping on the reduction of several kinds of interference. Pulse shaping is a technique that is known to be a good counter-measure against the degrading effects of the intersymbol interference caused by multipath propagation. The main goal of this project is to prove pulse shaping can also reduce the interference between the users of a DS-CDMA system. Consequently the users capacity of a system with such a protocol could be increased.

In order to analyse the effects of pulse shaping, a model has been implemented to simulate the transmission of bits and calculate the probability of a detection error for different noise levels. The simulations have been carried out for three modulation methods (BPSK, QPSK and OK-QPSK), for several measured indoor impulse responses and for different pulse shapes.

The first conclusion derived from the obtained results is that if OK-QPSK is used to modulate two carrier waves shifted 90°, the interference between both carriers due to the different path phase shifts of a multipath channel, can be reduced by some pulse shapes.

The most important conclusion is that pulse shaping can decrease the average interference between the users of a DS-CDMA system at the expense of introducing some heterogeneity in the cross-correlation function of their codes. Therefore, further research should determine whether the quality of service is actually improved by pulse shaping. Besides, some other techniques could be studied to minimize the negative effects of the cross-correlation function heterogeneity.

PREFACE

This report is the result of the research work carried out at the Department of Telecommunications and Traffic Control Systems, Faculty of Electrical Engineering, Delft University of Technology, within the Erasmus program. This work constitutes the final project of a five year course in industrial engineering performed at the Escola Tècnica Superior d'Enginyers Industrials de Barcelona, Universitat Politècnica de Catalunya.

As was mentioned in the summary, the purpose of this report is not only exposing and discussing the results of the research, but also giving an overview of the main issues related with this project for students and engineers not so involved with these subjects. For this reason, the report, especially the first chapters, has been written in a way to make it as clear and understandable as possible, explaining most of the terms encountered only in the telecommunication literature.

ACKNOWLEDGEMENTS

First of all, I would like to thank my parents, Prof. Dr. Ramjee Prasad and my school in Barcelona for giving me the opportunity of studying in another country and living such a great experience.

I wish to express my gratitude to Dr. Homayon Nikookar for all the time he has devoted in answering my questions and the interest he has shown for my work.

I would also like to thank Nicolás Kruijt for his comments and revisions of my report, Marco Moretti for his advises on my project, Neill Whillans for correcting my written English. and the three of them for their friendship and support.

TABLE OF CONTENTS

LIST OF ABBREVIATIONS

ACI	Adjacent Channel Interference
ADC	American Digital Cellular
AM	Amplitude Modulation
APK	Amplitude-Phase Keying
ASK	Amplitude Shift Keying
AWGN	Additive White Gaussian Noise
BER	Bit Error Rate
BPF	Bandpass Filter
BPSK	Binary PSK
B/U	Bipolar-to-Unipolar converter
CCI	Cochannel Interference
CDMA	Code Division Multiple Access
CP-FSK	Continuous Phase Shift Keying
CW	Continuous Wave
DE-BPSK	Differentially Encoded BPSK
DEM	Demodulator
DPSK	Differential PSK
DQPSK	Differential QPSK
DS	Direct Sequence
DSB	Double Sideband modulation
DSB-SC-AM	DSB-Supressed Carrier-AM
FDM	Frequency Division Multiplexing
FDMA	Frequency Division
FM	Frequency Modulation
FFT	Fast Fourier Transform
FSK	Frequency Shift Keying
FSR	Feedback Shift Registers
GMSK	Gaussian Minimum Shift Keying
GSM	Global System for Mobile communications

I	In phase
IFFT	Inverse Fast Fourier Transform
ISI	Intersymbol Interference
LOS	Line Of Sight
LPF	Lowpass Filter
LPI	Low Probability of Interception
MA	Multiple Access
ML	Maximum Length
MODEM	Modulator-Demodulator
MSK	Minimum Shift Keying
OOK	On-Off Keying
OK-QPSK	Offset-keyed QPSK
pdf	Probability density function
PM	Phase Modulation
PN	Pseudonoise
PRK	Phase Reversal Keying
P/S	Parallel-to Serial converter
psd	Power spectral density
PSK	Phase Shift Keying
Q	Quadrature
QAM	Quadrature AM
QPR	Quadrature Partial Response
QPSK	Quadrature PSK
RMS	Root Mean Square
SIR	Signal to Interference Ratio
SNR	Signal to Noise Ratio
S/P	Serial to parallel converter
SS	Spread-Spectrum
SSB	Single Sideband modulation
SSMA	Spread-Spectrum Multiple Access
TDM	Time Division Multiplexing
TDMA	Time Division Multiple Access

U/B	Unipolar-to-Bipolar converter
UMTS	Universal Mobile Telecommunication System
VSB	Vestigial Sideband modulation

LIST OF SYMBOLS

A	Amplitude
b(t)	Bit stream
$b_I(t)$	Inphase bit stream
$b_Q(t)$	Quadrature bit stream
b_m	m^{th} bit
B_d	Doppler spread
B_s	Swept bandwidth
B_i	Information bearing signal bandwidth
B_T	Transmitted signal bandwidth
c(t)	Code sequence
$c_I(t)$	Inphase code sequence
$c_Q(t)$	Quadrature code sequence
c_w	w^{th} chip
C	Code length
d	Modulation index
E_b	Energy per bit
$E[\cdot]$	Expected value
f_c	Carrier frequency in Hz (cycles/s)
f_d	Frequency deviation
g(t)	Pulse shape
$G_x(f)$	Power spectral density of signal x.
h(t)	Complex-valued impulse response
I	Interference wave power
k	Path index
L	Number of paths
m	Bit index
M	Number of different symbols
N	Noise power

N_o	One-sided noise power spectral density
P(r)	Spatially averaged received power at distance r from the transmitter
PG	Processing Gain
r	Distance between transmitter and receiver
r_b	Bit rate
R(w)	Discrete cross-correlation function
$R(\tau)$	Continuous cross-correlation function
s(t)	Signal time function
$s_r(t)$	Received signal time function
$s_{bb}(t)$	Signal lowpass equivalent time function
$s_I(t)$	In phase component of the transmitted signal
$s_Q(t)$	Quadrature component of the transmitted signal
S	Signal power
t	Time
T_b	Bit duration
T_c	Chip duration
T_m	RMS delay spread
Ts	Signal duration
$v_I(t)$	In phase correlation receiver integrator output
$v_Q(t)$	Quadrature correlation receiver integrator output
w	Chip index
y	Gaussian deviate
z	Uniform deviate
α	Path-loss law exponent
β_k	Gain of the k^{th} path
$\delta(t)$	Dirac delta function
ϕ	Phase
λ	Gaussian parameter
θ_k	Phase shift of the k^{th} path
ρ	Roll-off factor

τ_k	Propagation delay of the k^{th} path
τ_{mes}	Measurable time
τ_{res}	Resolution time
ω_c	Carrier frequency in rad/s
$(\Delta f)_c$	Coherence bandwidth
$(\Delta f)_{samp}$	Sampling frequency step size
$(\Delta t)_c$	Coherence time

1. INTRODUCTION

1.1 Digital Communications

Since the transistor was invented in 1948 and specially since integrated circuit technology was able to produce cheap digital circuits (1961) [Car], the growth in digital communications has not stopped growing and has continued to be used in more and more applications. At present, most kinds of communication systems are partially implemented with digital technology.

The main difference between digital and analogue communications is that in digital communications the time and the values are discrete. The information is codified into a bit stream of ones and zeros, so only two states have to be transmitted. In analogue communications the information is carried by a continuous wave, the input signal. In both kinds of communications an electrical wave is transmitted through a channel, however, in analogue communications this wave is the result of modulating a carrier wave suitable for the channel, with the input signal, while in digital communications the transmitted wave is the result of shifting between two different signals according to the codified bit stream[1]. In the receiver the process that takes place is the opposite process that carried out at the transmitter: in analogue communications the transmitted wave is demodulated and the output signal is obtained, while in digital communication the signals corresponding to ones and zeros are distinguished, usually by means of a filter and a decision device, so the original bit stream can be recovered.

Some of the main reasons why digital systems have been replacing analogue systems during the last years, are exposed below [Lee],[Spi] :

* **Data Communications:** As the use of computers spreads, more digital data is needed to be exchanged, and of course, digital communications is the most suitable way.

[1] In M-ary signalling schemes the bit stream is converted to a symbol stream. There are M different symbols and every symbol has its own electrical signal. So the shifting is done between these M signals instead of the two signals of the binary case.

* **Fidelity:** Digital systems allow the reproduction of signals with as much fidelity as desired, limited only by the first and last analogue parts to transduce and reproduce[2] the signal and also by the methods used. The main difference between analogue and digital communications, is that in long distance communications, it is more difficult for analogue systems to avoid the degrading effects of noise and distortion. With digital communications using enough quantization levels; coding, to detect and correct errors, and regenerative repeaters[3], it is possible to obtain the required bit error probability. Obviously, to get extreme low probabilities, a large amount of methods and devices will be needed. However, with analogue communications, it is almost impossible to transmit a signal without any noise or distortion, as the regenerative repeaters are amplifiers and filters that are not able to regenerate completely the transmitted signal. In addition to that analogue circuits add more retransmission noise to the treated signal.

* **Multiple access and Multiplexing:** When many users share a common transmission medium and there are no switches to make an independent connection between all of them, some kind of Multiple Access (MA) technique is needed. In analogue communications the most common way to provide access or communication between any two points is by assigning a different carrier frequency to each pair of them. This method is called Frequency-Division Multiple Access (FDMA). This kind of MA requires complicated and expensive bandpass filters (BPF). On the other hand, digital communications allow many more MA methods like Time-Division Multiple Access (TDMA) or Code-Division Multiple Access (CDMA), that are usually more efficient than FDMA. When instead of a common medium with an access for every user, there is a network that consists of point-to-point links (different mediums), but one of these links is simultaneously shared by many users, a multiplexing technique is needed. Just like MA methods, analogue communications allows only Frequency Division Multiplexing (FDM) while digital communications also allow Time Division Multiplexing (TDM). Besides, digital communications are more suitable to divide an information message into several so-called packets. Every packet consists at least of the information data and the source and destination addresses, so they can be

[2] to transduce means to transform a physical quantity that varies with time, like the pressure applied to a microphone membrane due to an acoustic wave, into an electrical signal, usually voltage or current. To reproduce means the opposite process.

[3] regenerative repeaters are devices that are placed between the transmitter and the receiver to retransmit the signal before it gets too weak.

sent independently and put together at the destination receiver. This technique is called packet switching.

* **Simulation:** Before fast computers were available, after thinking theoretically about a new electronic device, the only way to prove its features, was to build a prototype and to physically measure its performance. This process may be expensive and can take a long time. In addition to that, when the prototype is not working properly, it can be difficult to envisage the actual problem. Nevertheless, nowadays there are computers and software, that allow researchers to simulate their new devices. Simulating is usually cheaper than the physical construction of the device, and can be as useful to optimize all the components before they are actually bought. It is also easier to find what is the cause of a problem because the involved variables in the process are instantaneously available. Besides, it is possible to simulate a device under conditions difficult to achieve in reality or to test an expensive or dangerous component in extreme conditions. The advantage of digital communication is that as computers are digital devices, digital systems can be better simulated.

* **Flexibility:** Digital information can be treated by programmable devices. This enlarges considerably all the field of signal processing (some digital filters could never be implemented in analogue technology). At first, treatments were only done in time domain, as the computation time of the Fourier Transform[4] was too high. But, in 1965, after the implementation of a more efficient algorithm, known as Fast Fourier Transform (FFT) [Opp], a frequency domain treatment could be done in real-time. Besides, it may be easier and faster to modify any parameter or function of a programmable device than of an analogue filter for instance.

* **Privacy:** For communication systems where privacy is an important issue, only by applying an encryption code to the bit stream, can interception of the message be made difficult for anyone who has no knowledge of the encryption key. In analogue communications, it is a difficult task to make information unreadable for prohibited users.

[4] The Fourier transform is a mathematical operation commonly used to obtain a frequency domain representation of a time function.

* **Costs:** The costs of digital circuits have been decreasing significantly since they were first commercialised. Actually, in the beginning, costs were one of the points why most of the applications continued to use analogue technology. Digital systems dealing with physical signals, always need analogue-to-digital and digital-to-analogue converters and the regenerative repeaters are not simple amplifiers. However, with the improvement of the integrated circuit technology, large scale integrated circuits became cheaper, and the low prices of all these components make digital systems more competitive than the analogue ones..

Besides the need of the analogue-to-digital and digital-to-analogue converters, and the complexity of the regenerative repeaters, there are at least two more disadvantages of digital communications. The first one is that synchronisation is needed in order to detect the pulses at the right time, and this makes receivers more complex. The second disadvantage is that the bandwidth of a digitally encoded signal, is usually greater than the signal itself. Some modern modulation schemes are solving this latest problem though.

1.2 Mobile Systems

At present, for all the advantages seen in the previous section, most of the mobile communication systems are becoming digital. For instance, in Europe and some other countries, the current digital standard is Global System for Mobile communications (GSM) and it uses digital modulators and demodulators (MODEMs).

One aspect that makes mobile systems different from other kinds of communication systems, is the nature of the transmission medium. In many communication systems, the medium is an electrical wire designed to transmit a signal avoiding interference. In addition, in some applications, every terminal has its own wire to the network. An example could be the telephone network, where the link between the local exchange and every subscriber is a different wire.

In mobile systems instead of a wire, radio waves are used to carry the signal through the air. So in wireless communications, all the users transmit their information through the same medium, which means that this medium has to be shared. The established way of sharing "the free space" is by dividing the electromagnetic spectra into different frequency bands, and assigning each band for a different purpose.

To understand the mobile systems capacity problem and the ways to solve it, from now on it will be considered that every assigned band is subdivided at the same time into several smaller spectral bands. These smaller bands will be called channels and each channel can be multiple accessed by several users. Therefore, every channel has a bandwidth and the number of channels in the assigned band is simply the total bandwidth of the radio frequency band assigned for that purpose divided by the bandwidth of each channel. This number might be also called the channel capacity of the assigned band. The number of users that will be able to transmit through every channel, will depend on many factors, like the efficiency of the multiple access technique. Nevertheless, the number of users that each channel can support, is finite, and if the number of users is too high there might not be enough channels to satisfy the traffic demand.

Wireless systems have some important advantages over wired systems. Besides the main advantage of providing communication to mobile users, as described in [Pra1], the wiring cost can be the 50% of the telephone network investment. Specially in low populated areas, wireless systems can be a much cheaper solution. An added advantage is that terminals can be moved more easily to another stationary position.

At first, high equipment prices kept mobile communications away from most of the applications. Due to digital technology improvement, the use of mobile communications is increasing at a growth rate of 40% per year [Bra] and many market forecasts predict that in a few years there will not be enough available capacity [Feh]. This is why research is carried out to design a third generation of mobile communication[5], capable of supplying all the demand. In Europe the programme created to develop the third generation is called Universal Mobile Telecommunications System (UMTS), and besides increasing the spectral efficiency it should

[5] In the eighties analogue cellular systems were commercialised and the first generation began. The second generation started in the nineties with the introduction of digital cellular systems.

integrate a much wider range of services [Pra1]. The work seems to follow two directions, but actually both directions are very related and studying one leads to the other:

The first one is to try to minimize the number of channels needed in one area. This can be achieved by dividing the area to be covered in more and smaller cells (microcells), so that every cell supports less users, or by fitting more users in one channel. Some work is being done about this last point, focusing on different multiple access techniques and in increasing the bits per second that can be transmitted through one channel of a specified bandwidth. However, if the bit rate is too high, the Intersymbol Interference (ISI), specially important in multipath channels, may decrease the bit error rate (BER). Some filtering and equalization can reduce the effects of ISI and allow the use of higher bit rates. Particularly the filtering of the transmitted pulses before they are sent through the channel seems to be a very effective manner to reduce ISI, which will be shown later in this report. This technique is called pulse shaping. Finally, to minimize the channels needed, some research is being done on data compression, for instance, improving the voice coding so that fewer bits per second are needed to obtain an acceptable voice quality.

The second direction is to increase the channel capacity of the available radio frequency band. In this direction there are apparently also two options. The first one is to increase this assigned frequency band, but unfortunately this is not possible, or at least not in the short term, because most of the frequency spectra is already divided and assigned for a specific purpose. The only thing that could be done is to search for another part of the spectra that is not being very used for other purposes and that is also suitable for its physical propagation characteristics. Some studies are evaluating the possible employment of millimetre waves to see if their physical properties are suitable for mobile communications [Pra1]. In case that these studies succeeded, the bandwidth available would be probably enough to develop Mobile Broadband Systems (MBS) with data rates above 2 Mbit/s.

The second option, to increase the capacity of the available band, is to decrease the frequency bandwidth needed for each channel. A lot of research has been recently done in this direction. In fact, there are several ways to achieve this bandwidth reduction. The main way is to improve the modulation method. The result of the work that has been recently done on modulation schemes is Gaussian Minimum Shift Keying (GMSK) or $\pi/4$ Quadrature Phase Shift Keying ($\pi/4$-QPSK), that are respectively evolutions of the earlier Frequency Shift Keying (FSK) and Phase Shift Keying (PSK). As in the case of ISI reduction, filter design is also useful to minimize the out-of-band interference between two spectrally adjacent channels, adjacent channel interference (ACI), so that two different channels can be spectrally closer without interfering each other.

In fact, the bandwidth per channel is very related to the bit rate and the number of users fitted by the multiple access protocol. The higher the bit rate is, the wider the bandwidth, because higher baseband frequencies are needed to transmit the pulses. That is why the performance of a MODEM system is often measured in the bits per second that can be transmitted within a bandwidth of one Hertz ((bits/s)/Hz). Obviously, increasing the number of users of the same channel by means of a multiple access protocol, will be at expense of increasing the bit rate in TDMA, or the bandwidth in spread spectrum methods like CDMA, as will be explained further on this report.

1.3 Aims of the Project

The main goal of the project is as its title says, to see how efficiently some pulse shapes may improve the performance of Direct Sequence CDMA (DS-CDMA) in multipath fading channels. The results have been obtained by the means of simulating information being sent through some measured indoor radio propagation channels. The performance has been compared by the obtained BER, and several modulation methods will be also simulated.

Pulse shaping is a technique that has been mostly used to reduce the effect of ISI. In this project, pulse shaping will be used in a CDMA system to investigate if pulse shaping is also useful to avoid the interference of other users in the same channel, known as Cochannel Interference (CCI) or multi-user interference for the specific case of CDMA.

As was explained in the previous section, any technique that can improve the performance of a mobile communication system is of great importance, as it can be used to increase the capacity of the available radio frequency band.

The next chapter is intended to give an overview of the main modulation schemes that are available at present, starting with the three basic kinds: Amplitude Shift Keying (ASK), PSK and FSK and then going on to the methods used at present. It will conclude by justifying the choice of the three simulated modulation methods. In the third chapter, the most important characteristics of multipath fading channels will be discussed, and some measured impulse response of real indoor channels will be shown. Afterwards, chapter four, will explain the DS-CDMA protocol and exposes its main features. Chapter 5 describes every part of the simulated model: the transmitter, the pulse shape filter, the channel, the noise and the receiver. In chapter 6 the results obtained from the simulations are discussed. Finally, in chapter 7, some conclusions derived from the results and future recommendations are given.

2. MODULATION METHODS

Every communication system needs a modulator to convert the information to be sent into a waveform that can propagate through the medium used to transmit the signal. This conversion can be done in many ways and it should depend mainly on the kind of medium and information that needs to be sent. In this work, the information to be sent is a bit stream and the medium is the free space.

The selection of a modulation method for the studied model is one of the most important choices of the project. This decision will have great influence in the implementation of the model and in the usefulness of the results. For this reason, in this chapter the main modulation methods will be exposed and compared using different criteria.

At the end of the chapter, the choice of the modulation methods simulated on this work will be justified basing the decision on the conclusions derived from the schemes comparison and the currently used modulation methods.

2.1 Desired Features

The main aspects to be taken into account when selecting a modulation method for a digital mobile system should be:

* **Spectral efficiency:** As was discussed in the introduction, spectral or bandwidth efficiency is one of the main goals to be achieved by a modulation scheme for wireless communication. It can be measured by the number of bits that can be transmitted in one second using a bandwidth of one Hertz ((bit/s)/Hz). The inverse magnitude is called the bandwidth utilization and it is measured in (Hz/(bits/s)). The Power Spectral Density (psd) function of a modulated signal usually has a mainlobe around the carrier frequency (f_c) and many sidelobes. As can be seen in Figure 2-1, the power of the sidelobes decreases with (f-f_c). By filtering the sidelobes with a Bandpass Filter (BPF), the signal bandwidth can be decreased and the spectral efficiency improved. Filtering the sidelobes or spillover, always introduces some distortion to the waveform

and sometimes ISI. But, as long as the mainlobe is not too affected by the filter, the performance of the system will not be significantly decreased.

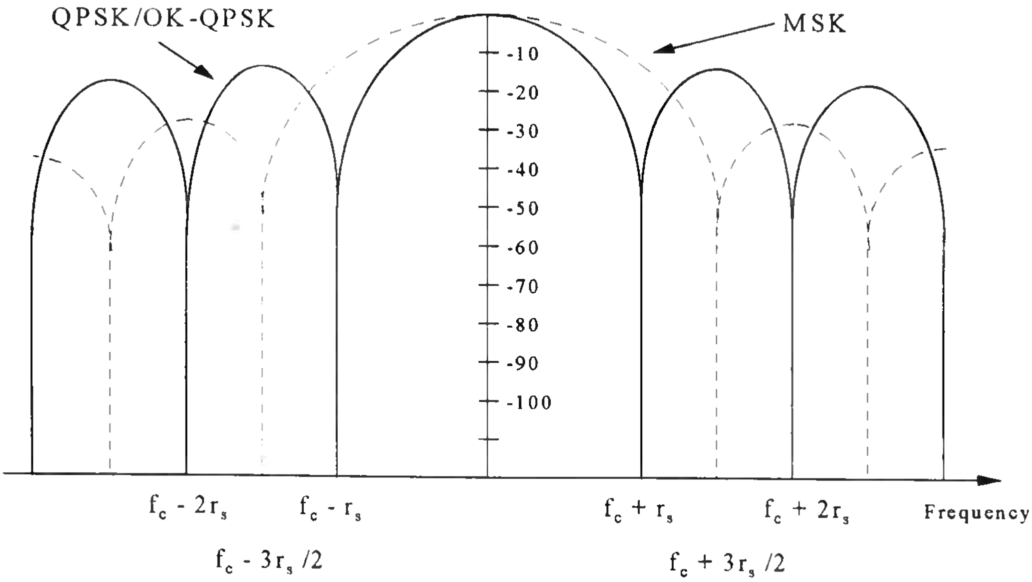

Figure 2-1 Unfiltered psds of QPSK, OK-QPSK and MSK signals [Agh]

Besides the need for spectral efficiency to overcome the problem of the limited assigned bandwidth, spectral efficiency also saves energy. The reason is that when the transmitted signal uses less bandwidth, the BPF in the receiver can have a narrower bandpass width limiting considerably the noise power. Hence the signal power is not required to be so high to obtain the same SNR.

* **Energy efficiency:** The most widely used measure of energy efficiency is the ratio E_b/N_o, where E_b is the energy per bit, and N_o is the one-sided noise psd. The reason is that the performance of a system always depends on the relation between these two values. It would make no sense to state that a system is more energy efficient than another merely because the E_b is lower. That system might operate in a less noisy environment and this could be the only reason why it was performing better.

In this report, in order to compare the results between different channels, the E_b will be the received energy and not the transmitted. When considering the transmitted energy, and dealing with channels having different attenuation effects, the comparison of the results is much more difficult as a poor performance could be due to a high attenuation of the signal.

Energy efficiency is an important issue in mobile systems, specially for the communication from the users' terminals to the base station (uplink). The energy to send the bits has to be provided by the terminal batteries, and this source is significantly energy limited, as batteries have to fit inside a portable terminal and cannot be too heavy.

An important relation between the bandwidth utilization and the energy efficiency is the SNR. This ratio, as was seen in section 2.1, is also used to describe how noisy is one channel. As its name says it is the relation between the signal and the noise power. This definition does not seem to do with spectral efficiency. However, considering that the received waveform is bandpassed through a filter having the transmitted signal bandwidth, the noise power (N) will be the one sided noise psd (N_o) multiplied by the transmitted signal bandwidth (B_T). On the other hand, the signal power is the energy per bit (E_b) divided by the bit duration or multiplied by the bit rate (r_b). Hence:

$$SNR = \frac{S}{N} = \frac{E_b \cdot r_b}{N_o B_T} = \frac{E_b / N_o}{B_T / r_b} \tag{2-1}$$

* **Low out-of-band radiation and near constant envelope:** Out-of-band radiation is the power radiated in frequencies outside the assigned spectral band. As was explained in the point about spectral efficiency, the assigned band usually corresponds to the mainlobe, and out-of-band radiation would be the power of the sidelobes. One way of comparing the out-of-band radiation of two modulation schemes is by observing how rapidly the power spectrum decreases around the carrier frequency. To quantify this, as it is described in [Oet], the attenuation of the power spectrum is calculated at a distance of $8/T_s$ from the centre frequency, where T_s is the signal duration. Another way of measuring out-of-band radiation, mentioned in [Mur], is by the ratio between the out-of-band radiation power in the adjacent channel and the power in the desired channel in dB. This ratio should be between -60 and -80 dB. Actually, it is quite simple to get high attenuations by filtering the signal with an efficient BPF. However, when filtering a signal modulated with Frequency Modulation (FM) or Phase Modulation (PM), as is discussed in [Car], FM-to-AM conversion can occur. This means that for instance, a PM wave with constant

envelope, after filtering the spillover or side-lobes, might no longer have a constant envelope. This should not be a problem for the demodulator to discriminate the signals. Nevertheless when amplifying the filtered signal with a nonlinear amplifier, or when the channel has nonlinearities, the sidelobes will be partially regenerated [Pas]. Unfortunately, to achieve energy efficiency, most of high power amplifiers must work near power saturation. Out-of-band radiation causes ACI, which in wireless communications can degrade the system performance considerably. So low out-of-band radiation or constant envelope after filtering the signal are important characteristics to consider.

* **Low sensitivity to ACI and CCI:** Adjacent channel interference, as has been already commented, is present in most of wireless systems, due to nonlinear amplifiers and to the high usage of a small portion of the spectrum. Nowadays, most of the mobile systems are cellular, which means that the coverage arc is divided into smaller parts called cells. Each cell has a base station and all the base stations are connected to the main network. One way to avoid interferences from adjacent cells, is assigning the frequencies so that the cells operating in the same frequencies are as far as possible from each other. However, there can still be interference between them and cochannel interference sensitivity should be an important criterion to compare modulation methods.

* **Low sensitivity to multipath fading:** Most of the channels in mobile systems show multipath fading. This is the reason why in this project the effect of pulse shaping is measured in multipath fading channels. Real environments have many reflection surfaces that lead to several possible paths for the wave to go from one antenna to the other. Each path has a different length, so the received waves have different delays and phases. The addition of all the different waves causes fading. Multipath fading will be explained in more detail in the next chapter. Fading due to multipath is often frequency selective, which means that signals with different frequencies undergo different amounts of fading. As a result of this phenomenon, some modulation schemes using spread spectrum techniques, perform better in mobile systems [Coo].

* **Low cost and complexity:** Last but not least, the economic aspect of an adopted solution is always very important. Specially the cost of the MODEM employed in the terminals, as each terminal should be available at a reasonable price. Sometimes it may be difficult to estimate the cost of a device because digital electronic technology develops rapidly. What today might be very expensive in a few years with large scale production and some improved techniques, can be much cheaper. Therefore, it is also very useful to compare the complexities of the different modulation schemes.

2.2 Methods Comparison

As was already mentioned in the introduction, there are three main kinds of digital modulators: ASK, where the amplitude of the carrier wave is modulated according to the input bits or symbols; PSK, where the phase is the characteristic of the carrier wave that is shift keyed between several possible values; and FSK, where as its name says, the frequency is shift keyed according to the transmitted information. A more recent method is the combination of ASK and PSK, which is called Amplitude-Phase Keying (APK). In this method the amplitude and the phase are shift keyed at the same time so better performance is obtained.

There is also another method that is more used in analogue communication, but can also be employed in digital communication when the bandwidth efficiency is very important. It is called Vestigial-SideBand (VSB) modulation. In this method the baseband digital pulses are shaped, usually by a raised cosine filter, to get a Nyquist pulse shape, and then modulated by a carrier wave. The spectrum of a real baseband signal is an even function ($f(x)=f(-x)$). This is why instead of translating all the spectrum of the baseband signal a distance of f_c, like in Double SideBand (DSB), it is enough to translate only the positive sideband or upper sideband. This is what is done in Single SideBand (SSB) modulation. However, better results are obtained if a trace or vestige of the lower sideband is also transmitted, which leads to VSB. The filter employed in VSB is also simpler than in SSB.

These main modulation methods have many variations. One of the ways to modify these methods is by changing the signaling scheme from binary to M-ary. In M-ary the number of bits that are transmitted in one signaling period is $\log_2 M$ instead of 1, so the amount of information transmitted at the same time is higher. As each symbol contains $\log_2(M)$ bits, there will be M different possible symbols. The modulator will transmit a different electric signal for every symbol. There is another kind of signaling scheme called partial response signaling. It is designed to maximaize the bit rate when the bandwidth is limited. This is achieved by letting the symbol pulses last for more than a symbol period, introducing a controlled amount of ISI. In the receiver, the decision is made taking into account the received previous symbols and the ISI introduced by them [Sha]. One of the disadvantages of this method is that when the decision device makes an error, the next output symbols are more likely to be also incorrect as their decision was influenced by the previous error symbol; this phenomenon is called error propagation. Error propagation can be prevented by precoding the symbol stream in such a way that the new sequence represents the original sequence by the consecutive symbol changes and not the absolute values [Car]. This method increases the symbol rate for a given bandwidth, at expense of energy efficiency as will be seen when the different efficiency criteria are discussed.

It is also important to note that a signal modulated with a determined scheme, can be detected by the demodulator using different schemes. For instance, the detection can be coherent or noncoherent. Coherent means that the receiver needs to generate a wave with the same phase and frequency as the transmitted carrier. This wave is usually called local carrier reference and it has to be generated from the received signal by a special circuit [Sha]. A noncoherent demodulator can be, for example, an envelope detector for ASK or a frequency discriminator for FSK. The detection method has also a direct influence on the performance of the system. Therefore when comparing the modulation methods the kind of detection should be specified.

2.2.1 Description of the main methods

This section describes only the most representative schemes of ASK, PSK and FSK methods, paying special attention to the ones that will be chosen to modulate the signal in the project simulations.

2.2.1.1 Amplitude Modulation Methods

The two ASK methods that are going to be discussed are Binary ASK (BASK), where the amplitude can take the values 1 and -1 and Quadrature Amplitude Modulation (QAM). QAM is actually the result of modulating two carrier waves shifted 90° with BASK modulation. Consequently two different bit streams can be transmitted at the same time.

* **BASK** is one of the simplest modulation methods there is. One of the ways to implement a BASK modulator is by using a Unipolar-to-Bipolar converter (U/B), which converts the input bits into 1 or -1, an impulse generator to obtain a positive impulse in case of a 1 and a negative impulse in case of a -1, a filter with an impulse response g(t), that convoluted with the input impulses will give the desired shape to the pulses, and then a multiplier does the product of the shaped pulses, g(t), with the carrier wave, $A\cos(\omega_c t)$[1], where A is its amplitude and ω_c its frequency. The result is actually a Double Sideband-Supressed Carrier-Amplitude Modulation (DSB-SC-AM) signal, s(t) [Agh]. And it has the form of:

$$s(t) = b(t)g(t - mT_b)A\cos(\omega_c t) \quad \text{for} \quad mT_b < t < (m+1)T_b \tag{2-2}$$

where:

$m = 0, 1, 2, \ldots$

$b(t) = b_m \qquad \text{for} \quad mT_b < t < (m+1)T_b$

Where m is the bit index, b(t) the bit stream, b_m is the m^{th} bipolar bit and can be 1 or -1, T_b is the bit duration and finally g(t) is the pulse shape, which equals 0 after the bit duration when no partial response signaling is used:

$$g(t) = 0 \quad \text{for } t < 0 \text{ and } t > T_b$$

[1] It will be considered in all the mathematical descriptions of this chapter that in the reference instant (t=0) the carrier phase equals zero. However all the equations could be rewritten as $A\cos(\omega_c t+\phi)$ where ϕ would be the random phase associated to the carrier wave.

* **QAM**. When another carrier wave of the same frequency but shifted 90° is also modulated, another bit stream can be transmitted. However, instead of transmitting two bit streams it is more common to transmit only one bit stream but at double speed. The input bit stream is converted into two bit streams of half the original rate by a Serial-to-Parallel converter (S/P). The resulting bit stream that modulates the 90° shifted carrier wave is called Quadrature (Q) bit stream, denoted by $b_Q(t)$ while the other one is called Inphase (I) bit stream, $b_I(t)$. Every group of consecutive two bits forms a symbol, also known as a dibit. Therefore the symbol rate is half the bit rate. This process is shown in Figure 2-3 and the whole QAM modulator is depicted in Figure 2-2.

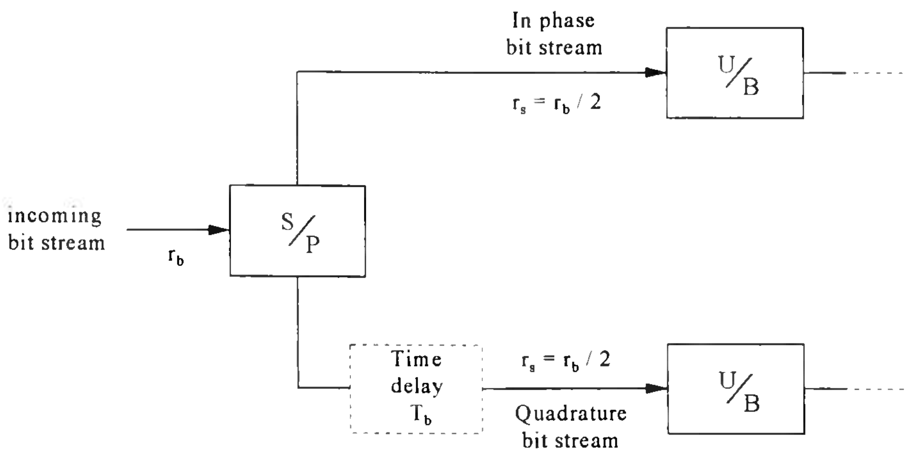

Figure 2-2a QAM/QPSK/OK-QPSK modulator (the time delay is only present in OK-QPSK)

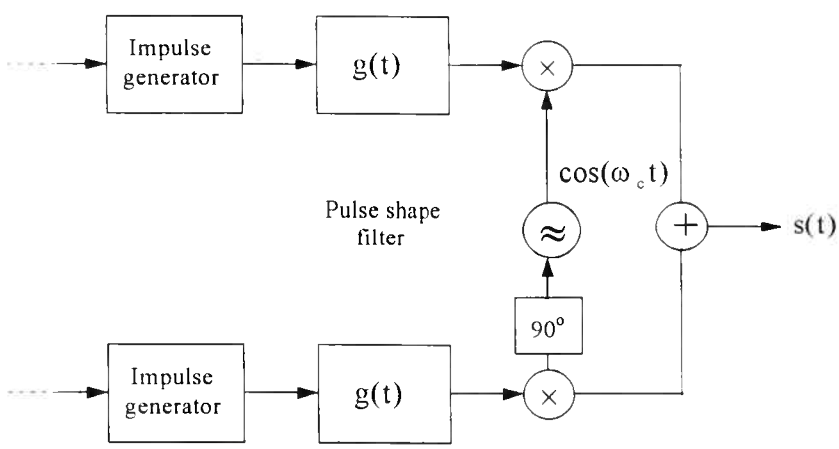

Figure 2-2b QAM/QPSK/OK-QPSK modulator

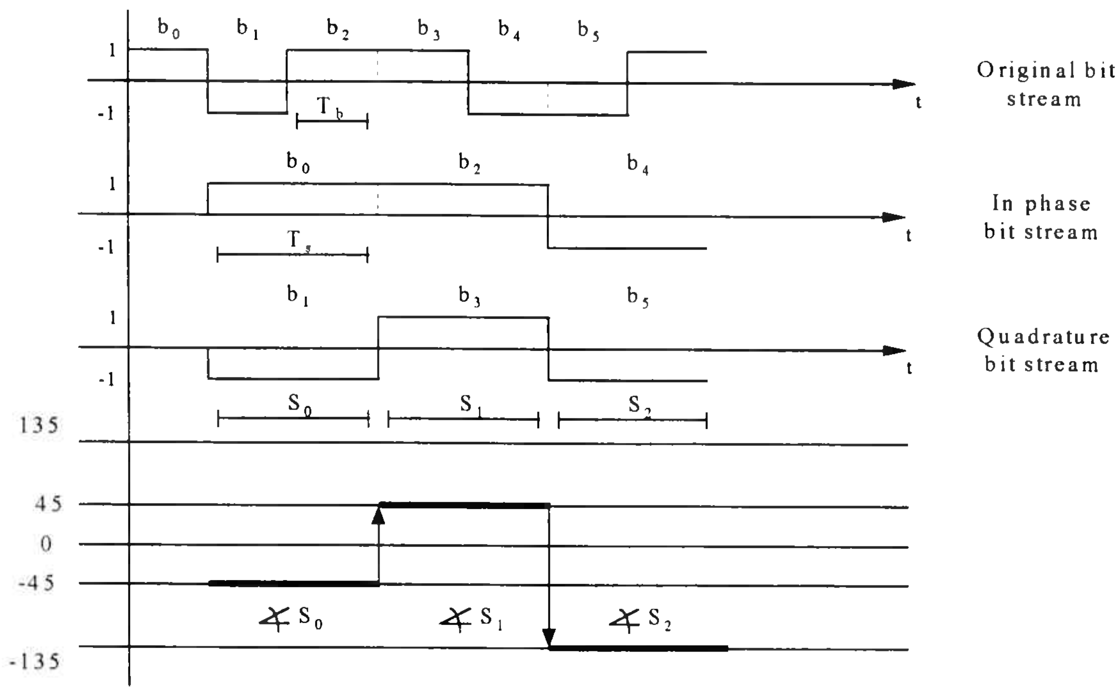

Figure 2-3 QAM/QPSK bit streams and phase changes

A QAM signal can be mathematically described by an equation very similar to the one used for BASK. In fact is the same equation where T_b is replaced by T_s and with another term for the Q carrier wave, which can be written as $A\cos(\omega_c t + \pi/2)$ or as $A\sin(\omega_c t)$:

$$s(t) = b_I(t)g(t - m'T_s)A\cos(\omega_c t) + b_Q(t)g(t - m'T_s)A\sin(\omega_c t) \qquad (2\text{-}3a)$$

$$\text{for} \quad m'T_s < t < (m'+1)T_s$$

where:

$T_s = 2 \cdot T_b$

$m' = 0, 1, 2, \ldots$

Where m' is the symbol index and g(t) is the pulse shape, which lasts a whole symbol period instead of a bit period like in BASK:

$$g(t) = 0 \quad \text{for } t < 0 \text{ and } t > T_s$$

This equation can be rewritten considering the bit period instead of the symbol period, as was done for BASK:

$$s(t) = b_I(t)g\big(t - (2m+1)T_b\big)A\cos(\omega_c t) + b_Q(t)g\big(t - (2m+1)T_b\big)A\sin(\omega_c t) \qquad \text{(2-3b)}$$

$$\text{for} \quad (2m+1)T_b < t < (2m+3)T_b$$

Where:

$m = 0, 1, 2, \ldots$

$b_I(t) = b_{2m}$ for $(2m+1)T_b < t < (2m+3)T_b$

$b_Q(t) = b_{2m+1}$ for $(2m+1)T_b < t < (2m+3)T_b$

2.2.1.2 Phase Modulation Methods

The correspondent PSK methods parallel to BASK and QAM are Binary PSK (BPSK) and Quadrature PSK (QPSK) respectively. Even if AM and PM methods are conceptually totally different, it will be seen below that for these four schemes, the resulting modulated signal shows no difference in some cases. Finally, Offset Keyed (OK-QPSK) will be also explained as it presents some advantages over QPSK.

* **BPSK**. According to the definition of PSK, BPSK should transmit ones and zeros shift keying the carrier wave phase. In order to maximize the phase difference between the two signals, one of the signal phases should be 0° and the other one 180°. However, most of BPSK transmitters are implemented just as the BASK transmitter described above. The reason is that it has exactly the same effect to shift the carrier wave 180° or to reverse its sign. So equation (2-2) also describes a BPSK signal. BPSK is also known as Phase Reversal Keying (PRK).

* **QPSK**. The idea behind QPSK is the same as behind QAM: to use another carrier wave shifted 90° to transmit information at a double rate. In the case of QPSK each carrier wave should be modulated by a BPSK modulator, but as a BPSK modulator is equivalent to a BASK modulator,

QPSK is also equivalent to QAM. Therefore equation (2-3) and Figure 2-2 are also valid for QPSK.

QPSK can also be viewed as 4-ary PSK, as the carrier wave phase is shift keyed between four values. Besides, the difference between two consecutive phase values is 90°, as it should be to maximize the performance in an ideal channel. To understand better this fact, it is very helpful to represent the signal constellation of a QPSK modulator. The signal constellation is nothing else than a polar plot, where each possible signal is represented by its corresponding amplitude and phase of the carrier wave. Applying some basic trigonometric equations it is very simple to derive from equation (2-3), the phase and the amplitude for each of the four possible dibits or symbols. The result is plotted in Figure 2-4.

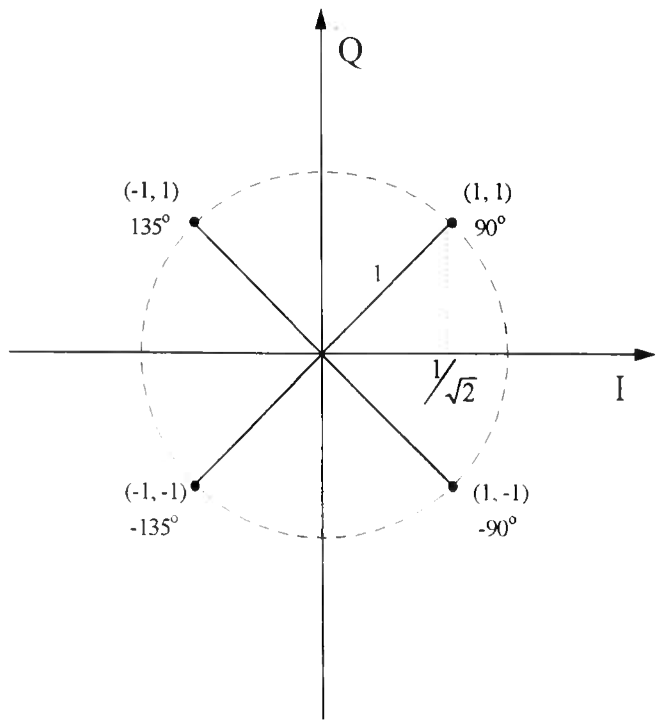

Figure 2-4 Constellation of Gray-Coded QAM or QPSK signal

For QPSK, another constellation could also be used to describe 4-ary PSK or QPSK signals. Instead of 45, 135, -135 and -45 degrees, 0, 90, 180, and -90 degrees could be represented. The difference is only a matter of phase reference, which has usually no effect in real systems.

A signal having a determined phase and amplitude can be represented by the I and the Q components (in a form similar to equation (2-3)), just like a point in a plane can be represented by its co-ordinates. This is the reason why one axis is denote by a 'Q' and the other by an 'I'.

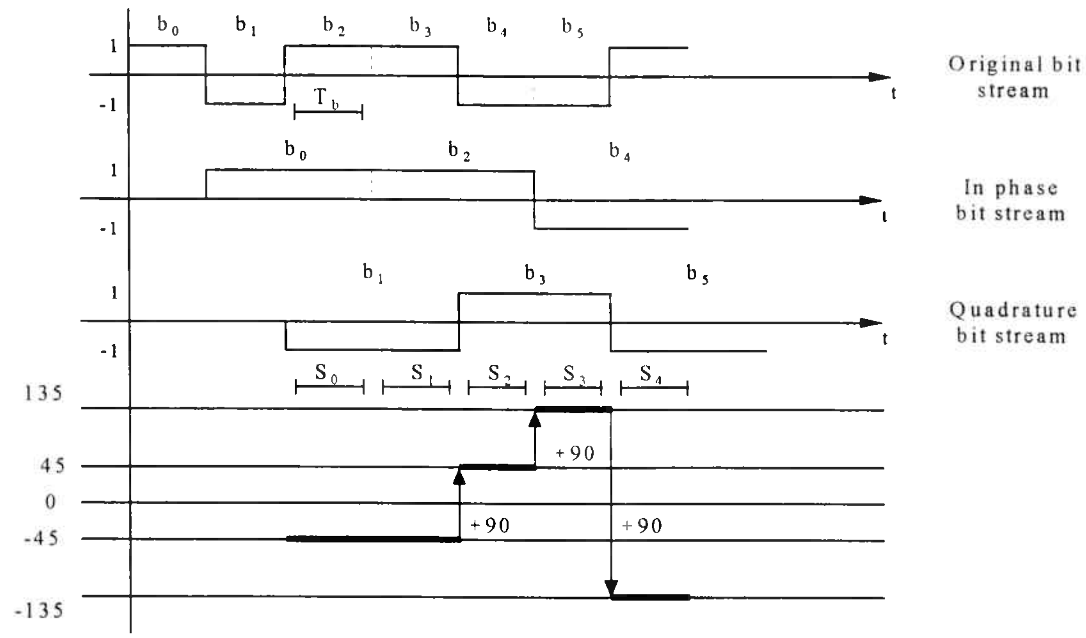

Figure 2-5 OK-QPSK bit streams and phases changes

* **OK-QPSK** The difference between OK-QPSK and QPSK is that in OK-QPSK a time delay of one T_b is introduced after de S/P in the quadrature branch (see Figure 2-2). The effect of this time delay is that the I and Q bit streams are no longer synchronized, and when a change occurs in one bit stream, the other remains the same (see Figure 2-5). The advantage of OK-QPSK compared to QPSK is that as only the I and the Q bit streams cannot change simultaneously and in consequence no 180° phase shift can occur. This fact can also be observed comparing the phases depicted in Figure 2-3 and Figure 2-5. Both modulation schemes have the same constellation but OK-QPSK only experiments 90° phase shifts when a Gray code[2] is used as only one bit of the dibits can change at a time. This is why it is sometimes called staggered QPSK. As will be seen further on this chapter, 180° phase shifts can lead to out-of-band radiation when nonlinear amplifiers are used.

[2] A constellation is said to be Gray-coded if the codes assigned to adjacent symbols only differ in one bit [**Agh**].

The equations to describe OK-QPSK are:

$$s(t) = b_I(t)g\big(t-(2m+1)T_b\big)A\cos(\omega_c t) + b_Q(t)g\big(t-(2m+2)T_b\big)A\sin(\omega_c t) \tag{2-4a}$$

$$\text{for} \quad (2m+2)T_b < t < (2m+3)T_b$$

$$s(t) = b_I(t)g\big(t-(2m+3)T_b\big)A\cos(\omega_c t) + b_Q(t)g\big(t-(2m+2)T_b\big)A\sin(\omega_c t) \tag{2-4b}$$

$$\text{for} \quad (2m+3)T_b < t < (2m+4)T_b$$

Where:

$m = 0, 1, 2, \ldots$

$b_I(t) = b_{2m}$ for $(2m+1)T_b < t < (2m+3)T_b$

$b_I(t) = b_{2m+2}$ for $(2m+3)T_b < t < (2m+5)T_b$

$b_Q(t) = b_{2m+1}$ for $(2m+2)T_b < t < (2m+4)T_b$

$g(t) = 0$ for $t < 0$ and $t > 2T_b$

2.2.1.3 Frequency Modulation Methods

There is a group of frequency modulation methods which seems to improve the features of conventional FSK. It is called Continuous Phase-FSK. And from this group Minimum Shift Keying (MSK) is one special modulation method that has been extensively studied as seems to be one of the best modulation methods there is.

* **CP-FSK**. The phase of a conventional FSK signal is usually discontinuous when a symbol change occurs. If these sudden phase changes are smoothed and the phase becomes continuous, FSK accomplishes better some of the criteria listed before. In CP-FSK the phase changes continuously with a derivate according to the symbol transmitted in that instant. Therefore the phase is the integral of the different changing rates experienced by the signal, and it gives also

information about the previous transmitted symbols. This is the reason why some CP-FSK MODEMs, observe a symbol signal for a longer time interval than one T_s before they decide which symbol was originally transmitted. The values showed in the tables of next section by **[Oet]** assume that the receiver of CP-FSK, observes the signal during 3 bit periods.

One characteristic of binary FSK MODEMs is the frequency difference between the two signals representing the logic states 1 and 0. The most common magnitude to quantify this frequency difference is the frequency deviation, which is half of the mentioned difference and it is denoted by f_d [Car].

The modulation index is a measure of the frequency deviation and according to [Oet] it is denoted by a d and it is defined as:

$$d = 2f_d \cdot T_b \tag{2-5}$$

* **MSK** is the name of a coherently detected CP-FSK having the minimum modulation index: 0.5. When two BPF followed by envelope detectors are used two detect a FSK signal, the minimum modulation index is 1, with less frequency distance the two signals would not be orthogonal[3] anymore [Oet]. This method received its name from the fact that when using a coherent receiver, the minimum modulation index is 0.5 [Pas].

If the g(t) function of the pulse shape filter of a OK-QPSK modulator in Figure 2-1 is a half-sinusoidal waveform, the resulting signal is equivalent to a MSK signal. This will be proved below:

From equation (2-4) the sinusoidal pulse shaped OK-QPSK signal can be written as:

$$s(t) = b_I(t)A\cos\left(\frac{\pi t}{2T_b}\right)\cos(\omega_c t) + b_Q(t)\sin\left(\frac{\pi t}{2T_b}\right)A\sin(\omega_c t) \tag{2-6a}$$

[3] In this context, two FSK signals are said to be orthogonal, if the sampled envelope of the output of the receiving filter tuned to the frequency of the first signal is zero when the other signal is transmitted and vice versa.

for $(2m+2)T_b < t < (2m+3)T_b$

Where:

$m = 0, 1, 2, \ldots$

$b_I(t) = b_{2m}$ for $(2m+1)T_b < t < (2m+3)T_b$

$b_Q(t) = b_{2m+1}$ for $(2m+2)T_b < t < (2m+4)T_b$

It is not difficult to derive from the previous equation that it can be also written as:

$$s(t) = A\cos\left(\omega_c t - b_I(t)b_Q(t)\frac{\pi t}{2T_b} + \Phi(t)\right) \quad \text{(2-6b)}$$

Where:

$$\Phi(t) = \begin{cases} 0 & \text{if } b_I(t) = 1 \\ \pi & \text{if } b_I(t) = -1 \end{cases}$$

From this equation the resemblance between OK-QPSK and MSK is more evident, as depending on the bit values the frequency is incremented or reduced $\pi/(2T_b)$ rad/s. However the sudden changes of $b_I(t)$ and $b_Q(t)$ might seem to make the phase of this signal discontinuous. Analysing the phase values just before and after a change of $b_I(t)$ and $b_Q(t)$ it will be shown that the phase is always continuous:

The function $b_I(t)$ changes its value in the instants: (2m+1) where m = 0, 1, 2... as was expressed in equation (2-6). Just before the change, the phase equals:

$$b_I(t)b_Q(t)\frac{\pi(2m+1)T_b}{2T_b} + \Phi(t) = \pm(m\pi + \frac{\pi}{2}) + \Phi(t) \quad \text{(2-7)}$$

Depending on the parity of m, the sign of $b_I(t)$, and the sign of $b_Q(t)$, the phase of the first term will equal $\pi/2$ or $-\pi/2$. If a change of sign in $b_I(t)$ occurs, then the first term of equation (2-7) will change its value from $\pi/2$ to $-\pi/2$ or viceversa. Nevertheless, as $\Phi(t)$ will also change its value from 0 to π or from π to 0 radians, it will cancel the change due to the first term and the phase will remain the same.

It is even simpler to analyse a change in $b_Q(t)$ as it occurs in the instants $2mT_b$ and $\Phi(t)$ cannot change at the same time. From equation (2-6) it is clear that at those instants the changing term of the phase can only take two values: π or $-\pi$ radiants. As both phases are actually the same angle, the phase is also continuous at these instants.

2.2.2 Methods features

In this section, all these modulation methods described above will be compared using every criterion that was discussed before. For this comparison some tables extracted from [Oet] and [Car] will be used. All the values of these tables, except those where the opposite is indicated, were obtained for ideal channels with only AWGN. The abbreviations and terms that appear in these tables and that have not been explained yet are:

OOK: On-Off-Keying. ASK modulation with amplitude levels 0 and 1. In Table 2-4 it is assumed that the receiver has an optimum variable threshold.

QPR: Quadrature Partial Response. The same as QAM but using partial response signaling.

DE-BPSK: Differentially Encoded Binary PSK. It is a coherently detected BPSK but due to its differential encoding, it allows a 180° of ambiguity in the phase reference. So in the receiver it is not known if the phase is 0° or 180°, but it distinguishes if the phase is the same or different from the previous bit

DPSK: Differential PSK. It is also differentially encoded but the difference with DE-BPSK is that it is noncoherently detected. This means that the phase is not tried to recover. the phase reference in this kind of modulation is the previous bit signal.

DQPSK: Differential QPSK. Two carrier waves shifted 90 degrees are modulated with DPSK.

* **Spectral efficiency:** Between the binary signaling methods the one that requires less bandwidth is VSB, which requires only a little bit more than half of the signaling rate [Car], so it can transmit almost 2 bits every second in a 1 Hz bandwidth. Actually, this is about the bandwidth stabilised by the Nyquist criterion [Pro], which states that the minimum bandwidth of an ideal channel able to transmit a bandlimited signal without ISI is half the bit rate. ASK and PSK have a mainlobe of twice the bit rate but if a BPF of only the bit rate is used, the amount of introduced ISI is not high[Car]. So their efficiency is about half of VSB. However, ASK and PSK can be very spectral efficient when using M-ary signaling schemes. Their theoretical efficiency is $\log_2 M$, which is the number of bits per symbol [Car]. If spectral efficiency was the only criterion taken into account, probably M-ary ASK or PSK with high values of M would be the best techniques. On the other hand, improving one feature is often at expense of another one. In the case of M-ary ASK and M-ary PSK, the improvement in spectral efficiency is at expense of power efficiency, specially ASK. This will be discussed when comparing the energy efficiency. FSK is the worst technique when spectral efficiency is required because the bandwidth has to contain at least all the frequencies corresponding to every symbol. Although the spectral efficiency of binary FSK is not much lower than that of binary ASK and PSK, when using M-ary signaling techniques, the spectral efficiency of M-ary FSK is not improved. Nevertheless, it was explained in the previous section that CP-FSK seems to outperform ordinary FSK in most of its features by just increasing the MODEM complexity. Besides it allows to reduce the frequency deviation, which has a direct consequence on the spectrum efficiency. MSK is in theory the most spectral efficient FSK method as its modulation index is only of 0.5. It can double the speed of conventional FSK schemes and achieves almost two bits/s/Hz, which is the same speed obtained with QAM and QPSK.

Table 2-1 Comparison of digital modulation systems with BER=10^{-4} [Car]

Modulation Scheme	Detection	r_b/B_T	E_b/N_o
OOK or FSK ($f_d = r_b$)	Envelope	1	12.3
DPSK	Phase comparison	1	9.3
DQPSK	Phase comparison quadrature	2	10.7
PRK (BPSK)	Coherent	1	8.4
MSK, QAM, or QPSK	Coherent quadrature	2	8.4
8-ary DPSK	Phase comparison quadrature	3	14.6
8-ary PSK	Coherent quadrature	3	11.8
16-ary PSK	Coherent quadrature	4	16.2
16-ary APK	Coherent quadrature	4	12.2

Table 2-11 of [Car] and Table 2-2 of [Oct] give the values of the speed (r_b/B_T) in (bit/s)/Hz and the energy efficiency measured by the E_b/N_o for a BER of 10^{-4} in an ideal AWGN channel, for several modulation methods. The difference between both tables is that the first one is more theoretical. The speed or bandwidth efficiency and the E_b/N_o values given are optimum. It should be noted that maximum power efficiency is only achieved when the whole signal spectrum is transmitted. As showed in Table 2-2, the E_b/N_o needed to obtain a BER of 10^{-4} is higher when the signal is filtered with a BPF with finite bandwidth. It should be mentioned that, many other pairs of values could appear in Table 2-2. It is always possible to increase the speed by filtering more the signal but at the expense of a lower power efficiency; Or viceversa, not filtering as much the signal and loosing spectral efficiency, in order to achieve a higher power efficiency. The optimum will depend on the specifications of every application. However, the values given are good examples of the speed that is possible to obtain without a significant loss of power efficiency.

Table 2-2 Relative signaling speeds of representative modulation schemes [Oet]

Type	Modulation Scheme	Speed ((bits/s)/Hz)	E_b/N_o (dB)
AM	OOK-coherent detection	0.8	12.5
	OOK-envelope detection	---[4]	---
	QAM	1.7	9.5
	QPR	2.25	11.7
FM	FSK-noncoherent det. (d=1)	0.8	11.8
	CP-FSK-coherent det. (d=0.7)	---	---
	CP-FSK-noncoherent det. (d=0.7)	1.0	10.7
	MSK (d=0.5)	1.9	9.4
	MSK-differential encoding (d=0.5)	1.9	10.4
PM	BPSK-coherent detection	0.8	9.4
	DE-BPSK	0.8	9.9
	DPSK	0.8	10.6
	QPSK	1.9	9.9
	DQPSK	1.8	11.8
	OK-QPSK	---	---
	8-ary PSK-coherent detection	2.6	12.8
	16-ary PSK-coherent detection	2.9	17.2
APK	16-ary APK	3.1	13.4

The values in these tables give evidence of what has been explained. All binary signaling methods can transmit less than 1 (bits/s)/Hz. On the other hand, 16-ary signaling schemes can theoretically achieve 4 (bits/s)/Hz, but in reality to have speeds around 3 (bits/s)/Hz they require higher powers. Another very spectral efficient method is QPR. The reason is that its pulses last longer and therefore it needs less bandwidth than QAM.

[4] The three dashes mean that no empirical data was available for those modulation schemes.

* **Energy efficiency:** In the preceding section, power efficiency was said to be compared by the E_b/N_o. However, E_b/N_o can take an arbitrary value using the same modulation method. In order to compare the power efficiency of two MODEMs, a predetermined performance should be specified. In this work and in the tables shown, the performance is measured by the BER, and the value chosen for the tables comparison is 10^{-4}. This value is usually adequate for most of the general purpose digital radio applications [Oct].

The most energy efficient modulation methods, according to Table 2-1, are PRK, MSK, QAM and QPSK, but the first one can only achieve a speed of 1 (bits/s)/Hz, as it only uses one carrier wave. It might seem a coincidence that the four schemes have exactly the same performance in an ideal channel, but there is an explanation for it. The reason is that even if conceptually PRK, QAM and MSK are completely different, it was explained in last section that they are in fact very similar. Although in an ideal channel they all have the same performance, it should be taken into account that in real channels, it is no longer this way. For instance, if the phase recovery circuit is not perfect, PRK is more energy efficient than the others because it is less sensitive to phase shifts as its signals are double spaced (in the signal constellation) than those from the other three methods. Another way to understand this, is by considering that the phase shifts introduces interference between the I and Q components.

These tables also give evidence that when noncoherent detection is employed in the receiver, the energy efficiency is worse than when using coherent methods. This agrees with the fact that coherent detection is the theoretical optimum method to distinguish between two signals. Obviously, the kind of detection has no influence on the speed. The speed only depends on the transmitted signal spectrum.

It was not difficult to foresee that M-ary signaling schemes for ASK would have a low power efficiency, as two signals are differentiated by their amplitude level, and to achieve the same BER performance, some amplitudes levels have to be higher than the amplitude used in BASK. QPR has also a poorer energy efficiency compared to QAM for example, because of the same reason. The ISI causes different signal levels [Car] and as M-ary ASK, the transmitted signal power needs to be higher.

For PSK M-ary signaling methods it is not so evident but it was also quite predictable. When increasing M, the phase difference between the signal decreases (Figure 2-4 and Figure 2-6) and to obtain the same BER more energy has to be transmitted.

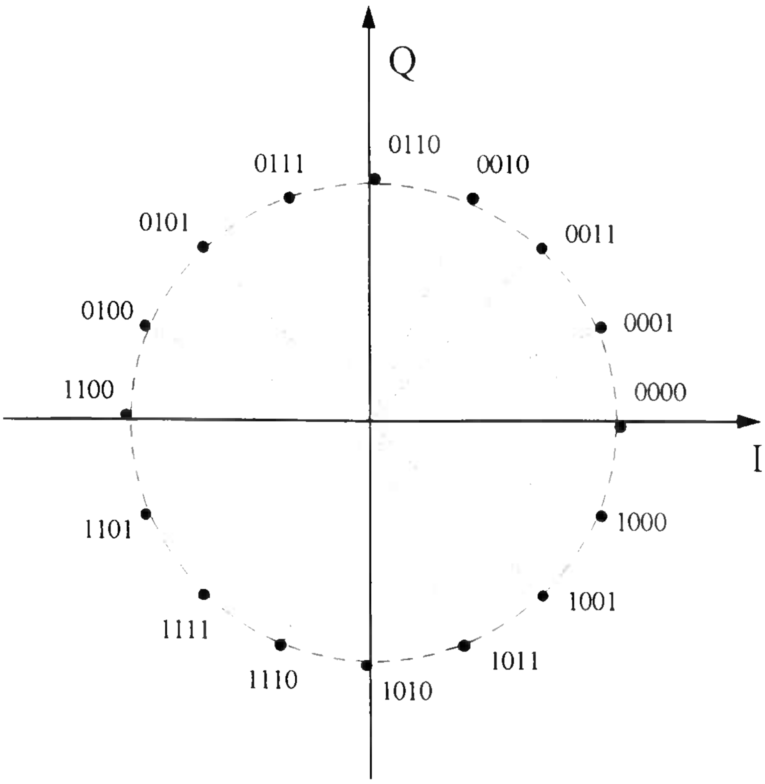

Figure 2-6 Constellation of a Gray-coded 16-ary PSK signal

Finally, it should be remarked that 16-ary-APK clearly outperforms 16-ary-PSK in power efficiency, which is the reason why this method has been studied. The reason is that APK not only detects the phase of the signal but also uses of the amplitude to differentiate two signals. From another point of view, APK signals are better distributed in the signal constellation space and as the distance between two signals is bigger than in 16-ary PSK, less errors are made by the decision device. This can be seen comparing Figure 2-6 and Figure 2-7.

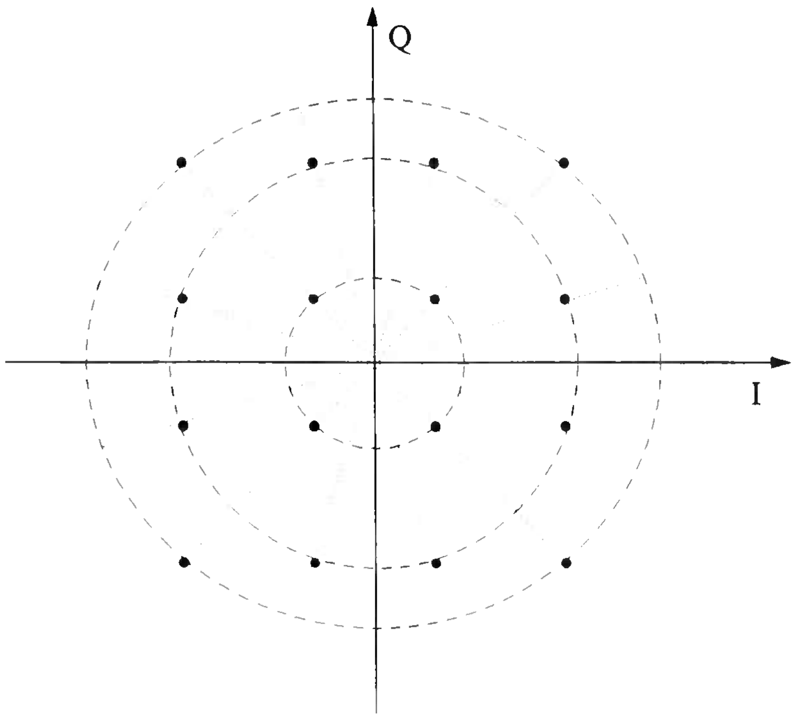

Figure 2-7 Constellation of 16-ary APK signal

* **Low out-of-band radiation and near constant envelope:** As described in the same paper by Oetting, the modulation scheme with less out-of-band radiation and faster sidelobes attenuation is CP-FSK. While ASK signals suffer an attenuation of 25 dB in 8/T Hz from the center frequency, and PSK 33 dB, CP-FSK achieves 60 dB. However, when some pulse shaping or other modifications arc introduced to ASK and PSK schemes, their spectral characteristics can be improved significantly. For instance when pulse shaping is applied to a PSK transmitter, the resulting modulation is actually CP-FSK, as the phase changes continuously and the earrier frequency is slightly modified by the rate at which the phase changes in time.

The reason why OK-QPSK performs better than QPSK, is that a 180^0 phase change, makes the envelope go to zero when the signal is bandhmited by a BPF [Pas]. As was explained before, the phase of an OK-QPSK signal experiences only 90° changes, which do not cause such important envelope variations. This is why after amplifying the signal with a nonlinear amplifier the regenerated out-of-band radiation is smaller for OK-QPSK. Usually, as bigger and sudden a change in a wave is, the higher frequency components the wave has. Therefore, smoothing the shape of the pulse or the amplitude, also helps in obtaining higher sidelobe attenuations, which are actually, higher frequency components. Although MSK has a mainlobe 1.5 times wider than QPSK or OK-QPSK, the bandwidth that contains 99% of the unfiltered signal power of QPSK and OK-QPSK is about $8/T_b$, but only $1.2/T_b$ for MSK [Pas].The spectral density functions of both signals can be observed in Figure 2-1.

Not only CP-FSK schemes have less spillover than other methods, in general most of the FSK schemes present about 50% wider mainlobes, but have a fourth-order spectral rolloff [Car]. Another method with much less spillover than QAM or QPSK but with more or less the same spectral efficiency is the already mentioned VSB.

Constant envelope is another important characteristic when using nonlinear amplifiers. That is why ASK schemes are not used in those cases. PSK and FSK are more suitable as long as bandlimiting does not cause envelope variations.

* **Low sensitivity to ACI and CCI:** Besides the amount of out-of-band radiation, it is also important to know how sensitive the performance of the system is to ACI and other kinds of interference as CCI. Table 2-3 shows also the E_b/N_o needed to achieve a 10^{-4} BER in the presence of Continuous Wave (CW) interference in the same frequency band. The table gives values for an interference wave power (I) 10 dB below the signal power and for a weaker interference of 15 dB. Unfortunately, there is no data available for CP-FSK or OK-QPSK schemes. The conclusion from the table is that the schemes using signals "further" from each other in the signal constellation diagram, as BPSK, are the less sensitive to interference, while the ones which use "closer" signals are more sensitive, as 8-ary-PSK.

Table 2-3 Performance of representative modulation schemes in the presence of CW interference [Oet]

Type	Modulation Scheme	E_b/N_0 (dB)	
		S/I = 10 dB	S/I = 15 dB
AM	OOK-coherent detection	---	---
	OOK-envelope detection	~20	14.5
	QAM	---	---
	QPR	---	---
FM	FSK-noncoherent det. (d=1)	14.7	13.3
	CP-FSK-coherent det. (d=0.7)	---	---
	CP-FSK-noncoherent det. (d=0.7)	---	---
	MSK (d=0.5)	---	---
	MSK-differential encoding (d=0.5)	---	---
PM	BPSK-coherent detection	10.5	9.2
	DE-BPSK	11.0	9.7
	DPSK	12.0	10.3
	QPSK	12.2	9.8
	DQPSK	>20	14.0
	OK-QPSK	---	---
	8-ary PSK-coherent detection	~20	15.8
	16-ary PSK-coherent detection	---	>24
APK	16-ary APK	---	---

* **Low sensitivity to multipath fading:** To see the effect of multipath fading in the different modulations schemes, the paper by Oetting gives Table 2-4 with the E_b/N_o needed to achieve a BER of 10^{-2}. The reason why the value of 10^{-2} was chosen instead of 10^{-4} is because the Rayleigh fading channel employed has degraded severely the system performance. To obtain a better BER without increasing too much the transmitted power, some error control coding or many other

diversity techniques can be applied. The concept of multipath fading, Rayleigh fading and some diversity techniques will be explained in detail in nexz

Table 2-4 Performance of representative modulation schemes on a Rayleigh fading channel [Oet]

Type	Modulation Scheme	E_b/N_0 (dB)
AM	OOK-coherent detection	17
	OOK-envelope detection	19
	QAM	14
	QPR	---
FM	FSK-noncoherent det. (d=1)	20
	CP-FSK-coherent det. (d=0.7)	13
	CP-FSK-noncoherent det. (d=0.7)	18
	MSK (d=0.5)	14
	MSK-differential encoding (d=0.5)	17
PM	BPSK-coherent detection	14
	DE-BPSK	17
	DPSK	17
	QPSK	13.5
	DQPSK	20
	OK-QPSK	13.5
	8-ary PSK-coherent detection	16.5
	16-ary PSK-coherent detection	21
APK	16-ary APK	18

* **Low cost and complexity:** The simplest MODEMs are those which use noncoherent detection, specially OOK and FSK. The most complex are the ones that use high M signaling schemes and specially APK. This can be seen in Figure 2-8 or in Table 2-1, where the schemes are in order of increasing complexity.

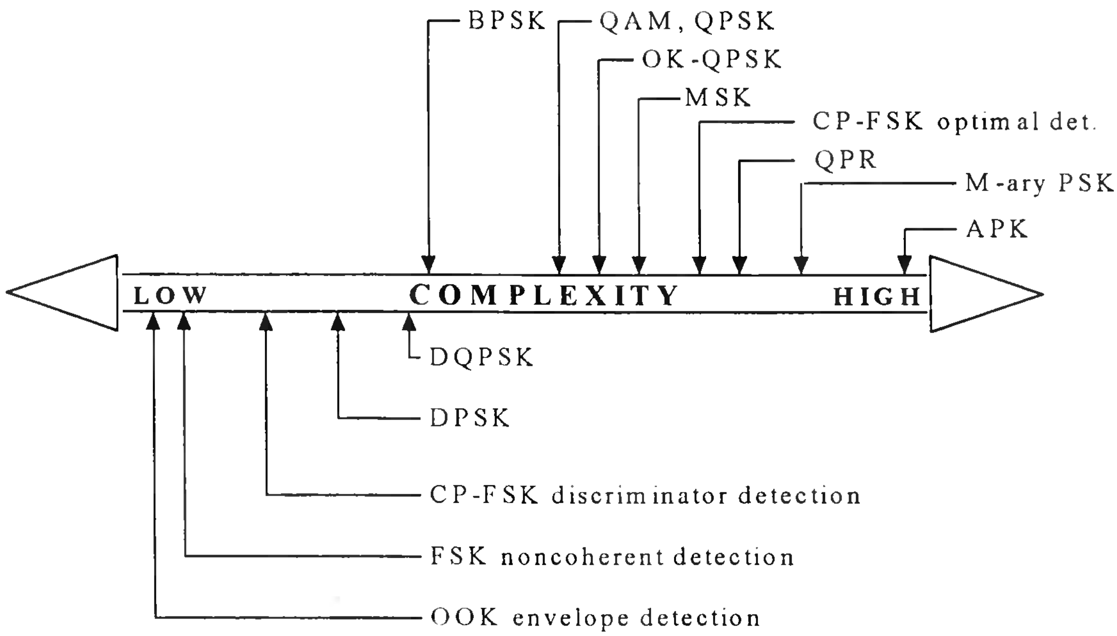

Figure 2-8 Relative complexity of representative modulation schemes [**Oet**]

2.3 Currently Used Methods

The modulation methods that are mostly used nowadays, are not any of the described until now. However, the schemes compared were the basic modulation methods, and a good knowledge of them makes it easier to understand the latest MODEMs principles. In Europe and some other countries, the chosen modulation method for the GSM system is GMSK, while in North America and Japan the modulation method employed in the digital second generation cellular systems is $\pi/4$-QPSK.

The previous comparison seemed to show that MSK was one of the best schemes. It is one of the most power efficient, its spectral efficiency is quite good, has low out-of-band radiation, has constant envelope and it is not too complex. Actually, MSK has some features that makes it very easy to recover the original two signals that needs its coherent receiver. Its synchronisation circuit is not too complex either[5]. For all these reasons, much research has been done in trying to improve MSK. The result of this research is GMSK. GMSK is basically MSK but adding to it a premodulation Gaussian Lowpass Filter (LPF). The effect of the LPF is an even better spectral efficiency and above all, a much sharper spectral cutoff [Mur]. As it has already been mentioned in this report, a fast spectral roll-off, or high sidelobes attenuation is very important in order to keep out-of-band radiation at a low level.

The scheme $\pi/4$-QPSK differs from normal QPSK in its phase transitions. In QPSK the phase can change 90° or 180°, but in $\pi/4$-QPSK the phase changes 45° or 135°. $\pi/4$-QPSK is like a compromise between QPSK and OK-QPSK as its maximum phase transition, 135°, is smaller than 180° but bigger than 90°, which is the phase change of OK-QPSK. The main advantage of $\pi/4$-QPSK over QPSK is the same of OK-QPSK over QPSK: it avoids the 180° phase shift that causes an important envelope variation when the signal is bandlimited. The reason why $\pi/4$-QPSK was chosen by the American Digital Cellular (ADC) instead of OK-QPSK, is that $\pi/4$-QPSK performs better in multipath fading channels and because OK-QPSK can only be coherently detected, while $\pi/4$-QPSK allows coherent detection but also noncoherent by means of a differential detector or by an FM discriminator [Agh]. This is why, the modulator, in the case of the second generation American standard, is differentially encoded. This way, each manufacturer is able to implement a different kind of demodulator. In addition to all these attractive features, it has been shown (see [Feh] and the references therein), that $\pi/4$-QPSK is even more spectral efficient than GMSK.

2.4 Simulated Methods

The methods chosen for the simulations of this work were PRK or BPSK, QPSK, and OK-QPSK Although none of these methods is really frequently employed nowadays in mobile systems, GMSK and $\pi/4$-QPSK are only variations of the studied basis. As was just described, GMSK is

[5] In [**Oet**] it is shown that coherent CP-FSK with d=0.7 seems to perform better than MSK, specially from the energy efficiency point of view. Nevertheless, it is more complex to implement the synchronization circuit and therefore the method is not so spread.

MSK with a premodulation LPF, and MSK is pulse shaped OK-QPSK. $\pi/4$-QPSK is just as QPSK but with different phase shifts.

If for instance, GMSK was chosen instead of BPSK, QPSK and OK-QPSK, there would be more guarantees that the results arc similar to those of a real GSM system, but this work could not be so easily applied to some other future modulation schemes. With the chosen basis, by only modifying some parts of the code programmed to simulate the model, results can be obtained for other similar modulation methods.

Another reason why this basis was selected is because the model of these modulation methods is not too complex to implement. Besides, QPSK is based on BPSK and OK-QPSK is based on QPSK. In fact, the only difference between QPSK and BPSK, is that in QPSK another carrier wave is used and between OK-QPSK and QPSK the difference is that the bit streams are shifted half a symbol period in the case of OK-QPSK. This way, the simulation can be first done using a relatively simple modulation scheme, BPSK, and after the results are analysed, QPSK is incorporated in the model making it more complex. Finally, when the results of the first two methods are understood, OK-QPSK is simulated.

An important issue to be discussed before finishing this chapter is the name chosen for the modulation methods. Even if it was already discussed when BASK, QAM, BPSK, and QPSK where described, it is worth to point out again that their modulators are identical. Therefore any of these pairs of names could have been chosen. If the second pair was finally selected, it was because BPSK and QPSK are the most often encountered names in the literature.

However from the conceptual point of view maybe BASK and QAM seem to be closer to the simulated MODEM. When the input pulses are shaped according to Figure 2-3 and equation (2-3), the only thing that changes in the transmitted signal is the amplitude. Strictly speaking, in BPSK, the pulses should modulate the carrier wave phase and not its amplitude. This way, when the input pulses were shaped, the phase transitions should be smoother but the amplitude should remain constant. However, this modulation would be more like CP-FSK. MSK is in consequence more like pulse shaped Offset Keyed QAM or amplitude shaped QPSK, but not pulse shaped QPSK. Nevertheless in the literature some authors talk about half-sinusoidal pulse shaped QPSK, or pulse weighting, referring to MSK [Agh] [Pas].

The pulse shaping that will be done in this project will always be amplitude pulse shaping, so it will be pulse shaping BASK and QAM or pulse shaping BPSK and QPSK, considering their amplitudes as the shaped pulses.

The detection in the receiver model will be coherent. As was already discussed, coherent detection allows lower BER and hence it saves energy. Besides, coherent detection is more complex to implement in reality, but in the simulated model it is relatively easy to program.

However the optimal receiver in ideal channels does not perform as good in multipath fading channels. Coherent detection is easily understood in ideal channels where only one pulse is received after sending one. In multipath channels, as it is explained in next chapter, many delayed replicas of the transmitted pulse are received through different paths and the synchronisation and the carrier recovery circuit can be done by tracking the first path signal, the strongest, an average of them or even each of them if a so-called RAKE receiver is used. The receiver implemented in this work will be explained later in more detail but does not track the phase of the received signals and therefore is not totally coherent. Nevertheless, it has the same structure as a coherent receiver for an ideal channel, and it would perform optimally in this kind of medium.

2.5 Concluding Remarks

In this chapter the main criteria that should be considered to choose a modulation method has been exposed and the most suitable modulation methods for wireless communication have been described and compared. As a result, three modulation methods (BPSK, QPSK and OK-QPSK) have been selected in order to make this work meaningful in the context of the research towards a more efficient mobile system.

3. RADIO PROPAGATION CHANNELS

Any communication system needs some kind of link between the source and the destination of the information. This link is known as the channel. The received signal is never identical to the transmitted signal, channels, and especially radio propagation channels, always degrade the signal somehow. Therefore a good knowledge and understanding of the effects introduced by the channel are fundamental in the design of a good communication system.

The objective of this chapter is to give an overview of communication channels in general, and more specifically, of radio channels. Most of the radio propagation channels present a phenomenon known as multipath fading. As the title of this project specifies, the effect of pulse shaping is intended to be measured in this kind of channels. For this reason, after exposing the main features of communication channels, multipath propagation will be explained and modelled in order to be simulated. With the help of this model, the effects of multipath propagation depending on the transmitted signal will be discussed.

The simulated channels are measured impulse response profiles, therefore, the last part of the chapter is devoted to describe the procedure followed in their computation. All the explanation is based on [Has1], which reports a comprehensive set of measurements in indoor environments. Some parameters exposed in the last section are very important as they set some of the validity bounds of the results obtained in this work.

3.1 *General Description*

The channel is the physical link between transmitter and receiver. When transmitting through an ideal channel, the received signal, is exactly the same signal that was sent by the transmitter. Unfortunately, there is not a single physical medium that behaves like an ideal channel. In reality, transmitted signals suffer four degrading effects:

* **Attenuation:** The signal power decreases due to power dissipation. The lost energy is the energy that was transmitted but never received in the destination. It can be due to the conversion to another kind of energy, like heat in an electric wire, or in wireless communication due to the fact that the receiving antenna does not receive all the transmitted energy. The energy loss depends on every medium, and in wireless communication it is basically a function of the distance between the transmitter and the receiver (r):

$$\frac{P(r_1)}{P(r_2)} \approx \left(\frac{r_1}{r_2}\right)^{-\alpha} \tag{3-1}$$

Where P(r) is the spatially averaged received power at distance r and α is called the path-loss law exponent [Sri] and usually takes the value of 2 in free space. In an indoor environment, it has been reported in [Sal] that this exponent takes lower values when the receiver and the transmitter are placed in the same hallway, but values around 3 or 4 in other cases[1]. [Pra1] mentions values up to 6 for buildings with metalized partitions. For long distance communications, repeaters or signal regenerators can be installed to decrease the attenuation level. As was mentioned in the introduction, in analogue communications repeaters are simply signal amplifiers, while in digital communication they receive the signal, obtain the original bit stream, and they transmit it again. If the received signal was not too degraded, the regenerated wave can be identical to the original wave.

* **Interference:** The received signal is often influenced by other manmade signals. Most of the electric machines, the high voltage lines, switching circuits and other electric devices, emit electromagnetic waves. However, in the case of wireless communication, the main interference comes from other signals in a range of frequencies close to the carrier wave frequency of the desired signal. Most of the times the electromagnetic waves coming from electric devices, have low frequencies compared to a radio wave, so their influence can be easily removed with a BPF. Nevertheless, when other transmitters use the same frequency, creating cochannel interference (CCI), or when other transmitters use the adjacent spectral band and generate out-of-band radiation, causing ACI, their interference is very difficult to remove from the desired signal.

[1] A hallway reflects the wave in such a manner that guides the signal towards the receiver. On the other hand, every wall between the transmitter and the receiver attenuates significantly the signal increasing the path loss law exponent.

* **Distortion:** Like attenuation, distortion is due to the communication system itself. The most apparent result of distortion is a change in the transmitted waveform shape. One kind of distortion is amplitude distortion [Car] caused by unequal attenuation depending on the sinusoid frequency. Another kind of distortion is delay or phase distortion, where the delays are not the same for different frequencies. These two first kinds can be denoted as linear distortion. Real channels are never completely linear. Most of the communication systems include transistor amplifiers that are merely linear in a small range of their input values.

When the system has only linear distortion, its effects can be almost totally cancelled by means of an equalizer in the receiver. An equalizer is a filter designed with a frequency response so that the final output is distortionless. To design such a filter the transfer function of the system should be previously known. However there are some devices called adaptive equalizers that can estimate the impulse response of the system an according to it adapt their filter parameters. A filter in the transmitter, shaping the transmitter pulses, can also reduce the effects of distortion.

Distortion can also be seen from the time domain point of view. The usual way to describe a channel in time domain, is its impulse response. As will be seen below in more detail, the impulse response of a wireless channel shows that the original transmitted impulse is received several times in the receiver. This is due to the phenomenon of multipath, that is explained in next section. Multipath is the main cause of distortion in wireless communication, causing fading and ISI.

* **Noise:** Noise is a random electrical waveform that is always added to the transmitted signal. It is due to internal and external sources. Between the internal sources the most important is thermal noise, which is caused by the motion of electrons. Their thermal agitation produces a weak current that generates the voltage waveform. An external source can be for instance the extraterrestrial radiation. A model of noise often used in theoretical analysis of communication systems is AWGN. Additive means that it is added to the transmitted signal. White means that the psd function is completely flat, all the frequencies have the same power density. And Gaussian means that it has a Gaussian Probability Density Function (pdf). Even if noise is not white over all the spectrum, its psd function is flat enough in a usual signal bandwidth, and the model does

not differ much from reality. However this model does not include some kinds of impulse noise as the one due to a lightning.

The effect of noise in the performance of a communication system, depends on the received signal power. This is why the signal to noise power ratio (SNR) appears so often in the literature. For high values of SNR, noise can be ignored, while for low values is sometimes the main problem of the system. This is the case of wireless communication, where attenuation is very important for long distances and the power of the received signal is usually very low. The transmitted signal power can not be increased too much because of the equipment limitations. Unlike the other kinds of degrading effects, noise is impossible to avoid completely. Not even in theory. Nevertheless, some filtering and modulation schemes can improve the noise immunity of the system very much.

3.2 *Multipath Propagation*

Due to the reflection, refraction and scattering of radio waves, a wave radiated by the transmitter, most of the times reaches the receiver by more than one path [Has2] (see Figure 3-1). This phenomenon is known as multipath. Multipath can have different effects on the received wave, and one of them is fading. These effects will depend on the multipath characteristics of the channel and the bandwidth of the transmitted signal.

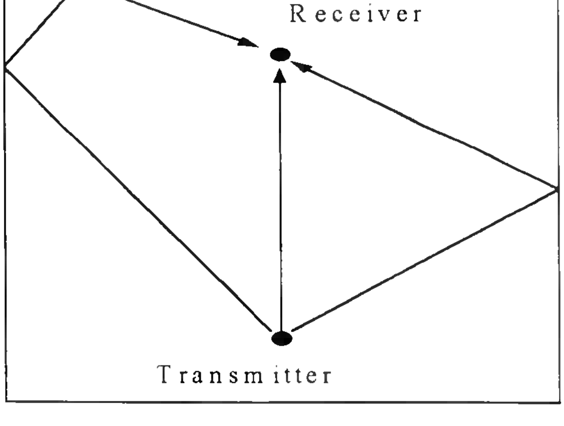

Figure 3-1 Multipath propagation

First multipath channels will be modelled by their lowpass equivalent impulse response and next, the coherence bandwidth and the coherence time are going to be defined. The first parameter gives important information about the frequency response and the impulse response of the channel in time domain. The coherence time is a measure of how quick are the time variations in the channel impulse response function. These two parameters, together with the transmitted signal bandwidth are the key to predict the effects of a multipath channel on the transmitted signal.

3.2.1 Mathematical Model

Almost all real communication signals are bandpass. Bandpass means that the spectrum of the signal is limited to a certain bandwidth around a center frequency, usually called the carrier frequency. When dealing with this kind of signals, it is very useful to work in baseband. This means that the negative part of the spectrum of the signal is ignored and the positive part is multiplied by two and translated to the origin in a way that the original response for the carrier frequency corresponds to the response for frequency 0. This way a signal can be represented just by its amplitude and phase:

$$s(t) = \mathrm{Re}\left[A(t)\exp\left(j\omega_c t + j\phi(t)\right)\right] = \mathrm{Re}\left[A(t)\exp\left(j\phi(t)\right)\exp\left(j\omega_c t\right)\right] \tag{3-2}$$

$$s_{bb}(t) = A(t)\exp\left(j\phi(t)\right) \tag{3-3}$$

Where s(t) is the signal time function, Re[·] means real part, A(t) is the amplitude time function, $\phi(t)$ is the phase time function measured with respect to the carrier phase $2\pi f_c$ and $s_{bb}(t)$ is the baseband equivalent signal or the complex envelope.

This simple interpretation of the lowpass equivalent function, is only true for narrow-band signals[2]. For wide-band signals the lowpass equivalent is obtained the same way, but the

[2] Narrow-band signals are those whose bandwidth is much smaller than its carrier frequency [**Hay**]

interpretation should be done using the concept of the pre-envelope and the Hilbert transform of the signal [Bel2].

The most common way to describe the channel of a communication system is by its impulse response in time domain, or its transfer function in frequency domain.

To work in baseband, not only the signal function has to suffer this transformation but also the impulse response of the system. This is why the mathematical model of the channel used in most of the papers is the baseband or lowpass equivalent impulse response [Sal]:

$$h(t) = \sum_{k=1}^{L} \beta_k \delta(t - \tau_k) \exp\left[j\theta_k\right] \tag{3-4}$$

Where h(t) is the complex-valued lowpass equivalent impulse response , L is the number of paths, β_k is the gain of the k^{th} path, θ_k its phase shift and τ_k its propagation delay. Finally, δ is the Dirac delta function.

The received signal will be the time convolution between the baseband signal and the described impulse response, just as if they were two bandpass functions.

It is very important to note that this model does not take into account that the parameters a_k, θ_k and τ_k, can vary in two dimensions, time and space [Tur3]. Time variations can be due to atmospheric turbulences [Ste], motion of people, or any change in the transmitter-receiver environment. Space variations are obvious as the paths depend totally on their surroundings. In addition to this, when the receiver or the transmitter move, space variations lead to time variations.

As can be seen in the references of [Has2], a considerable amount of papers have been recently published describing the statistics of these parameters. Even if the simulations carried out in this project do not consider the variation of these parameters in time, its effects will be also discussed.

3.2.2 Coherence Bandwidth

The complex-valued baseband impulse response described above can be viewed as a power delay density function, by only considering the gains of the profile and ignoring the path phase shifts [Jan]. One way to measure the temporal extent of a multipath channel profile is the Root Mean Square (RMS) delay spread [Sal], denoted by T_m. It is defined as the standard deviation of the power-delay profile, where the usual role of probabilities is played by the path gains to the power of two:

$$T_m \equiv \sqrt{E\left[\tau^2\right] - E^2\left[\tau\right]} \tag{3-5}$$

with

$$E\left[\tau\right] \equiv \frac{\sum_{k=1}^{L} \tau_k \beta_k^{\,2}}{\sum_{k=1}^{L} \beta_k^{\,2}} \tag{3-6}$$

and

$$E\left[\tau^2\right] \equiv \frac{\sum_{k=1}^{L} \tau_k^{\,2} \beta_k^{\,2}}{\sum_{k=1}^{L} \beta_k^{\,2}} \tag{3-7}$$

The coherence bandwidth, denoted by $(\Delta f)_c$ is defined as the bandwidth over which the signal propagation characteristics are correlated [Jan]. The same concept is sometimes called the correlation bandwidth, which is the width of the frequency correlation curve. This curve is obtained by transmitting two sinusoids and measuring the envelope correlation of the two received waves in function of the frequency difference between both sinusoids [Bel2].

When the only available description is the impulse response in time domain, a very simple method to obtain the order of magnitude of the coherence bandwidth is by calculating the reciprocal of the RMS delay spread:

$$(\Delta f)_c \approx \frac{1}{T_m} \tag{3-8}$$

To understand this relationship, a simplified multipath channel can be considered. This channel will consist of only two paths, one of them being a Line of Sight (LOS) path. The LOS path having no delay and both path gains being one. By applying equation (3-5), it is very simple to obtain that the RMS spread delay equals the delay of the non LOS path. When transmitting two sinusoids of frequencies ω_c and $(\omega_c+\Delta\omega)$ through these channels the received signals will be:

$$s_1(t) = \cos(\omega_c t) + \cos(\omega_c (t - T_m)) \tag{3-9}$$

and

$$s_2(t) = \cos((\omega_c + \Delta\omega)t) + \cos((\omega_c + \Delta\omega)(t - T_m)) \tag{3-10}$$

Their envelopes can be easily derived from their baseband equivalents, adding the I components and the Q components and calculating the modulus. However, by only analysing in more detail the preceding equations, the relationship is clarified below.

In both signals there is a wave with no phase shift and another shifted by $\omega_c T_m$ in the first case and by $(\omega_c+\Delta\omega)T_m$ in the second wave. It is obvious that if $\Delta\omega T_m \approx 0$, both envelopes will be almost equal. Then when $\Delta\omega << 1/T_m$, the two envelopes will have a correlation of almost 1.

The use of the coherence bandwidth is that knowing the transmitted signal bandwidth it will be very easy to know if the signal will suffer frequency distortion or not. When the transmitted signal bandwidth is much smaller than the coherence bandwidth, the signal might suffer envelope variations but will not be distorted. In this case, the channel is called frequency nonselecetive channel. When the transmitted signal bandwidth is bigger than the coherence bandwidth, the signal will suffer distortion and the channel is called frequency selective channel. It is important to note that the same channel can be frequency selective or nonselective depending on the transmitted signal bandwidth.

3.2.3 Coherence Time

When developing the mathematical model, it was explained that even if the described model does not take into account the time variations of a multipath channel, in reality these variations are one of the main causes of the severe degradation introduced by multipath channels in a communication system. The parameter that measures these time variations is the coherence time. Like the coherence bandwidth it is also related to the width of the time correlation function. The coherence time $(\Delta t)_c$ is defined in [Pra1] as the duration over which the channel characteristics do not change significantly.

In the frequency domain, the effect of the impulse response time variations, can be observed by transmitting a pure sinusoid and processing the received waveform in order to obtain its spectrum. Instead of the expected peak in the transmitted frequency, a wider spectrum should be seen. The resulting narrowband signal could also be a modulated wave whose envelope was changing the same way, or a sinusoid received by a moving receiver whose speed produced the same Doppler shifts [Ste]. This is why the width of the obtained spectrum is called Doppler spread, denoted by B_d.

It is quite clear, that a channel having slow time variations, will have a large coherence time and a small Doppler spread, while a fast changing channel will have the opposite characteristics. Just as the coherence bandwidth and the RMS time delay spread, the coherence time has a reciprocal relationship with the Doppler Spread [Pra1]:

$$\left(\Delta t_c\right) \approx \frac{1}{B_d} \tag{3-11}$$

Similarly to the frequency selectivity classification, the coherence time can be used to classify the channels. Those channels with a coherence time much smaller than the bit duration, are called fast fading channels, whereas the ones having a much bigger coherent time are called slow fading or quasi-static [Pra1]. Fast fading channels can also be called time selective and slow fading channels nonselective. The same comment given about the frequency classification of the channels can be mentioned about the time one, a channel can be time selective or nonselective depending not only on its own characteristics, but also on the transmitted signal.

3.3 *Fading and Multipath Effects*

As was explained in the previous section, the parameters of the complex-valued lowpass equivalent impulse response change in time. These variations can lead to a fluctuation of the received signal envelope. This phenomenon is called multipath fading.

Stein in [Ste] divides fading in short term fading, or rapid fading and long term fading. The first term includes changes in the channel transfer function of less than several seconds, while long term fading refers to changes with time scales of minutes or even years. Rapid fading is usually caused by multipath propagation, whereas long term fading is due to meteorological influences. However, there is another cause of fading, which are moving obstacles between the transmitter and the receiver that usually produces changes in the transfer function of some few seconds or even fractions of second. According to Stein's division they would belong to rapid fading but other authors consider them as slow fading [Fat]. In fact bit durations are in most applications shorter than one second, so the last classification would make more sense. Also for the shortness of usual bit durations, it is possible to consider that long term variations will only change the parameters of the chosen mathematical model but not its form. For this reason more attention will be paid to rapid fading.

3.3.1 Narrowband Signals

The effect of multipath in narrowband transmission is a fluctuation in the received signal envelope and phase [Has2]. When the bandwidth of the signal is inferior than the coherence bandwidth the channel is frequency nonselective, so the signal is not severely distorted. From the time domain point of view, this means that de RMS delay spread is shorter than the reciprocal of the signal bandwidth. The consequence is that the baseband envelope of the transmitted signal will not have changed significantly in a time interval equal to de RMS delay spread. Considering now the lowpass equivalent of the signal and the impulse response channel, if the signal is almost equal in the system impulse response duration, the convolution of the transmitted signal and the multipath profile, will be the vector addition of all the path components multiplied by the complex envelope of the transmitted signal (equation (3-3)) [Tur1]. This is the reason why narrowband transmission can be studied as if a pure sinusoid of constant complex envelope was transmitted. With the following example, it will be shown that small changes in the path delays can make the envelope of the signal drop down to extremely low values.

Taking again the example of the idealised bipath channel in section 3.2.2, see equation (3-9), the envelope of the received signal can change from its maximum value to zero, when the phase difference between the sinusoids propagated through each path changes from zero to 180°. Considering that the carrier frequency equals 1 GHz, which is a common value in indoor wireless communications [How], a phase difference of π radians, can be due to a delay increment of only 0.5 ns between both paths. As electromagnetic waves travel around the speed of light, a time difference of 0.5 ns corresponds to a path length difference of only 15 cm. Similarly, when the phase difference between the sinusoids propagated through each path changes from 90° to 270° the received signal experiences a phase shift of 90°.

A real channel has certainly more than two paths and it is very unlikely to happen that the received signal is completely cancelled. However, short term fading can cause envelope variations to fall down to 40 dB below the signal mean level, and a vehicle driving up to 60 mi/hr can experience random signal fluctuations occurring at rates of 100-1000 Hz [Jak]. From these values it is highly expectable to have a severe performance degradation of a mobile communication system.

The peaks and dips of the received signal envelope dependent on the phases of the reflected signals, is the most known explanation of multipath fading, and can also explain the dips experienced in the instantaneous transfer function spectrum of a multipath channel. This spectrum shows some dips for certain frequencies. These frequencies are the ones that make the instantaneous delays to produce destructive phase shifts. Because of the channel time variations, its transfer function is continuously changing, and when one of the frequency dips coincides with the transmitted signal frequency, a dip in the received signal envelope will occur.

In [Sri] RMS delay spreads from 50 to 250 ns are reported for 910 MHz, a common radio frequency in indoor wireless communications. As was explained in the example above, a 0.5 ns delay difference produces a phase change of π radians between the two received sinusoids. This is why most of the models consider that the phase shift of each path varies individually and randomly over a full $[0,2\pi]$ range. Central limit arguments lead to the conclusion that even with only a few of these kind of paths, having similar gains, the received signal envelope has a Rayleigh distribution [Ste]. Fading that fits to this model is designed by Rayleigh fading.

When there is a LOS path, its contribution to the received signal is usually more important than the ones from other paths, so it becomes a dominant component. Then the obtained fading is called Rician fading as the received signal envelope is distributed according to a Rician pdf.

The two fading models mentioned above, describe mainly short term fading in local geographical areas[3], but in larger areas, due to obstacles and other spatial inhomogeneities, there is also long term fading. As explained in [Sri], the two kinds of fading can be artificially separated even if real fading is the product of short and long term fluctuations. The fading caused by obstacles in the communication path from the transmitter to the receiver is also known as shadowing and it is better described by a lognormal distribution [Fat].

In order to improve the performance of mobile systems, several diversity techniques can be implemented to achieve better results. From all the available diversity techniques, perhaps the more specific for multipath fading is antenna diversity. It consists of employing several antennas separated several wavelengths. As the path lengths to both antennas are different, when the received signal in one antenna is in fade because of the path lengths distribution, the received signals in the other antennas will be rarely also in a deep fade. In the tutorial by Stein [Ste], many other diversity techniques are described in detail.

Finally, as explained in [Dix], spread-spectrum (SS) techniques can also improve substantially a wireless system performance. The reason has to be searched in the transfer function of a

[3] In **[Tur2]** local geographical areas are defined as areas having a hundred wavelengths or so in dimensions.

multipath channel. It has been already explained that the spectrum presents some dips at certain frequencies because of destructive interference between the received signals. The advantage of SS is clearly understood considering frequency hopping. In frequency hopping the carrier frequency is changed according to a predetermined sequence [Dix], and two consecutive frequencies will be very rarely in deep fade. The general improvement of SS systems in comparison to conventional systems, will be clarified in the next section.

3.3.2 Wideband Signals

When the bandwidth of the transmitted signal is bigger than the coherence bandwidth, like in most of SS systems, the effects of multipath propagation are very different from those experimented by narrowband signals. The frequency selectivity of the channel causes distortion due to, for example, the high attenuations of the signal components whose frequencies coincide with the transfer function spectrum dips. In time domain the evidence of a large RMS delay spread compared to the reciprocal bandwidth, which in the case of digital communications is around the bit period, is ISI. When one pulse of a much shorter duration than the RMS delay spread is sent through a multipath channel, a series of delayed attenuated pulses is received [Has2], [Sal].

The point that makes the difference between narrowband and wideband signals is that in narrowband signals, the transmitted pulse would have to be of a much longer duration than the RMS delay spread, so the different received signals would be overlapped and the only result that could be seen would be the vector addition of all the signals, as explained in the section 3.3.1.

It is described in [Tur3] that many real media, like an urban environment, experiment some natural clustering, for example groups of facades of buildings. Clustering means that if an impulse was transmitted, the received impulses propagated through different paths would frequently arrive in groups of impulses. In a very short period of time many impulses would reach the receiver antenna, then for a longer time no impulses would arrive, next in another short period another group of paths would arrive and so on.

Due to this phenomenon, a distinction between paths is made in most of the literature devoted to frequency selective channels. Those paths whose time delay difference is greater than the reciprocal of the transmission bandwidth, are called resolvable paths, whereas in the other case, they are called nonresolvable paths [Tur3]. The argument is similar to the one used to explain the difference between the effects on narrowband and wideband signals. The reciprocal of the transmitted bandwidth is a measure of how fast the complex envelope of the signal changes, or in digital communications, a measure of the bit duration or chip[4] duration in SS systems. When this value is bigger than the two path delay difference, the received two bits, chips or pulses will overlap and the receiver will not resolve the three pulses individually, it will resolve the vector additions of them both. In other words, as they would be overlapped, the receiver would never be able to distinguish them.

Returning to the mathematical model, by the next example it will be shown that nonresolvable paths do not have to appear in the baseband impulse response of the channel. Instead there will be only resolvable paths that will be as a matter of fact the vector addition of several nonresolvable paths, also called subpaths. Taking again the example of a two paths channel, if they are nonresolvable, according to the previous definition, their time delay difference should be shorter than the transmitted signal reciprocal bandwidth. Using the same argument used in explaining the result of multipath in narrowband transmission, the signal complex envelope will not change significantly between a time interval equal to the two paths delay difference. Looking at the problem from a more mathematical point of view, the received signal would be the result of the convolution between the complex-valued lowpass equivalent impulse response and the signal complex envelope, and according to equations (3-3) and (3-4) can be expressed as:

$$s_{bb}(t) = \beta_1 \exp(j\theta_1)A(t-\tau_1)\exp(j\phi(t-\tau_1)) + \beta_2 \exp(j\theta_2)A(t-\tau_2)\exp(j\phi(t-\tau_2)) \tag{3-12}$$

Taking into account that the amplitude and phase of the transmitted signal, denoted by A(t) and $\phi(t)$ respectively, can be considered constant during the time interval $(\tau_2-\tau_1)$, equation (3-12) can be written as [Tur1]:

[4] In DS-CDMA every bit is multiplied by a unique binary sequence called code. Each digit from this code is called a chip. This concept will be discussed in more detail in the next chapter

$$s_{bb}(t) = A(t - \tau_1)\exp(j\phi(t - \tau_1))[\beta_1 \exp(j\theta_1) + \beta_2 \exp(j\theta_2)] \tag{3-13}$$

Where $\beta_1\exp(j\theta_1)+\beta_2\exp(j\theta_2)$ would be the resolvable path, and $\beta_1\exp(j\theta_1)$ and $\beta_2\exp(j\theta_2)$ the two nonresolvable paths or subpaths. In consequence the mathematical model doesn't have to contain all the physical paths, only those which are resolvable for the receiver. This is why the described model is widely used when considering frequency selective channels but has only a theoretical meaning for frequency nonselective channels. In nonselective channels, there is only one resolvable path and the fading effects are due to the time changes of the gain and phase of this path.

The statistical time variations of the parameters of the complex-valued impulse response are not included in the model. The complexity would be considerably increased but the results would be similar. The reason is that the channels most of the times can be considered time nonselective as the bit or chip durations, in wideband signals arc usually higher than the coherence time. While coherence time can achieve values of milliseconds in mobile communications [Jak], bits last only several microseconds. In the simulations done in this project, the chosen way to include the time variations of the channel impulse response parameters, is to simulate transmission using the instantaneous impulse response measured in different locations. The average of the performances obtained for each profile, can be a good approximation of the real performance achieved when the receiver or the transmitter is moving around these locations.

From the time domain point of view, the ISI introduced by multipath propagation can degrade the performance of a communications system in orders of magnitude. However some techniques can control the effects of ISI. For instance, pulse shaping can improve the performance when ISI interferes only with adjacent symbols, but when ISI is stronger and time varying, the best solution is adaptive equalization. Digital adaptive equalizers can adjust their parameters by transmitting before the actual message a training sequence. More sophisticated versions adjust themselves continuously using error measures derived from the message sequence [Car].

In the preceding section it was mentioned that SS systems are less subject to multipath signal variations than conventional systems. From what has been explained until this point, the advantage of wideband transmission with respect to narrowband is not clear. Actually, the reader might think that because of distortion and ISI, that was not experimented in narrowband transmission, the performance of SS systems should be worse.

The reason why SS systems are said to be less subject to multipath signal variations is because their bandwidth is wider than the coherence bandwidth of the channel and it is impossible that all the spectrum of the signal is in a dip of the channel transfer function. Some of the frequency components of the wideband signal will certainly experiment high attenuations because of the dips, but hot the whole signal like in the narrowband case.

In the specific of DS-CDMA (explained in detail in the next chapter) the signal is spread multiplying every bit by a unique binary sequence called code. The digits of the code are denoted as chips. When the coded signal is received, it is multiplied again by the same code. The purpose of this process is that for high code lengths low cross-correlation values can be achieved between the diffent users' codes, reducing their mutual interferences. This will be clarified in the next chapter. As the delay differences between resolvable paths are usually bigger than the chip duration, if the autocorrelation function of the spreading codes presents also low values, the interference between the several received delayed versions of the same signal will be also weaker [Dix].

In 1958 a certain receiver called RAKE receiver was designed to outperform conventional receivers in a multipath environment [Pro]. The principle of this receiver is that when a wideband signal is transmitted and there are several resolvable paths, the receiver detects all the paths of the same signal, so a signal is received several times. This way ISI is not only reduced but used to improve the performance of the system.

3.4 *Simulated Profiles*

The simulated profiles are the complex-valued lowpass equivalent impulse responses measured in an office building. Therefore, the results obtained from the simulations are specific for indoor communications and in the context of the cellular concept, would correspond to a picocell environment. Outdoor environments exhibit different propagation characteristics as hallways, walls and other indoor obstacles have a great influence in multipath effects.

It is also important to note that as the purpose of the experiment was to obtain a series of static (only spatial dependent) impulse responses, the measurements were performed at night or on weekends when there was no moving personnel in the surroundings of the measurement set-up.

In the experiment from which the simulated data was acquired, 12000 impulse response profiles where measured inside two office buildings. The locations for the experiment were chosen according to a predetermined plan. This plan pretends to distinguish three kinds of positions variations in order to be able to model different statistical distributions for each group of data. The three categories are: small-scale, mid-scale and large-scale variations. Small-scale variations correspond to groups of 75 different locations inside a small area of less than 4 square meters. Mid-scale variations are in a wider range but all of them having the same antenna separation. However they exhibit great differences due to inhomogeneity of indoor environments, for instance, the profiles obtained when transmitters and receivers were both in the same hallway, have no similarities with the ones where both antennas where separated by several walls. Finally, large-scale variations include locations with different antenna separations. The distances between transmitter and receiver varied from 5 up to 30 meters [Has1]. The 75 simulated profiles correspond to a group of locations in the category of small-scale variations, at 5 meters from the base.

Another relevant parameter from the measurement procedure, is the bandwidth swept to estimate the transfer function. It is reported in [Has1] that the network analyser measured the frequency response from 900 MHz to 1300 MHz in 500 KHz steps. As mentioned in [How], frequencies around 900 MHz are commonly used in indoor communications. The center frequency of this band is 1100 MHz, therefore the lowpass equivalent model is only applicable to signals with a carrier frequency of also 1100 MHz.

3.4.1 Measurement Technique

In [Tur2] it is explained that most of the measurements carried out before 1970 consisted in observing the envelope variations of a received sinusoid. This kind of experimental data is useful to obtain fading distributions at particular frequencies, but it will only help understanding the multipath fading effects on narrowband systems.

At this point of this chapter, it is already clear that in order to simulate wideband signals transmission, the complex-valued lowpass equivalent impulse response is required. The first measurements to obtain the channel impulse response were done in the time domain by transmitting very short pulses, playing the role of impulses, and recording the received signal with high time resolution devices. The pulses should have shorter duration than the reciprocal of the simulated transmitted signal bandwidth. Otherwise, some resolvable paths would be overlapped and therefore not detected. This method and its results are reported in [Tur2], [Tur3] and [Sal].

Even if this seems the most simple method to measure the impulse response, more recently another method was implemented as it presents several advantages. This new method is described in detail in [How] and [Has1], and is the one used to obtain the simulated profiles. It consists of measuring the frequency domain transfer function in the spectral band where the signal is expected to be transmitted. The transfer function is obtained by sending many sinusoids of frequencies uniformly distributed along the measured bandwidth, and recording the received amplitude and phase shift of them. Then the complex-valued lowpass equivalent impulse response is calculated by means of the inverse FFT (IFFT)[5].

The advantages of this other method is that most of the time domain measurements provide only the magnitude of the time domain response [How]. In other words, only the delays and gains of

[5] Before the IFFT can be applied, the data has to be zero padded until the next number being a power of two. In the specific case of the described measurements, the IFFT was applied to 1024 samples, from which the first 801 values were the measured data and the rest were just added zeros.

the paths are available but not their phase shifts. The phase information is very important as will be shown in the chapter devoted to the obtained results. Another important advantage is that the transmitted sinusoids have a constant envelope, while the short pulses required in the first method change their envelope rapidly. This is a serious limitation when there are nonlinear components in the measurement system, specially for long distance measurements where high powers have to be transmitted and the effects of nonlinearities are more important. Finally, the set up for frequency measurements is easier and the measurement time is shorter when it is compared with some time domain techniques [How].

As the bandwidth swept is not the complete spectrum, the measured frequency response data was windowed by a minimum three-term Blackman-Harris window. The properties of this window are discussed in detail in [Har]. In the same paper the purpose and effects of windowing are also explained. For completeness, the general idea of windowing is given in the next paragraph:

When only a part of a function is considered, an implicit windowing is being done. In other words, it is as if the original functions was being multiplied by a rectangular function of the same duration in time domain or bandwidth in frequency domain. Multiplication in one domain is convolution in the other domain. Hence, windowing in one domain is convoluting with the Fourier transform pair of the rectangular function. The mentioned transform pair is the sinc function, so the inverse Fourier transform of the windowed measured frequency response data would be the convolution of the time domain real impulse response with the sinc function.

If instead of a rectangular function a special shape or weighting function is used to window the measured data, the process is similar but the real signal would be no longer convoluted with the sinc function. If the transform pair of the chosen weighting function is much narrower than the sinc function, the resultant function will be closer to the real time function.

The wider the window is, the narrower its transform pair gets. However for the same width, some windows have a narrower transform pair, and this is the interest of choosing a good weighting function. The resolution time in time domain is theoretically the reciprocal of the swept bandwidth [Opp]. However, after the zero padding, the windowing and other minor processes not described in this report, the final resolution is twice the expected resolution [Has1]:

$$\tau_{res} = 2\frac{1}{B_s} = \frac{2}{4 \cdot 10^8\,\mathrm{Hz}} = 5\mathrm{ns} \tag{3-14}$$

This resolution time determines also the path resolvability. Only those paths with delay differences of more than 5 ns will be resolvable, and will appear in the obtained channel impulse responses. These paths will be actually the result of adding subpaths with less delay difference. Therefore, this resolution time allows chip rates up to 200 Megachips per second. If higher chip or bit rates were required, the model would be not complete and a wider bandwidth should be swept. From the frequency domain point of view it is very clear that all the bandwidth used by the transmitted signal has to be swept. The simulations in this project are done by quite lower chip rates, so the resolution time of the measurements is not a practical limitation for this work.

The other important parameter that can be derived from the measurement procedure is the maximum measurable time domain delay. The range that can be determined by the IFFT is the reciprocal sampling frequency step size. This is explained in detail in [Opp]. The idea is that the Fourier transform of a finite duration signal, like the multipath impulse response, is done considering that the signal is periodic having a period equal to the finite duration interval. Hence, the frequency components of the periodic signal will be all multiples of the period reciprocal.

$$\tau_{mes} = \frac{1}{(\Delta f)_{samp}} = \frac{1}{5 \cdot 10^5\,\mathrm{Hz}} = 2\mu\mathrm{s} \tag{3-15}$$

Where τ_{mes} is the measurable time range and $(\Delta f)_{samp}$ the frequency step size. The calculated measurable range is more than sufficient as no paths were detected with delays longer than 500 ns.

3.4.2 Examples

The final data format consists of three files for each location profile. One indicating the path delays, another for the path gains in dBs and the third one for the phase shifts. The same parameters of the mathematical model in equation (3-4).

The files are series of 100 numbers. Every number corresponds to a bin. A bin is like a sample of the complex-valued impulse response. As was derived above, the resolution time is 5 ns, so every bin corresponds to a 5 ns interval. Only those bins with values above a threshold will be considered to contain a path in order to reduce the influence of the noise in the measurements. The numbers corresponding to those bins not containing a path are zero in the three files.

The first file contains actually the excess delays. The real delays are the excess delays plus the delay of the LOS path between the transmitter and the receiver. The LOS delays where subtracted because for most applications the useful values are the excess delays. Actually the numbers given in the delay files have to be multiplied by the resolution time to obtain the right excess delays.

The two figures below illustrate the impulse response of one of the simulated channels is

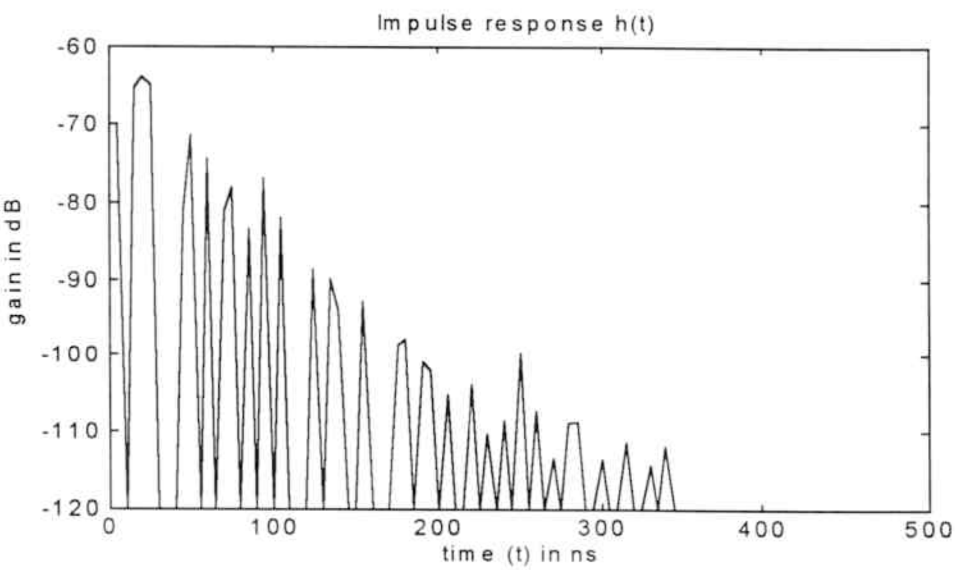

Figure 3-2 Path gains corresponding to location 70

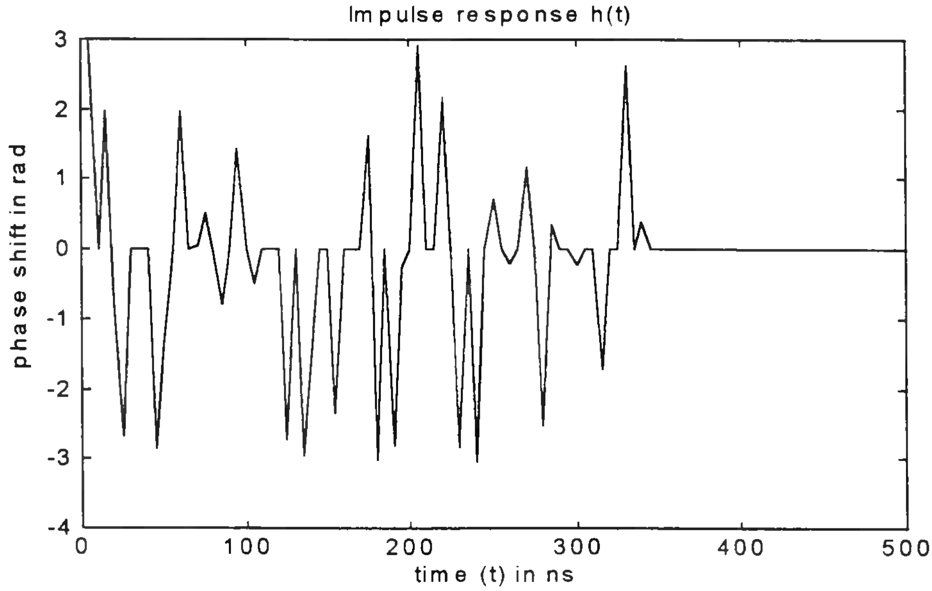

Figure 3-3 Path phase shifts corresponding to location 70

An average channel has been calculated from the 75 original profiles. The purpose of this channel is to simplify the multi-user simulations, as will be explained in chapter 5. The process followed to obtain the average channel is not an arithmetic mean as could be expected. It was observed, that a linear average was highly influenced by those paths less attenuated. Instead, the logarithm of the complex valued impulse responses was carried out. The average was done bin by bin and not for the 75 profiles, but only for those having a path in the corresponding bin. The resulting gain for a determined bin is the arithmetic mean of the path gain logarithms, and the average phase is the arithmetic mean of the corresponding path phase shifts.

The impulse response of the obtained average channel is plotted in the two figures below:

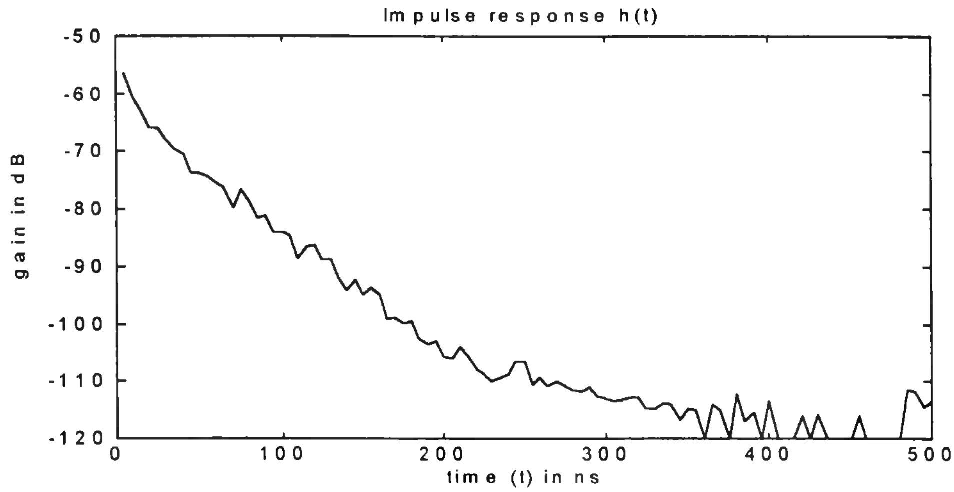

Figure 3-4 Path gains corresponding to the average channel

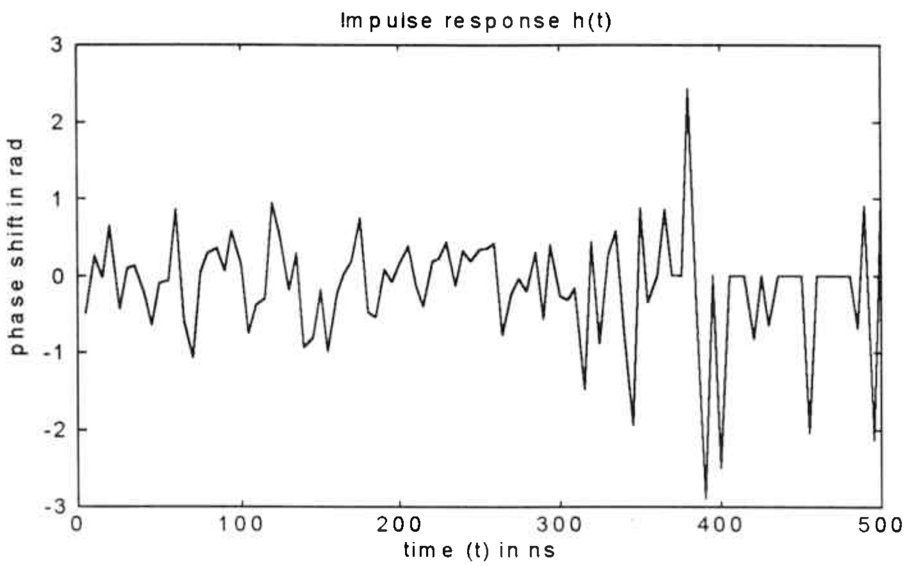

Figure 3-5 Path phase shifts corresponding to the average channel

Finally, the table in Appendix B shows the values of the average delay, the time delay spread, the coherence bandwidth and the average phase shift for every simulated channel including the average channel at the end. The most relevant values of Table B-1 are the time delay spreads. They are only of a few nano seconds. This might be due to the short distance between the transmitter and receiver antennas, as reported in [Has1]. This low values make this group of channel less frequency selective than usual radio propagation channels. This fact will be reflected in the results of chapter 6.

3.5 *Concluding remarks*

One of the most important characteristics of radio channels is their multipath propagation. Multipath propagation has two main effects: ISI in wideband signals and fading in narrowband signals. Fading was the first phenomenon studied and therefore these channels are often known as multipath fading channels. However, DS-CDMA systems transmit wideband signals, so the most important effect for this study is ISI.

The results presented in chapter 6, have been obtained simulating some measured impulse responses. The resolution of these profiles allow the simulation of transmission rates up to 200 Megachips per second. The results derived from the simulations with these impulse responses will only be valid for indoor environments, for antenna separations of about 5 meters and for carrier frequencies of approximately 1100 MHz.

4. DIRECT SEQUENCE CODE DIVISION MULTIPLE ACCESS

The first chapter of this report already introduced the need of a Multiple Access (MA) protocol for a mobile communication system, in order to reduce the interference between the different users. The protocol chosen to evaluate the performance of pulse shaping in this project was DS-CDMA. In this chapter its principles and main features will be explained.

It was mentioned in the introduction, that the first technique to share the free space, was FDMA. This MA protocol assigns every user a range of frequencies, or bandwidth, in which he is allowed to transmit. However, digital communications opened the doors to many other techniques, some of them showing great efficiency. TDMA is one of these protocols, where instead of assigning a spectral bandwidth to each user, it divides the time axis into frames, and each frame into slots. These slots are allocated between all the users according to their needs.

Even if TDMA is more flexible than FDMA and not too complex, when a user is not transmitting information he has still assigned a time slot, or a frequency bandwidth in the case of FDMA, so some capacity is wasted.

In CDMA instead of a time slot or a bandwidth, every user is assigned a code. This code is used to spread the signal spectrum. This is why CDMA protocols are also known as Spread Spectrum Multiple Access (SSMA) protocols. All the users of a CDMA system transmit in the same bandwidth and at the same time, so the signals interfere with each other. However, in the receiver each signal can be individually despread by using the original spreading code of the signal. Using appropriate codes, in the despreading process the other users' signals will remain spread and they will appear as noise when compared to the desired signal [Pras2]. CDMA capacity is limited by the SNR. When increasing the number of users, the SNR will also increase, and the system performance will degrade.

The main advantage of CDMA, compared to FDMA, and TDMA is that when a user is not transmitting, he is not causing interference to the other signals and therefore no capacity is wasted.

There are several ways to spread a signal with a determined code. Hence several CDMA protocols can be implemented. However this chapter will only explain the principles and the main features of DS-CDMA.

4.1 Principles

The method by which DS-CDMA spreads a message is by directly multiplying the message signal by the code sequence. A code sequence is a stream of bipolar binary digits taking the values of 1 or -1. As was mentioned in the last chapter, the binary digits of a code sequence are called chips. In order to spread the information signal spectrum, the chip duration T_c has to be smaller than the bit duration T_b.

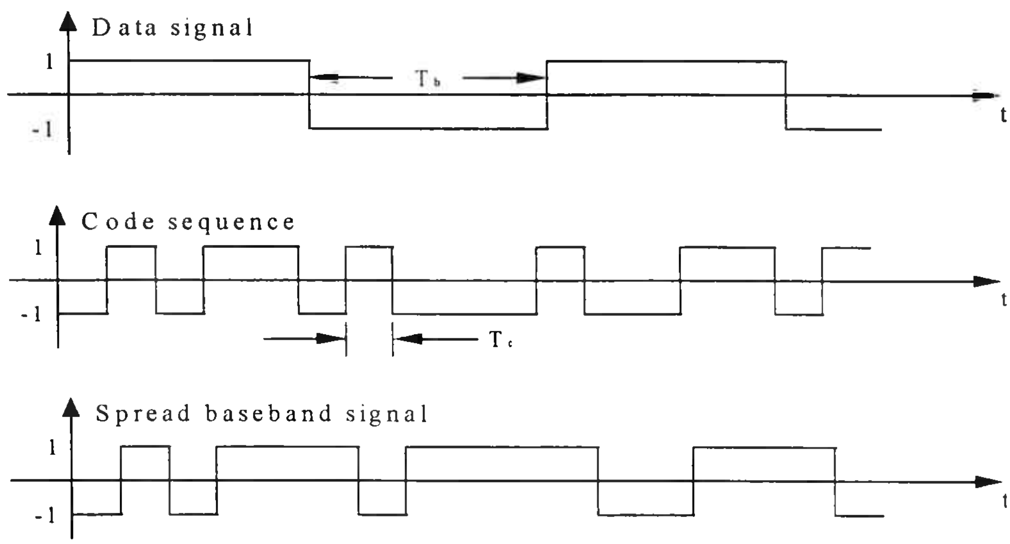

Figure 4-1 DS-CDMA spreading procedure of a data signal.

The second chapter explained that the theoretical bandwidth of a BPSK[1] modulated signal is the reciprocal of the bit duration T_b (see Table 2-1), and in general the information bearing signal bandwidth is proportional to the bit rate, with a factor that will depend on the modulation method speed. The result of multiplying a bipolar bit stream by a code sequence, is just another code sequence that could also be viewed as a bit stream of shorter bit duration (see Figure 4-1). Therefore the bandwidth of the multiplied signal is approximately the reciprocal of the chip duration.

The ratio between the final spread transmitted signal bandwidth B_T and the original data or information bearing signal B_i is called the processing gain, PG [Coo]:

$$PG \equiv \frac{B_T}{B_i} \approx \frac{T_b}{T_c} \tag{4-1}$$

From the frequency domain point of view, the multiplication by the code sequence is just the convolution of the message signal with another signal of a wider bandwidth. The result is obviously another signal having a bandwidth similar to the one from the code sequence. This is shown in Figure 4-2, where:

$$f_1 = f_c + \frac{B_m}{2} \qquad \text{and} \qquad f_2 = f_c - \frac{B_T}{2} \tag{4-2}$$

The spread signal is then used to modulate the carrier wave as if it was a bit sequence in a BPSK transmitter.

[1] The case of QPSK and OK-QPSK are similar to BPSK, as they can be viewed as two BPSK signals modulated with carrier waves shifted 90°. The only aspect that should be taken into account is that the spreading process is done independently to the I and the Q bit streams.

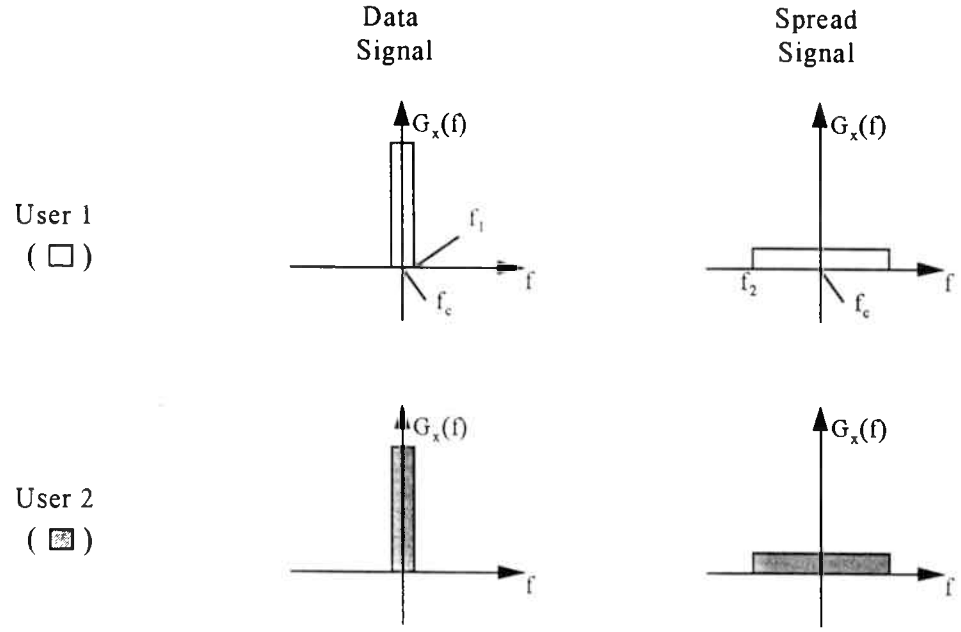

Figure 4-2 Psd functions of the data signal before and after the spectral spreading carried out by each user's transmitter.

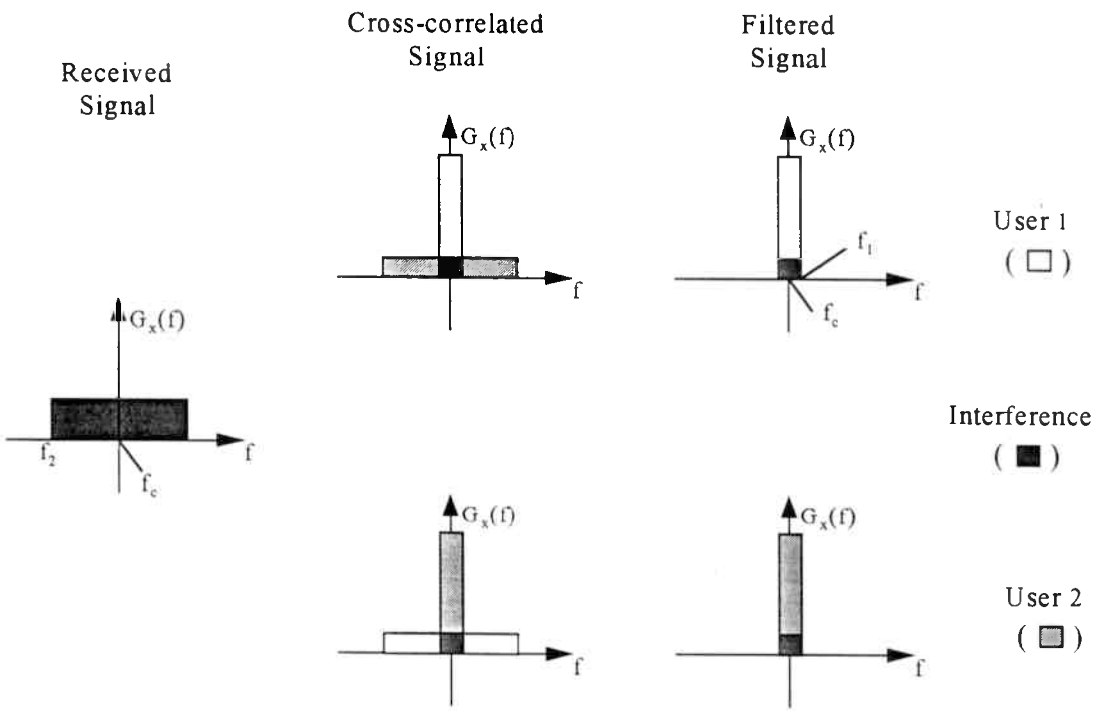

Figure 4-3 Psd functions of the received signal before and after the cross-correlation and filtering carried out by each user's receiver.

To despread the signal in the receiver, the signal is multiplied again by the same code. This process is called cross-correlation [Wib]. The result is exactly the original data bit stream, as any chip multiplied by itself always equals 1. Actually when more than one user is transmitting simultaneously, there are several signals in the same bandwidth. However, the signals originally spread with different codes remain spread after cross-correlation. Figure 4-3 illustrates the cross-correlation done to the same signal but by different receivers. Each receiver uses its own code to spread its user's signal. It is also made clear in this figure that in order to reduce the interference power from other users, the correlated signal can be passed through a narrowband filter centered in the carrier frequency. In the lowpass equivalent model, the narrowband filter is a lowpass filter. Specifically, the lowpass filter in the simulated model is an integrator with an integration time of T_b.

When the codes exhibit good correlation properties, the result of the cross-correlation and integration done in the receiver for other users' signals gives a very low result. The autocorrelation should be also almost zero to achieve good performances in multipath environments and make the synchronization easier [Pras2].

A common way to generate the codes is by means of a Pseudonoise (PN) code generator [Coo]. The codes generated by these devices are periodic sequences of C chips. These generators can be implemented by combining shift registers. They arc also denoted as Feedback Shift Registers (FSR), and linear FSR if they are combined linearly. A popular linear FSR is the Maximum Length (ML) FSR [Pras2]; with v storage elements it can generate a sequence of $C = 2^v - 1$ chips. Its autocorrelation function is:

$$R(w) = \begin{cases} 1 & w = 0, C, 2C, \ldots \\ -\dfrac{1}{C} & \text{otherwise} \end{cases} \tag{4-3}$$

So the longer the code is, the smaller the values of its autocorrelation function.The cross-correlation between several codes is also between acceptable margins compared to other code generators[Pras2]. However, the number of linear FSR that can generate ML codes is limited. To overcome this problem, another sort of code can be generated by modulo 2 adding the outputs of two different ML FSR. The resulting codes are known as Gold Codes and their main advantage compared to ML codes is that by shifting one of the ML sequences from which they are generated (with respect to one another), a new Gold code is obtained [Pras2]. Besides they show low cross-correlation values than ML FSR sequences [Pro].

4.2 Main Features

Spread-spectrum techniques were first used for military purposes. When radio communications started being of great strategic importance to co-ordinate the logistics of an army in a war, some techniques were developed to first *detect* the enemy signal, and then either try to *jam* it or to *decipher* it. This three processes are less likely to be successfully done to a SS signal as it presents the characteristics listed below [Coo]:

* **Low Probability of Interception (LPI) or covert operation**. As the signal power is spread through a large bandwidth, the power density is very low and the signal becomes very difficult to detect, specially when there are other interfering sources in the same band.

* **Antijamming capability**. To jam means to make a signal unintelligible by sending out another wave in the same bandwidth. To achieve the same signal degradation the power required is PG times higher in SS systems because the power has to be sent out in all the spread bandwidth.

* **Privacy**. A receiver is not able to despread the signal and recover the original message unless the right code is known. This feature might be also desirable for civil applications.

Besides, there is another property that is also related to military purposes but can be also useful in the civilian sector. Some navigation systems and radars, send a signal to determine distances by measuring the delay of the received signal. The time resolution is proportional to the reciprocal of the signal bandwidth. Therefore, SS signals will be able to measure distances with a higher precision.

Nevertheless, none of these features seems to determine why a CDMA protocol is being studied in a project related to mobile communications. Actually, the reader might think that SS systems are highly spectral inefficient and for only this reason they should not be considered in wireless systems. This argument is not so obvious if many users can transmit in the same bandwidth, and at the same time. At the beginning of this chapter it was already explained that one of the main reason why SS techniques are used in MA protocols is that they are interference limited, and therefore no capacity is wasted if a user is assigned a code but is not transmitting information. This characteristic becomes even more outstanding taking into account the bursty nature of data and that voice signals are intermittent with a duty factor[2] of approximately 3/8 [Sri]. If a voice activity monitoring system is introduced in the terminals, in order to stop transmission during silent periods, the capacity can be increased significantly [Jan]. Any other way to reduce other users interference will also increase the system capacity.

Compared to FDMA, TDMA and other CDMA protocols, DS-CDMA does not need any special frequency filters or any synchronization between users. The MA protocol can be just implemented by a simple linear FSR and by a binary multiplicator or a module 2 adder. Besides, the following properties of DS-CDMA will help understand why this protocol is considered in this thesis:

* **Soft handover**[3]. Cellular systems using FDMA or TDMA protocols usually divide all the available system bandwidth into several smaller bandwidths. Every cell is assigned one of these bandwidths in a way that the cells transmitting in the same bandwidth are as far as possible from each other in order to avoid CCI. As users of a CDMA system are differentiated by their codes, it is not required to assign a different frequency bandwidth to the adjacent cells and no frequency management is needed.. Assuming a cluster size[4] of one (all the cells transmit in the same bandwidth), soft handover can be achieved. When user A moves from cell 1 to cell 2 (see Figure 4-4), as long as his code is not allocated to another user in cell 2, his signal will gradually be

[2] The duty factor can be defined as the average time fraction where there is voice activity in a conversation.
[3] Handover is the procedure by which a terminal is handed over or reallocated from one base station to another during a connection.
[4] A cluster is the smallest group of cells where all the system bandwidth is used, and its size is the number of cells that it contains.

received by the base station of cell 2. Therefore, no change in frequency or time slot is required and a so-called soft handover can be experienced.

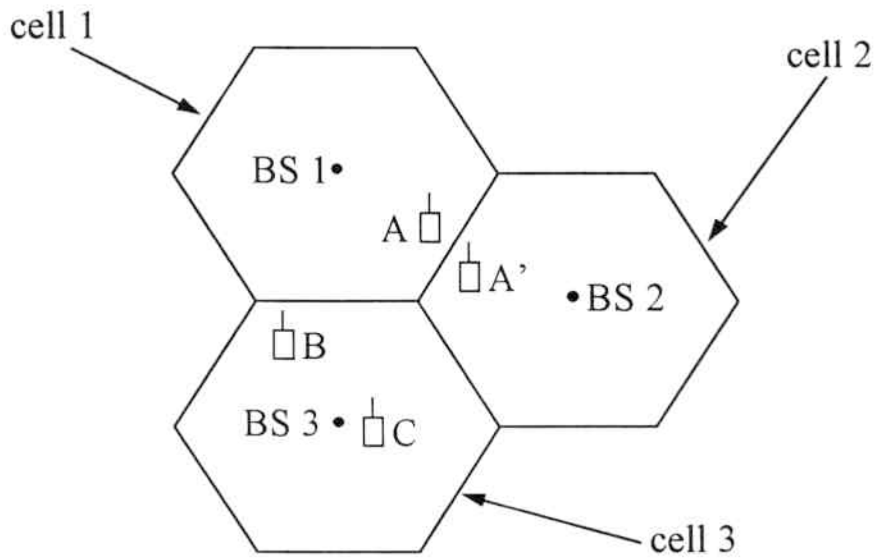

Figure 4-4 Diagram of a cellular system.

* **Multipath protection**. This issue was discussed in chapter 3. It was explained there that SS systems can outperform narrowband systems, specially with a RAKE receiver or other techniques that take advantage of the inherent diversity[5] of SS in multipath channels. When a conventional correlator receiver is used, the autocorrelation of the code sequence acquires great importance, as the receiver considers the delayed versions of the signal just as other interfering signals.

* **Interference rejection**. Similar to the antijamming property, when an additional narrowband wave is present in the same bandwidth, the interference is reduced by aproximately PG times. This is due to the fact that a narrowband signal is spread by the correlator receiver just as it was being codified.

Not all the features of DS-CDMA are advantages compared to other MA protocols. Some of them lead to disadvantages. The most significant are listed below:

[5]The name inherent diversity comes from the fact that in SS systems there are several resolvable paths, each one of them carrying the transmitted signal.

* **Near-far effect**. Due to the path-loss law (see section 3.1) in uplink communications, the signal received from terminals close to the base station will be more powerful compared to those signals coming from terminals located in the boundaries of the cell. This implies that the signal-to-interference ratio can be very low for those signals coming from further users. To solve this problem a pilot signal can be continuously transmitted by the base station. The terminals receiving a high power signal should transmit at lower levels than terminals receiving a weaker pilot signal [Jan]. Despite the accuracy of some power control algorithms, due to fading and other factors, the received power is never equal for all the users.

* **Codes synchronization requirement**. An important limitation of the bit rate and the processing gain is the capability of the synchronization circuit to acquire and maintain the synchronization of the locally generated code sequence with the received signal. When the chip rate takes values of 10-20 MHz the chip time is less than one microsecond and it is usually below the boundaries of the synchronization circuit [Pras2].

* **Multi-users interference**. It has been made clear in this chapter that CDMA protocols are interference limited systems. The reason is that the cross-correlation between several codes is low but not zero and when the number of users increases, the signal-to-interference ratio rises and the system performance gets degraded. This problem is made worse in a cellular system. Adjacent cells can use the same bandwidth, and the fact that makes a handover softer, also decreases the system capacity. Not only the rest of the users of one cell cause interference, but also the users of adjacent cells. Specially those near the cell limits, as user B in Figure 4-4. User B is further from his base station (BS3) than user C, therefore if their terminals have a power control algorithm, the power sent out by user B should be stronger than the power transmitted by user C. In fact the power sent out by user B will be of the same order of magnitude than the one sent by user A, considering that cells 1 and 3 are similar. As the distance between user A to his base station (BS1) and the distance from base station 1 to the user B is not too different, user B will cause almost the same interference to the base station 1, as the users of cell 1.

4.3 Concluding remarks

Except for the three disadvantatges listed above, the rest of DS-CDMA features seem to prove that it can be a suitable protocol for certain applications. Specially for those where interference can be minimized (with voice monitoring for instance), it could be more efficient than traditional protocols. The reason is that unlike other protocols, the capacity of CDMA is limited by the multi-user interference. This fact is precisely the characteristic of CDMA that makes it more likely to improve its performance by choosing the right pulse shape. If pulse shaping is able to reduce the multi-user interference, the capacity of DS-CDMA will be increased without any doubt.

5. MODEL DESCRIPTION

In this chapter, the model used to obtain the results is going to be explained. This model is based on the concepts discussed in the previous three chapters. Obviously, the model is not completely equivalent to a real communication system; some assumptions have been considered in order to simplify the model. These assumptions are of great importance to establish under which conditions the results of the simulations are meaningful in reality.

Another important issue that will be presented in this chapter are the pulse shapes that were simulated. A mathematical description will be given and some time domain and frequency domain plots will be shown.

The model of the studied digital communication system consists of a transmitter, that modulates the input bits, a channel modelled by its discrete time impulse response h(t), Additive White Gaussian Noise (AWGN) added after the channel, and the receiver, that demodulates the received signal, samples the result and decides whether the output bit should be a 0 or a 1. The model does not consider the source of the data, which could be, for instance, the result of transducing a physical variable and converting the analogue signal to a digital bit stream. This process could be done by an analogue-to-digital converter which samples the signal, quantizises the samples in one of the possible levels and encodes each level into a binary code that may include some error control coding redundancy. The recovery of the source information is not studied either, as none of these processes are part of the aims of the project. As was discussed in the introduction, the value chosen to measure the performance of the different pulse shapes and modulation methods, is the BER, which does not depend on where the input bits come from or what is done to the output bits, as long as the probability of transmitting a one is the same as transmitting a zero.

5.1 Transmitter

The transmitter is basically the QPSK or OK-QPSK modulators shown in Figure 2-2 of the second chapter. As was explained there, the BPSK modulator would be only the I branch of those modulators. However these modulators do not have any MA capabilities. A transmitter, in order to operate in a CDMA communication system, should also have a code generator, and for DS-CDMA a multiplier to obtain the SS signal from the information bearing signal and the code sequence. It is important to note that the code generator always repeats the same sequence of length C. Finally, in the simulations the data source consists of a random bit generator with equal probabilities for ones and zeros. In Figure 5-1 the transmitter model for the most complex modulation scheme, OK-QPSK, has been depicted.

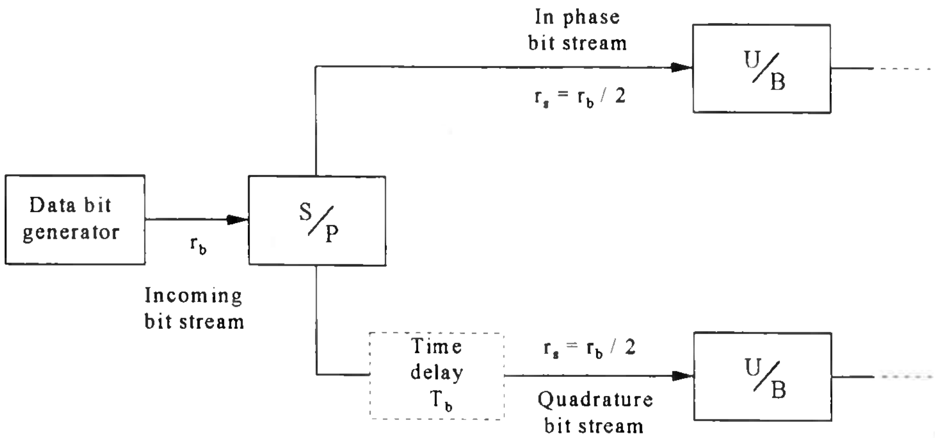

Figure 5-1a DS-CDMA OK-QPSK transmitter model

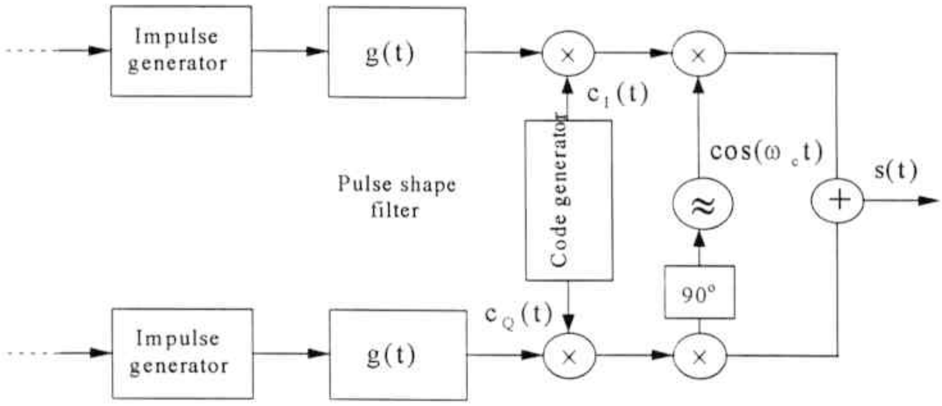

Figure 5-1b DS-CDMA OK-QPSK transmitter model

The most relevant aspects of Figure 5-1 are that in the case of QPSK, instead of one code sequence, each user may be assigned two code sequences, one for every carrier wave. In this way, the coding is also useful to avoid the interference between both carrier waves in the presence of phase shifts in the receiver. For receivers not sensitive to path phase shifts, the same code should be assigned for both carrier waves as the number of codes with suitable corrletion properties is limited. The other comment that can be given to this figure, is the point in the modulator where the signal is spread. If the coding was carried out just before the impulse generator, the chips would play the role played before by the bits and the pulse shape filter would shape the chips instead of the bit pulse. However, in this project the effect of the bit pulse shaping is studied, as the chip shaping has been already discussed in [Cha]. Actually, the effect of pulse shaping in CDMA can be compared to the effect of a multi-level code, as shown Figure 5-2.

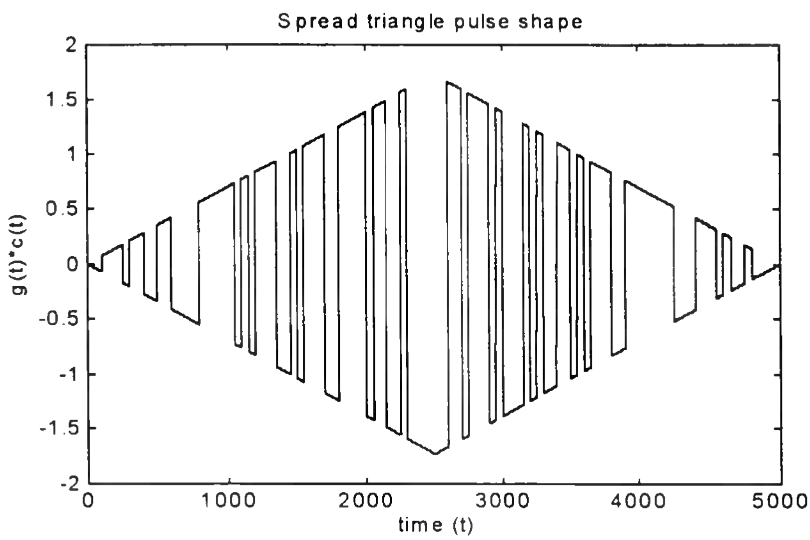

Figure 5-2 Product of a triangle pulse shape by a spreading code

A real transmitter has of course many more components. Most of them are not concerned with the kind of study carried out in this project. However, most of the real transmitters have a BPF and a power amplifier at the end of the modulation process. The purpose of the BPF is to reduce out-of-band radiation. This function is partially accomplished by the pulse shape filter. Although the pulse shaped signal has already lower sidelobes, if a severe BPF is introduced, the transmitted signal will be distorted compared to the just modulated one and therefore the performance of the real system can be slightly different from the results obtained with the described model. The discrepancies can be more important if the real power amplifier is working in saturation, as the simulated signals present considerable envelope variations for some pulse shapes.

5.1.1 Code Generator

In the last chapter the main ideas about code generators where already given. Nevertheless, the code generator in the simulated model is not based on Feedback Shift Registers (FSR). As the purpose of this project is not to calculate the maximum capacity of a CDMA system or to give exact values of the minimum achievable interference, the model code generator is just a random chip generator. The reason why this generator was chosen is its simplicity and the fact that the random data bit generator was already implemented and could be easily reused[1].

The chosen value for the processing gain[2] is 100. It is a usual value in commercial applications of CDMA systems as it is high enough to achieve low cross-correlations between codes (and therefore low multi-user interference) but it does not spread the signal beyond a too wide a bandwidth. Besides the system bandwidth limitation, when the signal is largely spread, the chip duration can be too short for the synchronization circuit of the receiver.

In order to compare the correlation properties of the random codes with the ones of ML FSR codes or Gold codes, a program to calculate the auto-correlation and cross-correlation was implemented (see appendix A.1). The properties of the random codes vary considerably depending on every code, so the auto-correlation and cross-correlation functions were calculated by generating a sufficiently large amount of sequences. This amount is 10^5, as for this quantity significant variations were not observed on the values given by the program.

The auto-correlation and cross-correlation between the codes were calculated according to the following equation [Opp]:

[1] It should be mentioned that time constrains played a major role in utilizing this random generator.
[2] The PG equals the code length if it is considered that the PG can be approximated by relation between the bit and the chip duration.

$$R(w) = \frac{\sum_{i=1}^{C} c_i^1 c_{i+w}^2}{C} \tag{5-1}$$

Where C is the code length, and R(w) is the cross-correlation when the c^1 and c^2 are different code sequences and the auto-correlation when they are the same sequence.

An example of the cross-correlation function of two random generated codes of length 100 is plotted in Figure 5-3.

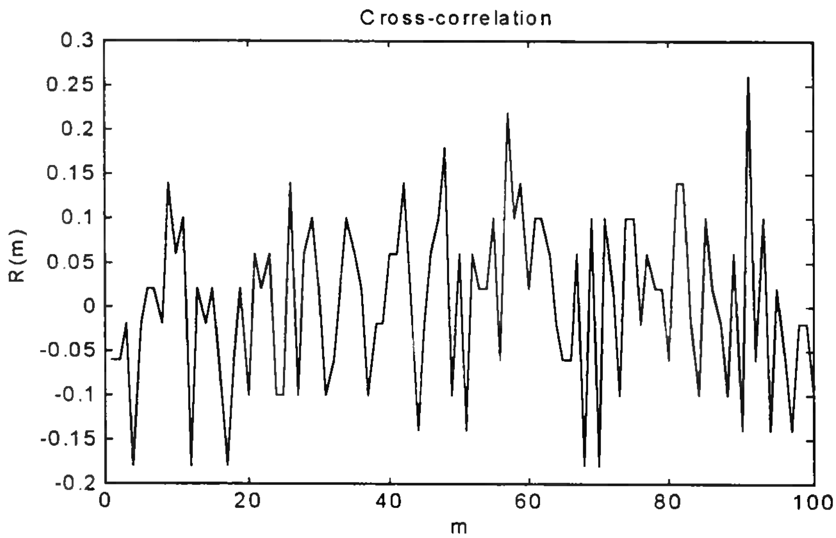

Figure 5-3 Cross-correlation function of two generated codes

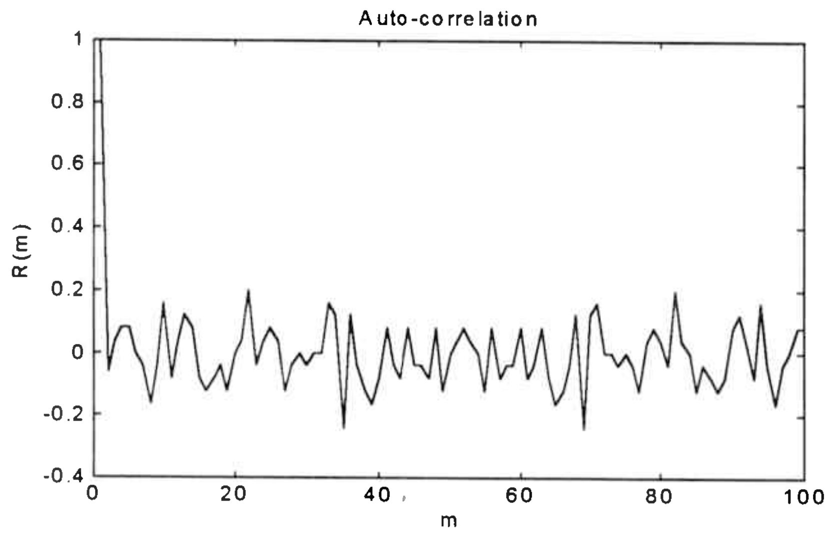

Figure 5-4 Auto-correlation function of a generated code

This example of the cross-correlation function seems to show a maximum value of 0.26. However, the maximum peak cross correlation value detected in the 10^5 functions, was 0.48. The same process was done for the auto-correlation function an a peak of 0.52 was observed. Figure 5-4 shows an example of the auto-correlation function of a random generated code. In both plots, only one period of the function is shown.

According to equation 4-3, the peak value of the autocorrelation function of a ML FSR code is 1/C, which in the considered case equals 0.01. As the value for the generated codes is 50 times higher, the system should perform rather worse in a multipath environment as was discussed in chapter 3. However, the chip duration that has been used is 100 ns and the time delay spread of the simulated channel is 64 ns, as will be seen in next chapter. Therefore, the time difference between the paths will not be more than a few chip durations and the autocorrelation function will not play a decisive role.

On the other hand, the cross-correlation peak has great influence on the multi-user interference of CDMA. The cross-correlation peaks for some ML FSR sequences and Gold codes are given in [Pro]. For a code length of 100 chips, the cross-correlation of ML FSR sequences would show peak values between 0.32 and 0.36, while Gold codes values would be between 0.27 and 0.13.

These values are also lower than the peak obtained for the generated codes (0.48) but they have the same order of magnitude, especially compared with ML FSR sequences.

After this brief analysis, it is possible to state that the results obtained with random generated codes will show performances that could be improved if codes with better correlation properties were used. Nevertheless, it will be still possible to observe the effect of pulse shaping on a CDMA system.

5.1.2 Modulator

In this section, the equations given in the second chapter for QPSK and OK-QPSK will be modified in order to describe a coded signal. The conversion is quite simple, as only the code sequence c(t) has to be multiplied by the shaped pulses. Only the equation for coded OK-QPSK is given as, those corresponding to QPSK and BPSK, are very similar:

$$s(t) = b_I(t)c_I(t)g\big(t-(2m+1)T_b\big)A\cos(\omega_c t) + b_Q(t)c_Q(t)g\big(t-(2m+2)T_b\big)A\sin(\omega_c t)$$

$$\text{for} \quad (2m+2)T_b < t < (2m+3)T_b \tag{5-2a}$$

$$s(t) = b_I(t)c_I(t)g\big(t-(2m+3)T_b\big)A\cos(\omega_c t) + b_Q(t)c_Q(t)g\big(t-(2m+2)T_b\big)A\sin(\omega_c t)$$

$$\text{for} \quad (2m+3)T_b < t < (2m+4)T_b \tag{5-2b}$$

Where:

$m = 0, 1, 2, \ldots$

$w = 0, 1, 2, \ldots, C$

$b_I(t) = b_{2m}$ for $(2m+1)T_b < t < (2m+3)T_b$

$b_I(t) = b_{2m+2}$ for $(2m+3)T_b < t < (2m+5)T_b$

$b_Q(t) = b_{2m+1}$ for $(2m+2)T_b < t < (2m+4)T_b$

$c_I(t) = c_{I,w}$ for $(2m+1)T_b + wT_c < t < (2m+1)T_b + (w+1)T_c$

$c_Q(t) = c_{Q,w}$ for $(2m+2)T_b + wT_c < t < (2m+2)T_b + (w+1)T_c$

$T_c = 2T_b/C$

$g(t) = 0$ for $t < 0$ and $t > 2T_b$

Where $c_{I,w}$ is the w^{th} chip of the I code sequence and $c_{Q,w}$ the w^{th} of the Q sequence. As was explained in chapter 3, the simulated channel impulse responses are given in the lowpass equivalent form. Therefore, in section 5.2, the previous equation will be also shown in the lowpass equivalent form. All the factors multiplying $\cos(\omega_c t)$ will be the real part and all the terms of $\sin(\omega_c t)$ the imaginary part.

5.1.3 Pulse Shape Filter

The pulse shape filter is one of the main components of the model as the purpose of this project is to determine the performance of the system for different pulse shapes.

In literature about pulse shaping, especially the one devoted to ISI reduction, most of the pulse shape filters described are bandlimited. This is due to the fact that most of the channels are also bandlimited and if the pulse bandwidth exceeds the channel bandwidth, some distortion or ISI might occur. Considering the case of an ideal channel and a matched filter in the receiver, the pulse shape that allows the highest bit rate within a limited bandwidth is the sinc function [Sha], which satisfies the Nyquist criterion mentioned in the second chapter. However it cannot be implemented with a physical filter, as its frequency response is rectangular. Therefore filters with a raised cosine frequency characteristics are also studied. Their bandwidth, to achieve the same bit rate, is wider but practical filters can approximate their frequency response more accurately. Besides, small synchronization errors would lead to important amounts of ISI in the case of the sinc pulse shape while the performance would not be so degraded with a raised cosine filter.

The frequency response of a raised cosine pulse shape filter is described by the equation below [Pro]:

$$G_{rc}(f) = \begin{cases} T_s & \left(0 \le |f| \le \frac{1-\rho}{2T_s}\right) \\ \frac{T_s}{2}\left\{1+\cos\left[\frac{\pi T_s}{\rho}\left(|f| - \frac{1-\rho}{2T_s}\right)\right]\right\} & \left(\frac{1-\rho}{2T_s} \le |f| \le \frac{1+\rho}{2T_s}\right) \\ 0 & \left(|f| > \frac{1+\rho}{2T_s}\right) \end{cases} \quad (5\text{-}3)$$

Where T_s is the symbol duration, and ρ is the so-called roll-off factor. The roll-off factor can take values from zero to one. When it equals zero the frequency response is a rectangle and the impulse response is the sinc function. When it equals 1, the bandwidth is the symbol rate. The filter impulse response of these filters is [Pro]:

$$g_{rc}(t) = \frac{\sin(\pi t / T_s)}{\pi t / T_s} \frac{\cos(\pi \rho t / T_s)}{1-(2\rho t / T_s)^2} \quad (5\text{-}4)$$

A very common way to implement digital filters is by a shift register containing the sampled impulse response values [Sha]. The impulse response of a raised cosine filter is not time limited but it equals almost zero for high time values. Hence, by implementing long pulse shape digital filters, the frequency response can be well approximated.

However, for simplicity, all the pulse shapes that have been tested, are time limited to one bit period. Besides, even if it is not a reasonable solution to study the pulse shaping effect on the ISI introduced by bandlimited channels, the purpose of this work is to study the effect in a CDMA system. It was shown in [Cha], that the performance in a CDMA system of time-limited chip pulses is about the same compared to the one for bandlimited chip pulses. In the mentioned paper, the pulses were time limited to one chip period, and the principles that are explained to understand the achieved multi-user interference reduction can be also applied to bit pulse shaping.

The simulated pulse shapes are divided in four groups. For each kind of pulse shape the mathematical expression of its time domain and frequency domain function is given. The time function will be only described during the symbol period as for other time values all the pulse functions equal zero. In most of the cases, the time function is implicitly time limited by a simple rectangular window. Other windows could be also used to improve their spectral features, as described in [Har]. In fact, the forth group consists of products of different pulse shapes that can be also viewed as windowed pulses. The plotted functions of all the pulses are normalized to make them energy equivalent:

$$g_p(t) = \frac{g(t)}{\int_0^{T_s} (g(t))^2 \, dt}, \tag{5-5}$$

where $g_p(t)$ is the normalized function of the pulse shape g(t). In all the figures, it is considered that the symbol period lasts one second and only the modulus of the frequency response[3] is shown.

5.1.3.1 Rectangular, Triangular and Sinusoidal Pulse Shapes

The first group consists of the most simple geometric shapes: the rectangular pulse, the triangular pulse and the half-period sinusoidal pulse, which is the one used to obtain a MSK signal from OK-QPSK.

The rectangular pulse can be defined as:

$$g(t)=1 \tag{5-6}$$

And its Fourier transform is:

$$G(f)=T_s \mathrm{sinc}(fT_s)\exp(-j\pi fT_s) \tag{5-7}$$

[3] The plotted frequency response has been obtained taking 100 samples of the impulse response, zero padding the samples up to 1000 samples, and calculating the DFT (see appendix A.2).

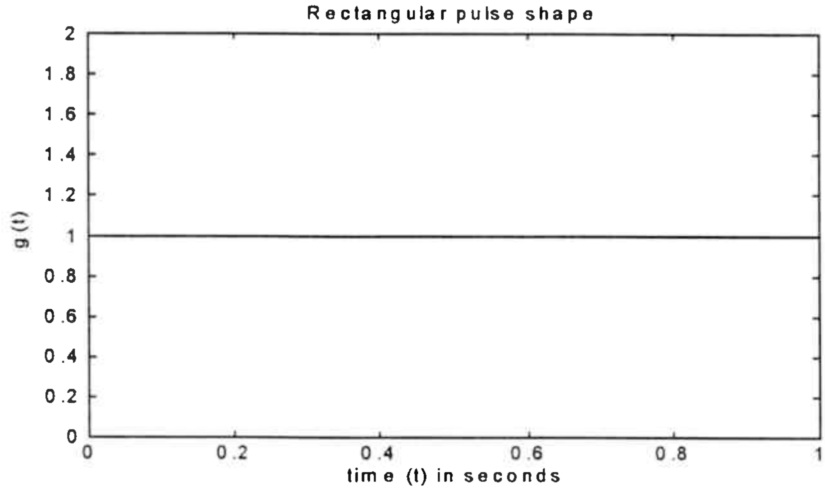

Figure 5-5 Impulse response of a rectangular pulse shape filter

It can be observed in Figure 5-6 that the main lobe is very narrow but due to the sudden step of the rectangular shape, there is almost no roll-off. The low peaks observed are caused by the zero crossings of the sinc function.

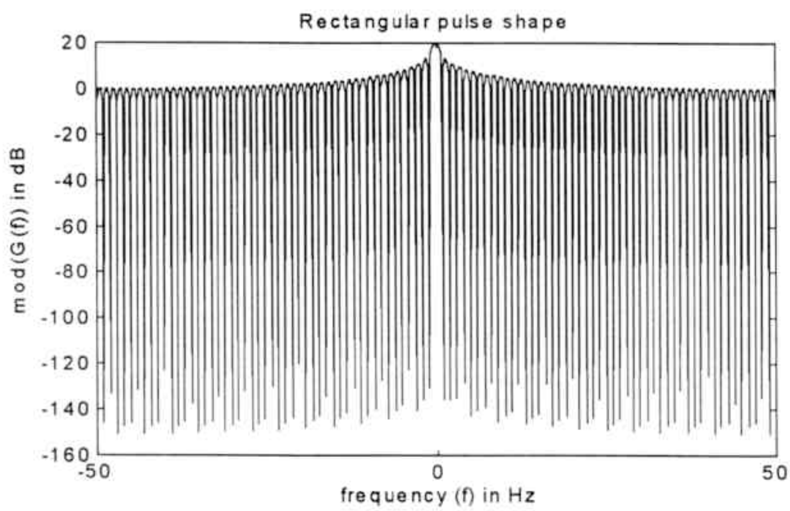

Figure 5-6 Frequency response of a rectangular pulse shape filter

The triangular pulse shape can be defined as:

$$g(t)=\begin{cases}\dfrac{2t}{T_s} & (0\le t<T_s/2)\\[2ex] \dfrac{2(T_s-t)}{T_s} & (T_s/2\le t<T_s)\end{cases} \tag{5-8}$$

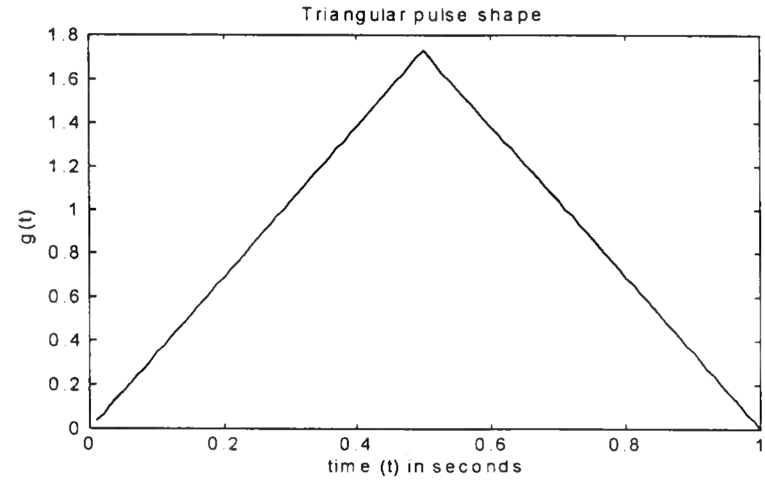

Figure 5-7 Impulse response of a triangular pulse shape filter

And its Fourier transform is similar to the square function of the rectangular shape Fourier transform as the convolution in time domain of two rectangular shapes is a double length triangle shape:

$$G(f)=\frac{T_s}{2}\mathrm{sinc}^2(fTs/2)\exp(-jfT_s) \tag{5-9}$$

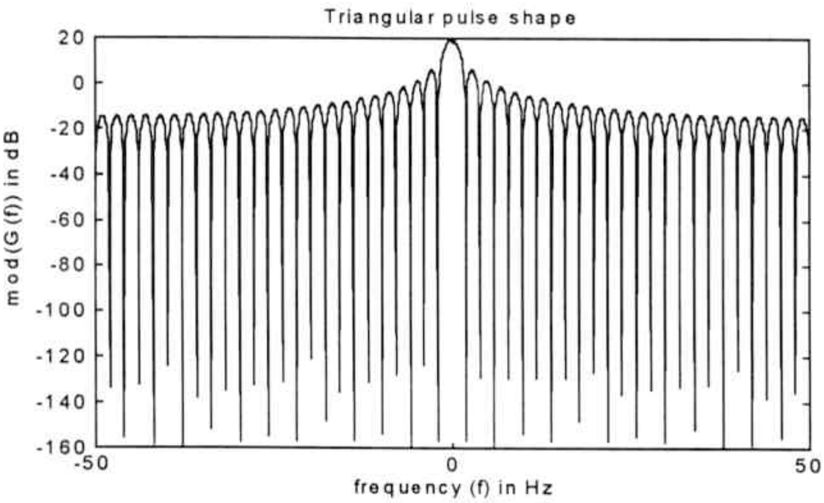

Figure 5-8 Frequency response of a triangular pulse shape filter

It can be seen in Figure 5-8 that the main lobe is wider than the one of the rectangular shape. However, about twice roll-off is observed. According to [Cha] the bandwidth where the 95% of the energy is contained, is only half of the one observed for the rectangular pulse shape.

The sinusoidal pulse shape can be defined as:

$$g(t) = \sin\left(\frac{\pi t}{T_s}\right) \tag{5-10}$$

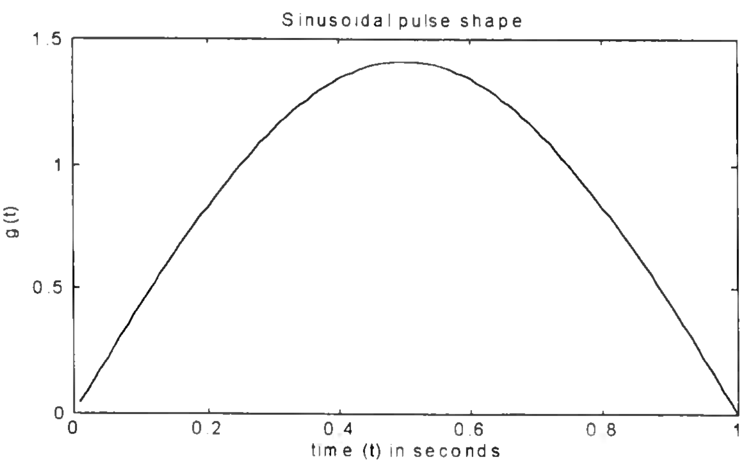

Figure 5-9 Impulse response of a sinusoidal pulse shape filter

Its Fourier transform can be obtained by convoluting the sinus Fourier transform by the rectangular shape Fourier transform:

$$G(f) = \frac{jT_s}{2}\left(\mathrm{sinc}\left(fT_s - \frac{1}{2}\right) - \mathrm{sinc}\left(fT_s + \frac{1}{2}\right)\right)\exp(-j\pi fT_s) \qquad (5\text{-}11)$$

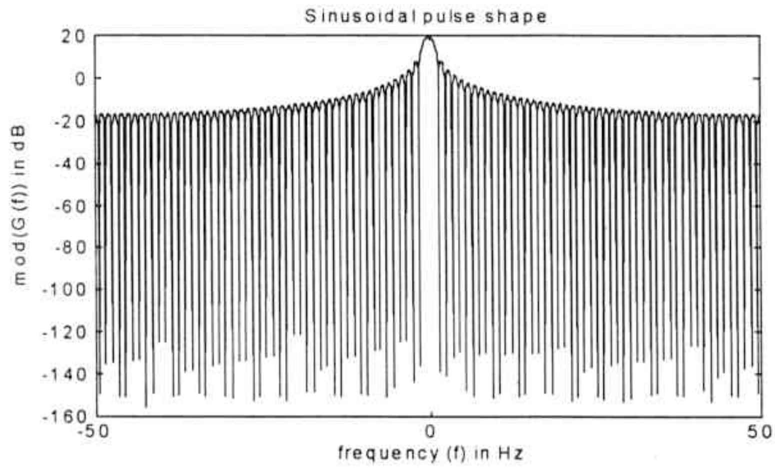

Figure 5-10 Frequency response of a sinusoidal pulse shape filter

Figure 5-10 shows that the main lobe is wider than the one of the rectangular shape but narrower than the one of the triangular shape. The roll-off is about the same than the one of the triangular pulse shape though. According to [Cha] the bandwidth where 95% of the energy is contained, is slightly lower than the one of the triangular pulse shape.

5.1.3.2 Gaussian Pulse Shapes

The second group of pulse shapes are the ones having a shape similar to a Gaussian pdf. They can be mathematically described by the following equation [Hay]:

$$g(t) = \frac{1}{\lambda}\exp\left(-\frac{\pi(t - T_s/2)^2}{\lambda^2}\right) \qquad (5\text{-}12)$$

Their unwindowed[4] Fourier transform is:

$$G(f) = \exp(-\pi\lambda^2 f^2 - j\pi f T_s) \tag{5-13}$$

Where λ is a parameter that can take any positive value. When λ tends to zero, the pulse shape tends to be an impulse (or in mathematical terms to the Dirac delta function), and when λ tends to infinity, the pulse shape tends to be the previously described rectangular shape. The flexibility introduced by this parameter, together with the fact that all its derivates are continuous, make Gaussian pulse shapes very useful from an experimental point of view.

To see the influence of λ on the Gaussian shape, several impulse responses are plotted in Figure 5-11 for the λ:

················ $\lambda = 0.1$ — — $\lambda = 0.3$ — – — $\lambda = 0.5$

———— $\lambda = 1.1$

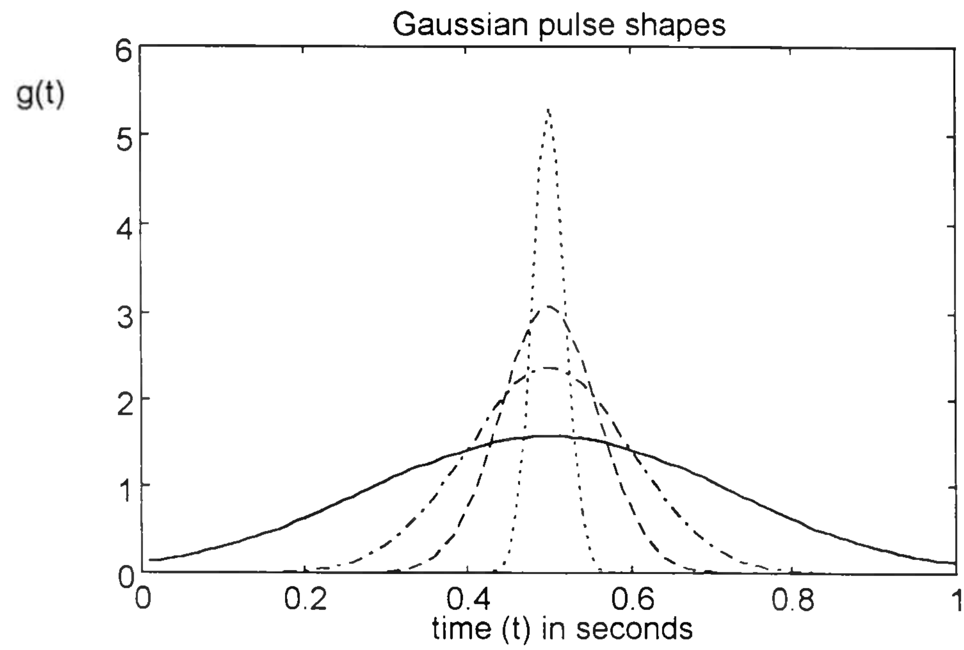

Figure 5-11 Impulse response of a Gaussian pulse shape filters

[4] To obtained the windowed Fourier transform. the unwindowed version should be convoluted with the given Fourier transform of the rectangular pulse shape.

The frequency response for the illustrative cases of $\lambda = 0.1$, $\lambda = 0.5$ and $\lambda = 1.1$ are shown in Figure 5-12, Figure 5-13 and Figure 5-14 respectively:

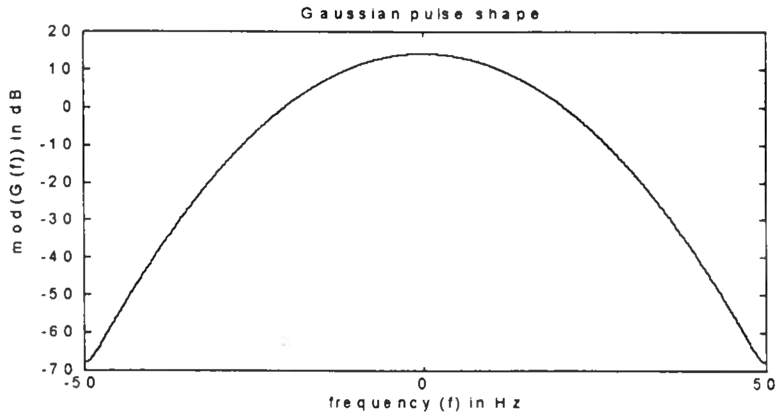

Figure 5-12 Frequency response of a Gaussian pulse shape filter for $\lambda = 0.1$

Due to the small width of the pulse, the main lobe of its frequency response is very wide. However it shows a very fast roll-off. To know the frequency response for a wider spectral range, more samples of the impulse response should be taken. It is also noted that there are no low peaks on this figure. This could be explained considering that the pulse shape takes very low values outside the symbol period, and therefore windowing has not an important effect.

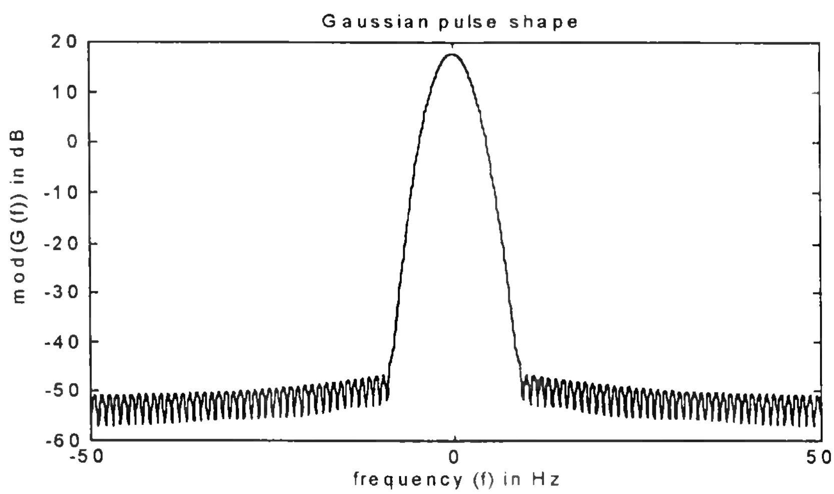

Figure 5-13 Frequency response of a Gaussian pulse shape filter for $\lambda = 0.5$

For $\lambda = 0.5$ the width of the main lobe is significantly reduced but the spectral roll-off is still very fast. Compared to the shapes of the first group, it has a considerably wider main lobe but its roll-off is much faster. Therefore this shape seems to be a good candidate to achieve a sharp cutoff.

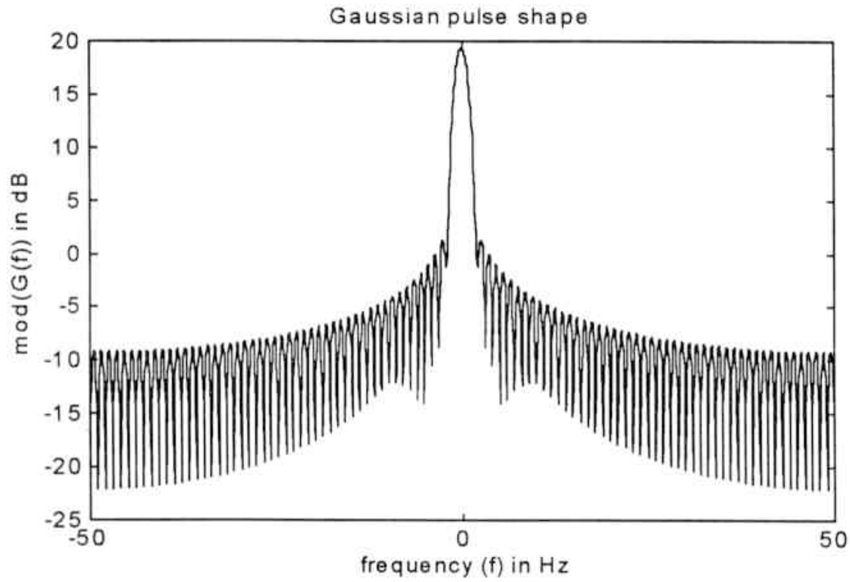

Figure 5-14 Frequency response of a Gaussian pulse shape filter for $\lambda = 1.1$

Figure 5-14 does not seem to have the good features of the last pulse shape. Its main lobe is narrower but its spectral roll-off is relatively slow. Compared to the pulse shapes of the first group, it has a wider main lobe but its spectral roll-off is not faster than the ones of the triangular or sinusoidal pulse shapes.

5.1.3.3 Raised Cosine Pulse Shapes

The third group consists of the raised cosine pulses described at the beginning of this section. The unwindowed and zero centered[5] equations where also given there (equations (5.3) and (5.4)). As will be seen in the figures below, the roll-off factor does not change the shape as much as the

[5] To obtain the equations of the half symbol period centered represented pulse shapes, a time delay of $T_s/2$ should be introduced, which in frequency domain is equivalent to the following factor: $\exp(-j\pi T_s f)$

parameter λ of the Gaussian pulse shapes. However, introducing a scaling factor, it is possible to narrow the pulses until the desired width, at expense of increasing the signal bandwidth.

As in the previous group, some pulse shapes will be plotted for different values of the roll-off factor. Figure 5-15 shows the shape of the sine function main lobe ($\rho = 0$) and the main lobe of raised cosine functions with rollof factors of $\rho = 0.6$, and $\rho = 0.9$.

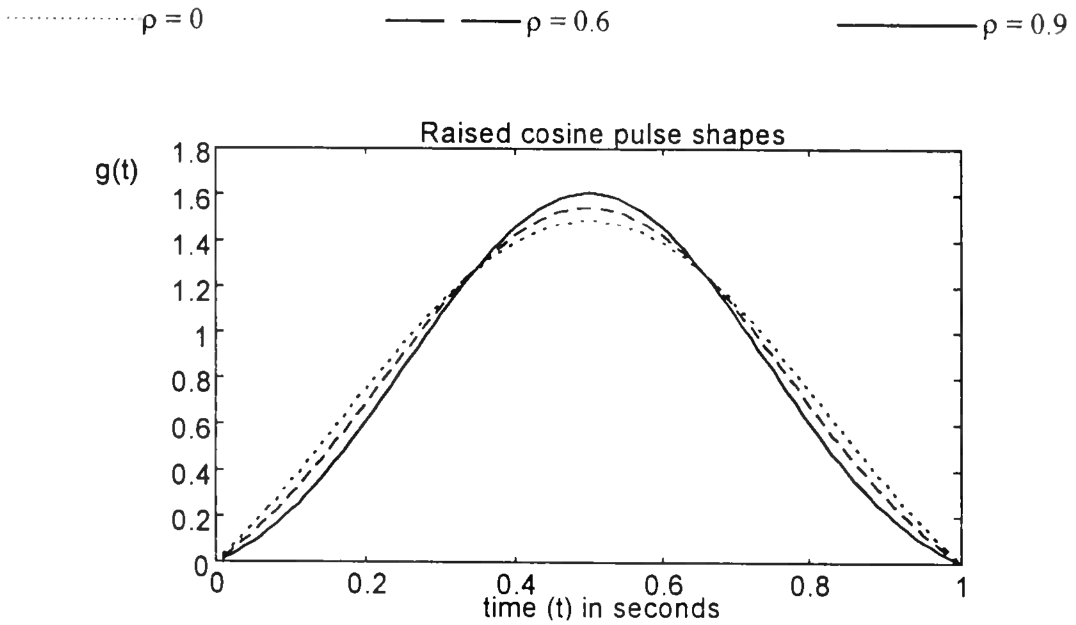

Figure 5-15 Impulse response of a raised cosine pulse shape filters

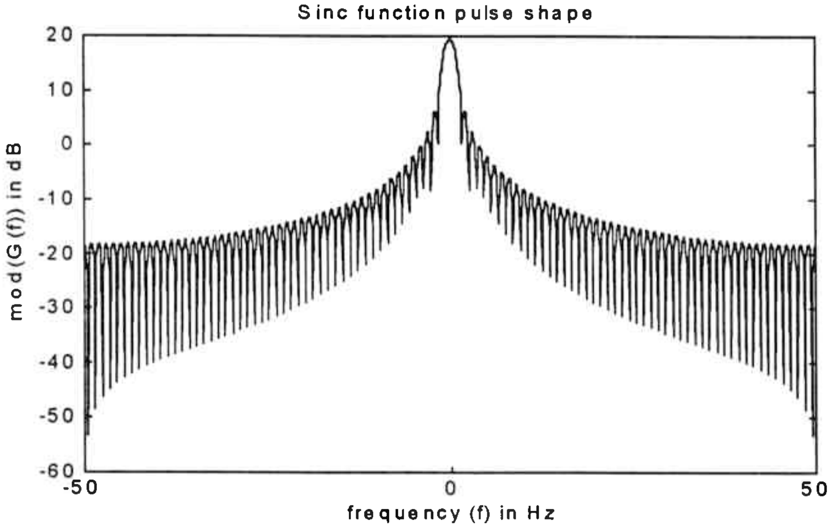

Figure 5-16 Frequency response of the sinc function main lobe filter

From Figure 5-15 and Figure 5-16, it can be stated that no important differences are observed between the sinusoidal and the raised cosine pulse shapes, only the amplitude is slightly increased when the roll-off factor takes higher values. Nevertheless, as mentioned before, when a scaling factor is introduced the shape can achieve totally different features as shown in Figure 5-17.

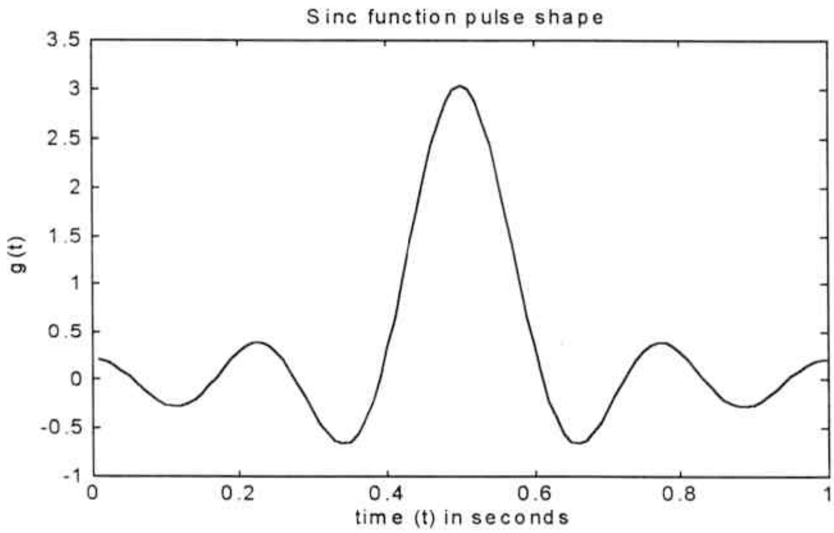

Figure 5-17 Impulse response of a sinc(4.5t) pulse shape filter

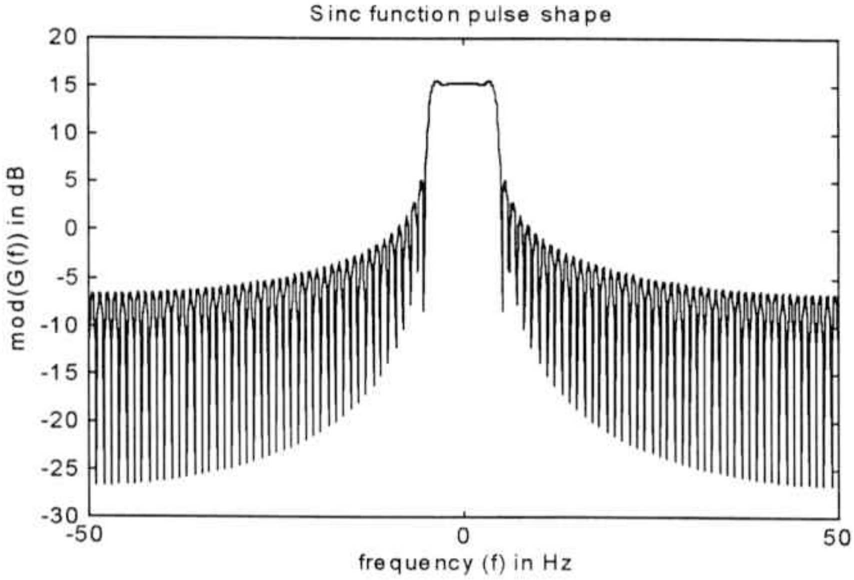

Figure 5-18 Frequency response of a sinc(4.5t) pulse shape filter

It can be observed in Figure 5-17 and Figure 5-18 that due to narrower time domain main lobe, the frequency domain main lobe is wider than the one of the previous sine function plotted. Besides, the original rectangular shape of the sinc function Fourier transform is better appreciated as the windowing in this case is less severe.

5.1.3.4 Windowed Pulse Shapes

Finally, the last group includes the products of all the previously described shapes. Hence, their Fourier transforms will be the convolution of the respective Fourier transforms. Many other windows and shapes could also be tested but improving the spectral characteristics of the pulse shapes is not the main goal of this project, and the presented basis has been considered to be enough to evaluate the effects of pulse shaping in a CDMA system. The example given for this group of shapes is a raised cosine main lobe pulse shape with a roll-off factor of 0.9, windowed with a triangular pulse. The result is plotted in Figure 5-19 and Figure 5-20.

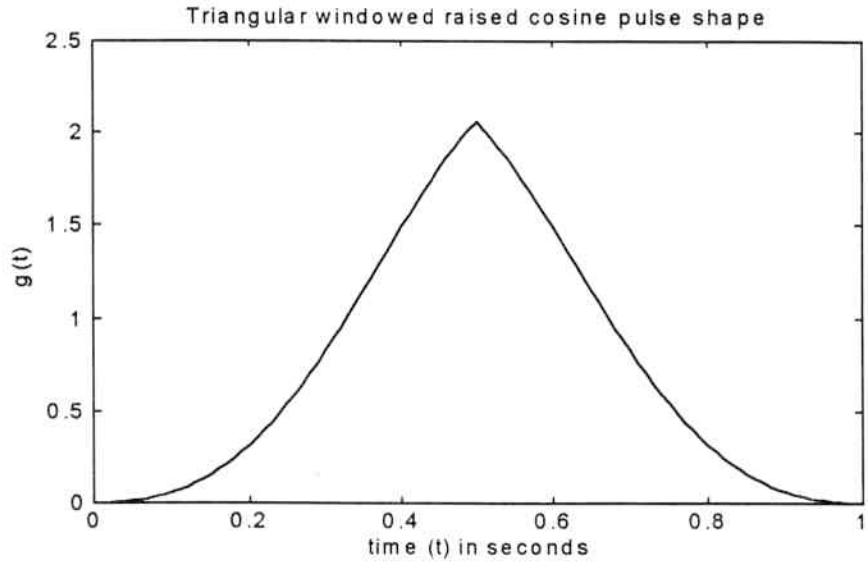

Figure 5-19 Impulse response of a triangular windowed raised cosine pulse shape filter

Figure 5-20 shows that the use of special windows can change significantly the spectral characteristics of some pulse shapes.

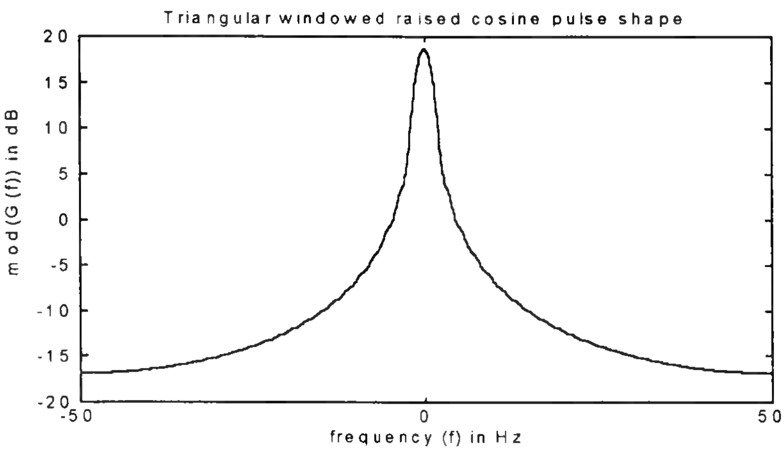

Figure 5-20 Frequency response of a triangular windowed raised cosine pulse shape filter

The case of a signal spread by a code sequence, can also be viewed as if its original pulse shape was windowed by the spreading code sequence. Therefore, the spread spectrum can be obtained by convoluting the spreading code Fourier transform with the original pulse shape spectrum. Figure 5-21 and Figure 5-22 show a random spreading code sequence of length 100 chips and its Fourier transform:

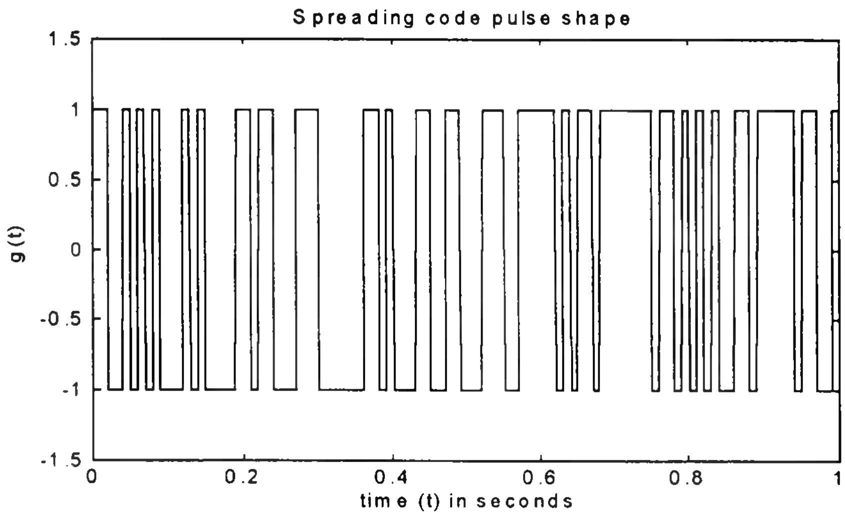

Figure 5-21 Spreading code sequence

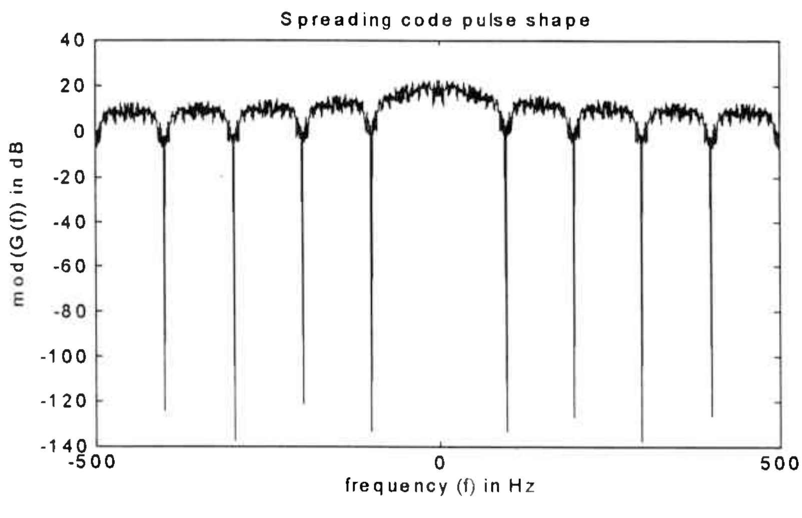

Figure 5-22 Discrete Fourier transform of a spreading code

As was expected, the spectrum of a code sequence is about 100 times wider than the one of a rectangular pulse.

5.2 Channel and Noise

It was explained in chapter 3 that a transmitted signal suffers four main degrading effects before it reaches the receiver antenna: attenuation, distortion, noise and interference. To model the first two effects, some measured real channels have been used. The simulated received signals have been obtained convoluting the channel impulse responses with the transmitted signals. Then, AWGN is added to the convoluted signal to simulate noise. Finally, the fourth effect, interference, will be only considered when measuring the performance of pulse shaping in DS-CDMA, where the multi-user interference is one of the main causes of error.

5.2.1 Channel modelling in a multi-user system

Chapter 3 explains in detail why multipath fading channels can be modelled by their lowpass equivalent time impulse response. The impulse response consists of a series of resolvable paths specified by their delay, gain and phase shift. The convolution of such channels with a signal, like the one described in equation (5.2), does not present major difficulties.

In a real multi-user system, every user transmits and receives from a different location and the paths between his terminal and the base station are totally different from the ones of another terminal. However, for simplicity and to save computation time, the simulations of CDMA in a multipath channel have been done using only one common channel for all the users. The impulse response of the common channel was obtained averaging all the impulse response profiles corresponding to the 75 locations within the same "local area" [Has1]. The averaging process is also explained in chapter 3.

Equation (5-2) represents the spread signal of one user. However, several users transmit instantaneously in a CDMA system and as a common channel is considered all the transmitted signals can be added together and convoluted. When adding all the signals it should be taken into account that in most of the real CDMA systems the different users' signals are not mutually synchronized. This is not reflected in equation (5-2), but it has two important consequences when the signals are added. First of all, the bit streams of the different users cannot have their origin at the same instant, and therefore, some random delays should be included in the signal description of equation (5-2). The distribution of the random delays be considered uniform in the interval $[0,T_s]$, as longer delays would only shift the random bit sequence. Besides, this fact will be the main reason to justify the multi-user interference reduction achieved by pulse shaping, as will be explained in the next chapter. The second consequence is the carrier waves phase reference. In chapter two it was mentioned that the carrier wave could also be written as $A\cos(\omega_c t+\phi)$ where ϕ is a random phase. For the case of only one signal, this random phase only affects the time or phase reference, and can be omitted. However, when different asynchronous signals are considered, every user should have a different random phase.

This last point has no particular effect in a real system, for the reason that the different users' paths are independent and their phase shifts are uniformly distributed in the interval $[0,2\pi]$, as was explained in chapter 3. Therefore the phase difference between the users' carrier phase does not affect this distribution. However, if a common channel is modelled, and the different users' signals are added together, this random phase should be considered.

If all the carrier waves were perfectly synchronized, all the I components could be added together to obtain the final I component, and the same addition could be done for the Q components. This is what has been done in the simulated model. It was considered that the complexity introduced by the carrier random phase would not contribute significantly to improve the reliability of the results. Actually, the fact that a common averaged channel is simulated is already an important simplification of the real system behaviour. Besides, as the effect of pulse shaping on the performance of CDMA is expected to be caused by the time shift between the different users' bit streams, the common channel and carrier random phase considerations should not affect the pulse shaping effect.

5.2.2 Noise

Noise can be modelled as an additive white Gaussian random variable, for the range of frequencies simulated in this project (a brief discussion is also given in chapter 3). A simple way to generate such a variable is to first generate a uniform deviate, and then apply a transformation method to change its pdf. One of these methods is the Box-Muller method, explained in [Pre]. According to this method, a Gaussian deviate can be obtained from the equation below:

$$y = \sqrt{-2\ln z_1}\cos(2\pi z_2) \tag{5-14}$$

Where z_1 and z_2 are two independent random variables uniformly distributed in the interval [0,1]. It is shown in [NR] that the pdf of y is Gaussian with a zero mean and a variance of one. The samples of AWGN have also a zero mean but their variance is the power of the simulated noise. However, the variance can be adjusted multiplying the Gaussian deviate with variance one (y) by the desired standard deviation.

Most of the results are presented in figures where the BER is plotted for different levels of noise. As was explained in chapter 2, the noise level is usually determined by the SNR or in the case of the curves of the next chapter by the ratio E_b/N_o. It is important to note that the signal bit energy has been measured at the receiver, which in the simulated model means the signal convoluted with the channel impulse response. The transmitted energy is not considered because the performance of the same MODEM in two channels with different amounts of attenuation could not be fairly compared.

5.3 Receiver

The aim of the receiver is to demodulate the received signal, decide whether the received bit is a zero or a one and try to recover the original message. It is exactly the same process that takes place in the transmitter but in reverse order.

The main structure of most of the receivers consists first of a filter, that should give a different output for each transmitted signal; followed by a sampler, to sample the filter output at the instant when the filter output is more influenced by the demodulated bit, and finally, a threshold device decides whether the transmitted bit was a zero or a one depending on the sampled value.

Chapter 2 explained that the filter implemented in the model of the receiver is a matched filter. As shown in [Car], in the case of time-limited pulses transmitted through an ideal channel with just AWGN, matched filtering is the best method to process the signal in order to remove the influence of noise without introducing ISI. The impulse response of a matched filter is given by:

$$h(t) = s_2(T_b-t) - s_1(T_b-t) \tag{5-15}$$

Where s_1 and s_2 are the signals corresponding to the logic states 1 and 0. A receiver capable of approximating in practice this impulse response is the so-called correlation receiver or integrate and dump filter [Sha]. It is depicted in Figure 5-23.

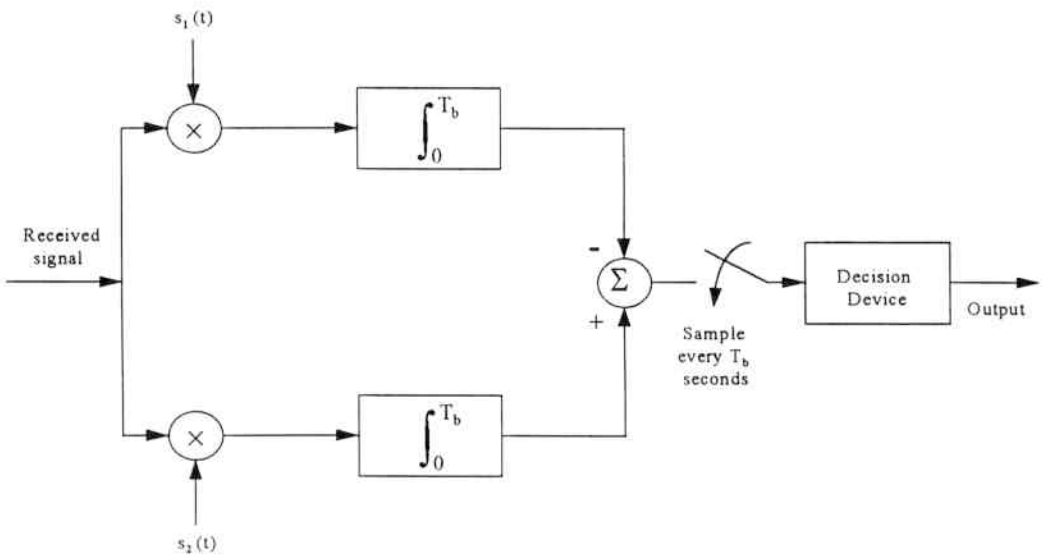

Figure 5-23 Correlation receiver

It is shown in Figure 5-23 that the correlated signal is integrated for one bit period, the sampling is carried out at the end of the integration and the threshold device makes its decision based on the instantaneous sampled value. This proceeding is optimum for ideal channels and signals time-limited to one bit period, however for other signalling schemes or for certain channels, more sophisticated methods could be implemented. For instance, some decision devices observe the signal for several bit periods before they make a decision.

Analysing the correlator receiver for the case of BPSK, it is possible to derive a simpler version. The signal s_1 is the same signal as s_2 but phase shifted 180°, in consequence the phase shift only changes the signal sign:

$$s_2(t) - s_1(t) = s_2(t) + s_2(t) = 2s_2(t) \tag{5-16}$$

Therefore the two branches of Figure 5-23 can be reduced to only one branch. The remaining signal does not have to be multiplied by two because the decision device has the threshold set at zero. If the integrator output is positive it decides that the transmitted bit was a 1 and if it is negative it decides a -1. Therefore any factor applied in the filtering process will not change the decision.

When a spreading code is applied to the signal, the signal should be despread before the lowpass filtering in order to concentrate the signal power in less bandwidth. In such way, the noise and the interference in the rest of the spectrum can be removed and the SNR is made as high as possible.

Besides, when a quadrature modulation method has been used in the transmitter, the first process that should be carried out is to separate the I from the Q carrier waves, as they have been codified with different sequences. This can also be done by two correlators. One in phase with the I carrier wave and the other in phase with the Q carrier wave. The reason is that the integral of the product of both waves (cos·sin) equals zero for a carrier wave period so only the influence of the same wave remains after the integration. Actually, the process of the I and Q components separation is not carried out in the program code because the signal is always simulated in the lowpass equivalent model with the real part corresponding to the I component and the imaginary part to the Q component.

As the carrier waves have already been correlated with the signal, before the signal integration is carried out, only the pulse shape has to be correlated with the despread signal. Finally, the original bit stream is recovered from the bipolar I and Q bit stream by a Bipolar-to-Unipolar converters (B/U) and a Parallel-to-Serial converter (P/S). In the OK-QPSK scheme, as the Q bit stream was delayed one bit period. a time delay should be introduced before the P/S in the I branch. In Figure 5-24 all the mentioned devices and processes are depicted.

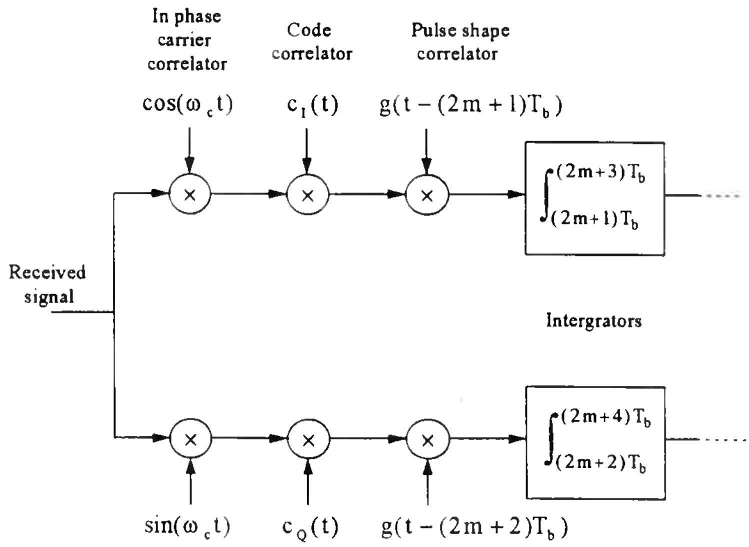

Figure 5-24a DS-CDMA OK-QPSK receiver model

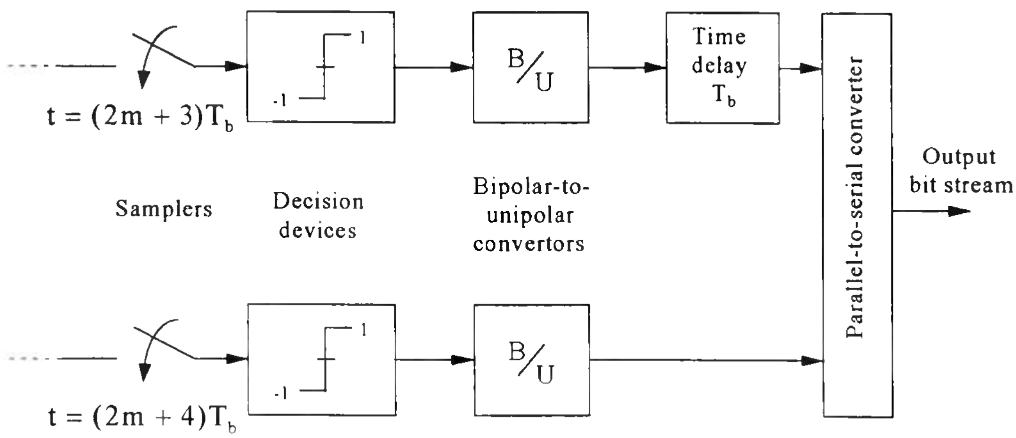

Figure 5-24b DS-CDMA OK-QPSK receiver model

Figure 5-24 does not show all the complexity involved in a real receiver. The model receiver is rather simple to implement because in the simulation program the timing and all the data used in the transmitter is also available in the receiver source code. Nevertheless, in the physical receiver, accurate synchronization with the received signal is needed in the correlators, the integrate and dump filter and the sampler. Besides the I and Q carrier waves cannot be as easily recovered as in the program. Special circuits have to be designed to achieve the required synchronization and to lock to the phase of the signal carrier wave. Small errors in the synchronization or in the carrier recovery circuits, can lead to a severe degradation of the system performance. In fact, all real receivers experience some phase recovery or synchronization error due to imperfections in the circuit. Therefore, the performances obtained with the simulations of this model might be difficult to achieve with a real receiver. In order to make the model closer to reality, some random phase or timing error could be introduced, however, it was considered that it would not improve the model capacity to test the pulse shaping effects.

As will be confirmed with the results in the next chapter, the modelled receiver is optimum for an ideal channel but in a strong multipath frequency selective environment its detection capabilities can be severely degraded. In addition to the ISI present in all the signals propagated through multipath frequency selective channels, one of the main causes of the experienced degradation is the fact that every path has an independent randomly distributed phase shift over the interval $[0,2\pi]$ as discussed in chapter 3. The tracking of the carrier wave phase can only be done to the signal propagated through one of the paths but cannot be done for all the received signals according to the preceding receiver description.

In chapter 3 it was also mentioned that some receivers lock to the strongest path signal (selection diversity), others to the first arriving signal, and RAKE receivers can lock to several paths at the same time. However, the model does not lock to any real path signal. It locks to a virtual LOS path signal presenting no phase shift. Certainly, the receiver model could be improved to achieve better BERs in multipath fading channels, but study and development of a better receiver for multipath environments was left for further research. It was also considered that locking to one of the path signals would improve the system performance, but would not suppose a great enhancement of the receiver capabilities because the phase shifts of the other signals would still be randomly distributed.

Besides the basic components described in this section, real receivers can also present some other devices and methods. For instance, a sequence known to the receiver can be transmitted periodically in order to estimate the channel impulse response, and an adaptive equalizer can be used to reduce the effect of the channel distortion. However, the studied model does not include any of them as they are not the object of this study.

5.4 Concluding Remarks

After the description of the transmitter, the channel and the receiver, it can be concluded that the considered model can be improved in many ways in order to make it more similar to a real CDMA communication system. However, even if the results obtained from the simulations can differ from real measurements, the effect of pulse shaping can be appreciated and well understood as will be seen in the next chapter. Besides, the model simplifications should not have a significant influence on the reliability of the conclusions derived from the results.

All the assumptions and descriptions explained in this chapter are reflected in the implementation of the simulation program included in appendix A.3.

6. RESULTS

This chapter exposes and discusses the results obtained by simulating the model described in the last chapter. The main goal of these results is to evaluate the performance of DS-CDMA in a multipath fading channel for different pulse shapes. However, before presenting the effects of pulse shaping in a DS-CDMA system, the results of several simulations for only one user will be shown. The purpose of these first simulations is to observe the influence of pulse shaping in multipath fading channels. Besides, one of the effects experienced in a simple single-user system will be useful to understand the promising results achieved by pulse shaping the bits of a DS-CDMA transmitter.

It has been mentioned several times in this report that the effect of pulse shaping would be measured simulating the transmission of bits and calculating the BER, however, it has not been justified yet why the chosen method has been simulation and not any other. The best method, from the accuracy point of view, is experimenting with real systems, but experimenting a multi-user system with different pulse shapes, would require a great amount of means and time. Another way is to analyse the problem from a theoretical point of view and intend to obtain the optimum pulse shape function. This method might be used for a very simple model, but the complexity introduced by an accurate model of multipath fading and DS-CDMA, makes the mathematical analysis of the problem quite difficult to manage. Simulation is a tool half way between real measurements and theoretical analysis. It allows a higher grade of complexity compared to a merely mathematical study, but it does not require the means involved with real measurements.
Besides, it was pointed out in the introduction, that digital systems can be better simulated on computers than the purely analogue ones.

Before explaining in detail every figure, some general assumptions about the procedure followed to obtain the results is going to be explained bellow:

The system performances have been compared plotting the BER obtained for different E_b/N_o ratios. For this purpose a high amount of bits were simulated to be transmitted, propagated through a determined channel and received by the correlator receiver. Then the output bits were compared with the input bits, and the errors were counted. At the end the error bits were divided by the total amount of generated bits and the BER was obtained. As in some simulations the BER takes very low values, the required number of generated bits was very high. Therefore, the computation time required to achieve high accuracy in the results was very long. It was considered that accuracy is not the main object of this work so one significant digit is enough to compare the effects of pulse shaping. This assumption is confirmed by the results, as pulse shaping improves the performance in some cases by several orders of magnitude.

In order to appreciate the general effect of pulse shaping on a certain system (with a determined MODEM, bit rate, or group of channels) two shapes have been simulated: the rectangular pulse, corresponding to the "non-shaped" case, and a main lobe sinc pulse, corresponding to the shaped case. For those systems presenting a significant performance enhancement with the sinc function pulse shape, more simulations have been carried out to determine the optimum pulse shape. The sinc functions was chosen to represent the general pulse shape because it is one of the most considered pulse shapes in the literature and besides, it shows a relatively good performance in all the cases where pulse shaping has some effect.

Finally, it should be mentioned that in most of the figures the performance of the system in an ideal channel has been plotted with a continuous line. This curve gives a reference of the best performance achievable and can also be useful to compare easily different plotted BERs. Besides, due to the similarity between the three simulated modulation schemes, their performance in an ideal channel is exactly the same and does not depend on the pulse shape. This issue was already discussed in chapter two.

6.1 Single-User Simulations

It was explained above that the first simulations have been done for only one user in order to understand the pulse shape effects in a simpler system. The three described methods (BPSK, QPSK and OK-QPSK) have been simulated at a bit rate of 1 Mbps and afterwards at 10 Mbps to observe better the effects of ISI. These bit rates have been chosen for three reasons. The first one is that transmission at several bit rates was simulated and it was seen that for 1 Mbps ISI did not degrade significantly the system performance, while for 10 Mbps important ISI effects were observed in some channels. The second reason is that 1 Mbps is a usual bit rate in some MODEMs. Finally, the studied time delay spread of the simulated impulse response profiles (see section 3.4.2) presented values in the order of several nanoseconds. A bit rate of 1 Mbps implies a bit duration of 1000 ns. Therefore,m it can be expected that for this rate there will be almost no influence of ISI. However, a bit rate 10 times higher should not introduce a great amount of ISI, because the bit duration would still be 10 times longer than most of the channel time delay spreads.

A possible explanation of why the performance is degraded at 10 Mbps is that the time delay spread is a good variable to be compared with the bit duration when the receiver locks at one of the strongest paths. Nevertheless, it was explained in the last chapter that the receiver modelled locks at a virtual LOS path with no phase shift. Therefore, when there is not a LOS path, the receiver starts correlating the received signal before the paths carrying the signal of the right bit have reached the receiver. In consequence, not only the time delay spread should be taken into account to predict the system performance, but also the average delay of the profile. When this average takes a relatively high value compared to the time delay spread, the corresponding location will probably present an obstructing object between the transmitter and the receiver antennas, and the obtained BER will be lower.

6.1.1 Pulse shaping average performance

The average performance has been calculated simulating all the 75 impulse response profiles of the studied local area, and then averaging the 75 obtained BER for every noise level. As it has already been explained above, these simulations have been carried out at a bit rate of 1 Mbps for the three considered modulation schemes, and considering only a rectangular and a sinc main lobe pulse shape.

The meaning of the line styles used in this section is listed below:

Modulation methods:

.... BPSK —— —— OK-QPSK — – — QPSK

Pulse shapes:

oooo Rectangular pulse shape **** Sine function pulse shape

The phases given in the channel profiles, are distributed from -90° to 90°. However, it is well known (a detailed explanation is given in chapter 3) that real path phase shifts are randomly distributed between the interval -180° and 180°. Therefore, it has been considered that the given phases are only distributed in this interval due to the process by which they were obtained, but they should be multiplied by two in order to make simulations as real as possible.

However, in Figure 6-1 the BERs obtained with the phase shifts distributed between the interval [-90,90] are plotted in order to understand better the effect that phase shifts have on the system performance.

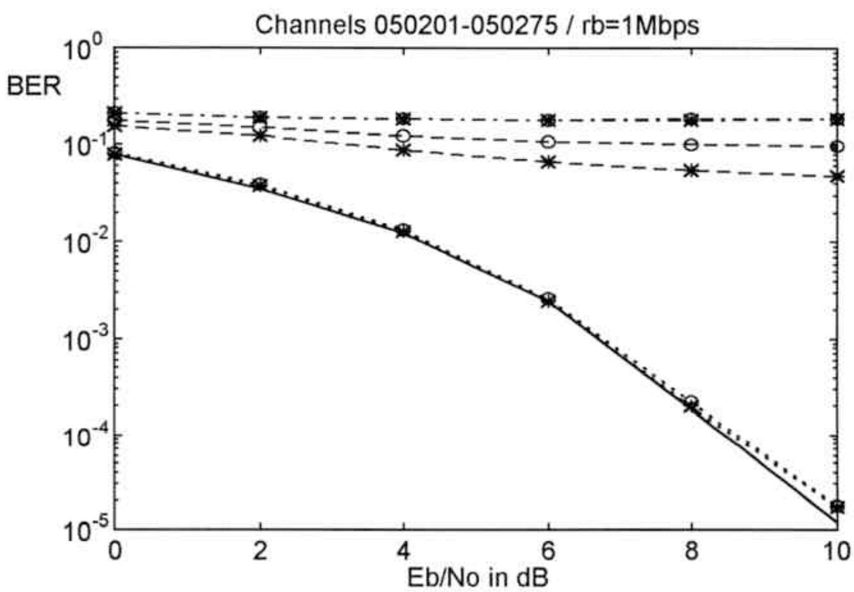

Figure 6-1 Average performance in channels presenting phase shifts in the interval [-90°,90°]

Figure 6-1 shows that when the path phase shifts are lower than 90°, the performance of BPSK is almost like the performance achievable in an ideal channel. However the BERs for QPSK take values near 0.5, which means that there is not any real detection as a random receiver could achieve the same BER. The performance of the third modulation scheme, OK-QPSK, is also very degraded but it is clearly better than the performance of QPSK. Besides, pulse shaping seems to have a positive effect.

The discussion below, will clarify the great difference observed between the performance of BPSK and QPSK and afterwards, the behaviour of OK-QPSK will be justified.

The output of the correlator receiver explained in the last chapter, could be geometrically viewed as the scalar product between the received signal vector and the originally transmitted signal, represented in the signal constellation diagram described in chapter 2. The reason is that the one period integral between to sinusoids is proportional to the scalar product between two vectors having the amplitude and phase of the sinusoids.

In BPSK when there is no phase shift, the received signal is in phase with the originally transmitted signal, so the correlator receiver output is maximum. As the phase shift increases, the scalar product decreases and when both signals are in quadrature, the output of the correlator receiver is zero. In fact, this is the principle of all quadrature modulation schemes. For phase shifts between 90° and 180°, the scalar product is negative and in the absence of noise, the correlator receiver would always decide that the output bit was the opposite of the transmitted bit.

The same reasoning may be applied to each correlator of the QPSK demodulator. The main difference is that due to the other carrier wave, the transmitted signal vector is already 45° shifted from both reference carrier waves. Figure 6-2 shows the QPSK constellation, already depicted in chapter 2, adding the received signal (s_r) in the case of a single path channel with a phase shift of θ_k:

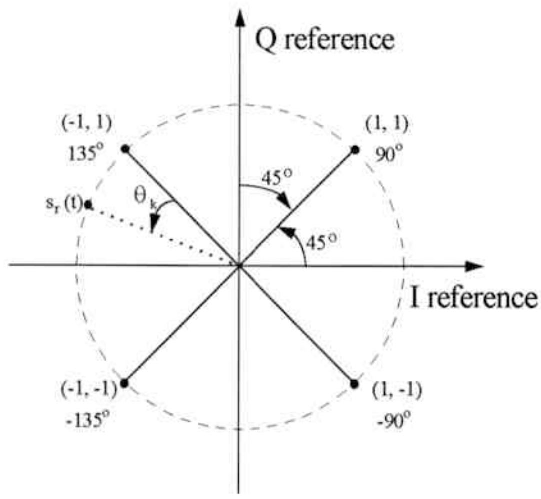

Figure 6-2 Path phase shift effect on the QPSK signal constellation

Therefore, for QPSK, phase shifts higher than 45° will already make the I or the Q correlator give the opposite output bit in the absence of noise, and phase shifts.

To understand the improvement experienced by OK-QPSK compared to QPSK and the effect of pulse shaping, some mathematical analysis based on the OK-QPSK modelled transmitter and receiver of last chapter will be needed.

First the lowpass equivalent equation for a transmitted OK-QPSK signal is going to be rewritten in equation (6-1) considering that the carrier wave amplitude equals one:

$$s(t) = s_I(t) + js_Q(t) = b_{2m}g\big(t-(2m+1)T_b\big) + j\big[b_{2m+1}g\big(t-(2m+2)T_b\big)\big] \tag{6-1a}$$

for $(2m+2)T_b < t < (2m+3)T_b$

$$s(t) = s_I(t) + js_Q(t) = b_{2m+2}g\big(t-(2m+3)T_b\big) + j\big[b_{2m+1}g\big(t-(2m+2)T_b\big)\big] \tag{6-1b}$$

for $(2m+3)T_b < t < (2m+4)T_b$

Where $s_I(t)$ is the I component of the transmitted signal, or its real part in the baseband equivalent, and $s_Q(t)$ the Q component. The rest of the terms have been explained in chapter 2. When this signal is propagated through a single path channel of gain one, delay zero and phase shift θ_k, the received signal is:

$$s_r(t) = \left(s_I(t)\cos(\theta_k) - s_Q(t)\sin(\theta_k)\right) + j\left(s_I(t)\sin(\theta_k) + s_Q(t)\cos(\theta_k)\right) \tag{6-2}$$

Equation (6-2) can be derived from multiplying equation (6-1) by the complex representing the phase shift, or by geometrical reasoning from Figure 6-2. Considering only the Q bit detection[1], the sampled value of the correlation receiver at $t = (2m+4)T_b$ will be the result of integrating the received Q component correlated with the pulse shape:

$$\begin{aligned}v_Q\left((2m+4)T_b\right) &= \int_{(2m+2)T_b}^{(2m+3)T_b} g\left(t-(2m+2)T_b\right)\left[b_{2m}g\left(t-(2m+1)T_b\right)\sin(\theta_k) + b_{2m+1}g\left(t-(2m+2)T_b\right)\cos(\theta_k)\right]dt\\ &+\int_{(2m+3)T_b}^{(2m+4)T_b} g\left(t-(2m+2)T_b\right)\left[b_{2m+2}g\left(t-(2m+3)T_b\right)\sin(\theta_k) + b_{2m+1}g\left(t-(2m+2)T_b\right)\cos(\theta_k)\right]dt\end{aligned} \tag{6-3a}$$

Where v is the Q integrator output. This equation can be rewritten as:

$$\begin{aligned}v_Q\left((2m+4)T_b\right) &= b_{2m+1}\cos(\theta_k)\int_{(2m+2)T_b}^{(2m+4)T_b}\left[g\left(t-(2m+2)T_b\right)\right]^2 dt\\ &+\sin(\theta_k)\left[b_{2m}\int_{(2m+2)T_b}^{(2m+3)T_b} g\left(t-(2m+2)T_b\right)g\left(t-(2m+1)T_b\right)dt\right]\\ &+\sin(\theta_k)\left[b_{2m+2}\int_{(2m+3)T_b}^{(2m+4)T_b} g\left(t-(2m+2)T_b\right)g\left(t-(2m+3)T_b\right)dt\right]\end{aligned} \tag{6-3b}$$

Which is equivalent to:

$$\begin{aligned}v_Q(2m+4) &= b_{2m+1}\cos(\theta_k)\int_0^{2T_b}\left[g(t)\right]^2 dt +\\ &+\left(b_{2m} + b_{2m+2}\right)\sin(\theta_k)\int_0^{T_b} g(t)g(t-T_b)dt\end{aligned} \tag{6-3c}$$

[1] Analogue results are obtained considering the I bit detection inverting the roles of the I and Q bit streams.

Following the same steps for the transmitted QPSK signal it can be derived that equation (6-3) for conventional QPSK is:

$$v_Q(2m+3) = b_{2m+1}\cos(\theta_k)\int_0^{2T_b}[g(t)]^2\,dt + b_{2m}\sin(\theta_k)\int_0^{2T_b}[g(t)]^2\,dt \tag{6-4}$$

The comparison between equations (6-3) and (6-4) will lead to the understanding of Figure 6-1. Both equations have two main terms: one term multiplied by $\cos(\theta_k)$ and another multiplied by $\sin(\theta_k)$. The first term contains the bit from the Q bit stream, which the Q correlation receiver is supposed to demodulate, and the other term contains bits from the I bit stream. To prove the coherence of these equations, two cases can be considered: first case is an ideal channel, where the phase shift would be zero (θ_k=0) and therefore the Q demodulation would not be influenced by the I bit stream. The second case, is a single path channel with a phase shift of 90°, where the value of the bit being demodulated will not have any effect on the integrator output, as the roles of the I and Q carriers would be inverted.

The main difference between both equations is that in equation (6-3) the second term contains two bits from the I bit stream, while in equation (6-4) only one bit appears; besides, the function integrated is not the same. The reason why offset keying improves the performance is that in equation (6-3) the two I bits are different, they cancel each other, and the term causing the interference from the I carriers becomes zero. In addition to this, the probability of a pair of consecutive bits being different is 0.5. Hence, the BER of QPSK in the absence of noise and for a channel with a phase shift of less than 90° should be decreased by a factor of two applying offset keying. This can be checked in the less noisy part of Figure 6-1.

On the other hand, the performance enhancement achieved by pulse shaping is due to the different integrated functions. In QPSK this function is the pulse shape filter impulse response to the power of two. As all the pulse shapes have been normalized in order to be energy equivalent, pulse shaping should not have any effect on the Q integrator output. However, in the case of OK-QPSK, the function integrated is the product of two pulse shapes shifted by a bit period. It can be easily calculated that for most of the shapes described in the last chapter, the result of the first integration in equation (6-3) is higher than the result of the second integration. Therefore the interference of the I bit stream in the Q integration output can be significantly reduced.

For instance, for a triangular pulse shape, the second integration is reduced a 50% of the value obtained for a rectangular pulse shape. Another example is a rectangular pulse shape time limited to only one bit period. In this case the second integral equals 0 and the BER can be the same as in an ideal channel for phase shifts in the interval [-90,90]. For higher phases the cosine would be negative and the output bits would have the opposite value of the corresponding input bit. This conclusion will be confirmed in section 6.1.3.

Before averaging the probabilities for every E_b/N_0 and every pulse shape, the values of the BER for each channel were analysed. An important amount of inhomogeneity was observed. In some cases there were even differences of several orders of magnitude for the same conditions. In consequence, the average of the BER obtained for each of the 75 simulated channels is not an optimum measure of the global performance of the system in that location. Actually, the calculated average gives a pessimistic measure of the real performance. The next example will clarify this last statement:

Supposing that instead of 75 channels, the simulation consists only of ten different impulse response profiles, and that, for certain conditions, in 9 of this ten profiles the obtained BER is 10^{-5}, but in the other channel only 10^{-2}, the resulting average probability would be of about 10^{-3}. However, if instead of 10^{-5}, for the nine profiles a BER of 10^{-4} was obtained, the probability would be of the same order. This example proofs that the most degrading channels have much more influence on the average BER than the better ones. Therefore in the next subsections, those profiles having similar characteristic will be grouped, and an average BER probability will be given for each group. This values will be more meaningful than a total average and at the same time the inhomogeneities between the 75 profiles will be shown.

To end this section, two more figures are given to confirm the hypothesis considered to justify the better performance of BPSK compared to the one observed for QPSK.

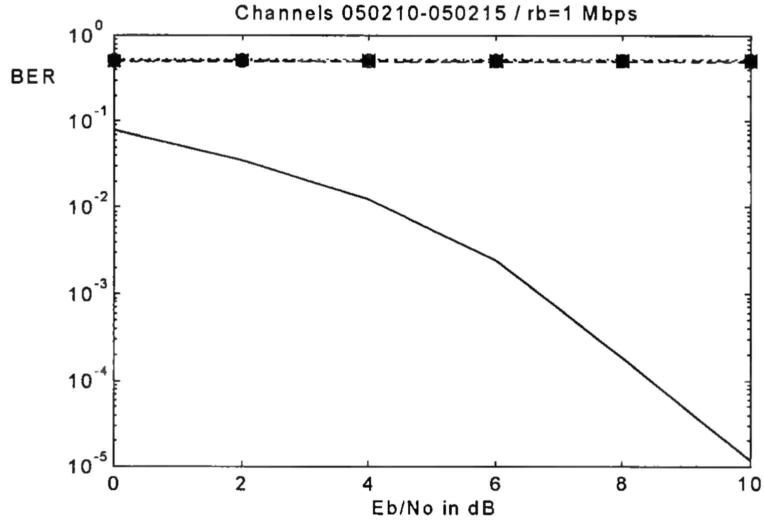

Figure 6-3 Average performance in channels presenting phase shifts in the interval [-180°,180°]

Figure 6-3 shows that the BPSK performance is also severely degraded for phases distributed in the whole interval. This result could be expected according to the explanation given above.

The performance of BPSK in Figure 6-1 is almost as the performance in an ideal channel, therefore it is obvious that ISI does not have an important influence for the simulated bit rate. However, to illustrate this fact, the model was simulated under the same conditions but artificially considering that all the phase shifts equalled zero. The result is shown below in Figure 6-4:

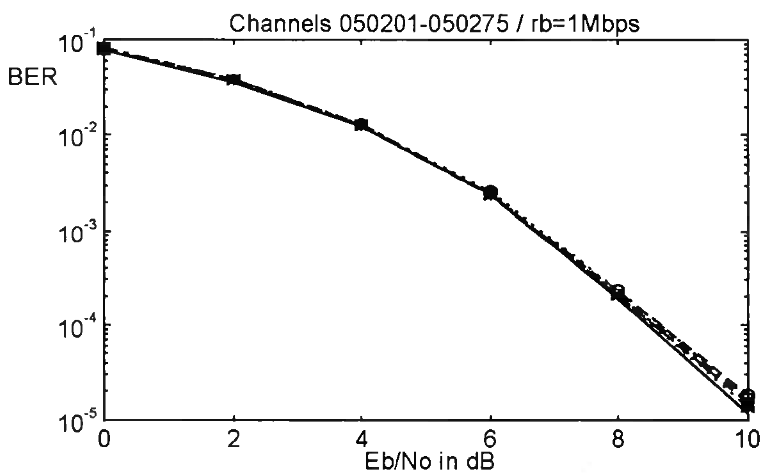

Figure 6-4 Average performance in channels with no phase shift

It can be definitely concluded from this last figure that none of the modulation methods is seriously affected by ISI at a bit rate of 1 Mbps. This fact was already foreseen in the beginning of section 6.1. However, the error due to the phase shifts makes an acceptable detection almost impossible for the modelled receiver. As was anticipated in the receiver description, a more sophisticated receiver should be implemented to achieve better performances in multipath environments.

6.1.2 Pulse Shaping as an ISI counter measure

This section intends to review the known use of pulse shaping to reduce the effects of ISI. For this purpose the bit rate is risen up to 10 Mbps as was mentioned in the introduction of section 6.1. All the Figures of this section were obtained with the same assumption considered before in Figure 6-4, the path phase shifts will not be taken into account in order to appreciate only the degradation caused by ISI.

Last section made clear that the different performances achieved by QPSK and OK-QPSK are due to the different influence that the interference between the I and Q carriers in the presence of multipath phase shifts has on both schemes. Hence, when no phase shifts are considered, identical performances are obtained and only the BERs of BPSK and QPSK are plotted in this section.

First the average performance in the 75 channels corresponding to the same local area, for a bit rate of 10 Mbps is given in Figure 6-5.

Modulation methods:

.... BPSK — — — QPSK

Pulse shapes:

oooo Rectangular pulse shape **** Sinc function pulse shape

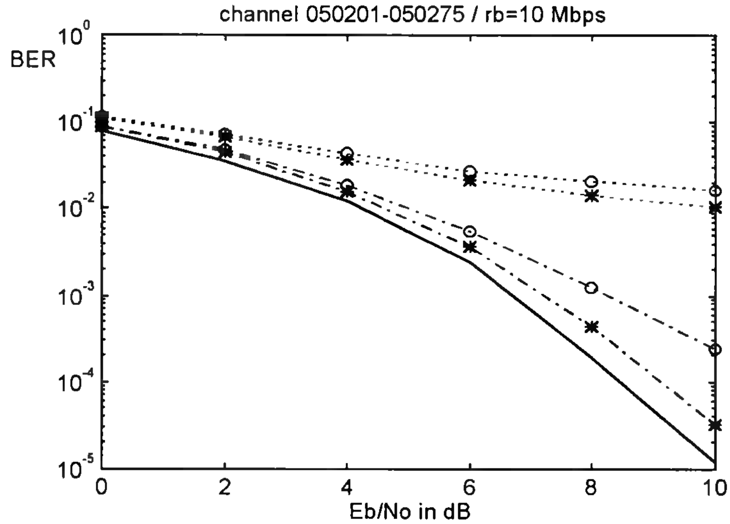

Figure 6-5 Average performance in channels with no phase shifts for a bit rate of 10 Mbps

A great difference between the performance of QPSK and BPSK is observed in Figure 6-5. This is due to the fact that in QPSK the symbol duration is twice the bit duration and consequently the influence of previous symbols is not so important. As was expected, the effect of pulse shaping is clearly appreciated when the bit rate is high enough to introduce some ISI. Specially when the performance is still not too degraded, pulse shaping can decrease the BER in almost one order of magnitude for an E_b/N_o of 10 dB. Another way to measure the performance enhancement is by calculating the energy that could be saved for a determined BER. For a BER of 10^{-4} it can be predicted that at least 2 dB could be saved which means that the transmitted power could be reduced almost 37%.

To illustrate the variance observed between the obtained BERs for similar conditions but in different channels, the impulse response profiles corresponding to locations 57-62 have been simulated for a bit rate of 20 Mbps. The results have been plotted in Figure 6-6. Table B-1, in appendix B, shows that the selected channels have a delay of about two nanoseconds, which is very low considering that the resolution time is 5 ns.

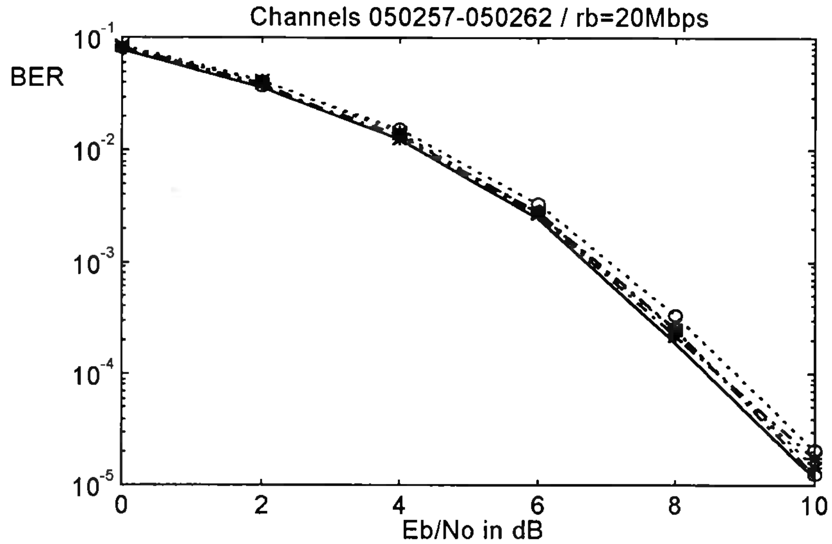

Figure 6-6 Performance in channels with low time delay spreads and with no phase shifts for a bit rate of 20 Mbps

Figure 6-6 gives evidence of the already mentioned inhomogenity between the 75 tested profiles. Even if the bit rate has been doubled (compared to Figure 6-5), the performance in these channels is still close to the one achieved for an ideal channel. This plot also confirms the influence of the time delay spread on the experienced ISI. Although the curves are all in the same region, the improvement achieved by pulse shaping and by QPSK can still be appreciated.

The last part of this section is devoted to the optimization of a pulse shape in order to reduce the effect of ISI. A mathematical aproach to the problem is quite complex and there is not a general optimum pulse shape, because the pulse shaping performance depends on the channel impulse response. Therefore several kinds of shapes have been simulated in a rather homogeneous group of channels (68-78) and for a bit rate of 10 Mbps. These channels have relatively high delay spreads (see Table B-1) so that the effect of pulse shaping is more clearly appreciated. A very important remark that should be given at this point, is that the results of this optimization will only give an idea of those shapes performing better in these concrete kind of channels.

As no phase shifts are considered, the curves obtained for QPSK could also be obtained simulating BPSK at a double bit rate. Therefore only the BPSK BERs have been plotted. It should be noted that in order to distinguish better the performances of each pulse shape, the E_b/N_o

range has been extended up to 12 dB. The pulse shapes have been grouped according to the analysis in chapter 5. The performances for each pulse shape are compared below:

In Figure 6-7 the triangular and sinusoidal pulse shapes are compared with the rectangular pulse shape that represents the non shaped case. The correspondence between line styles and pulse shapes is illustrated below:

·················· Rectangular —— ——Triangular — — — Sinusoidal

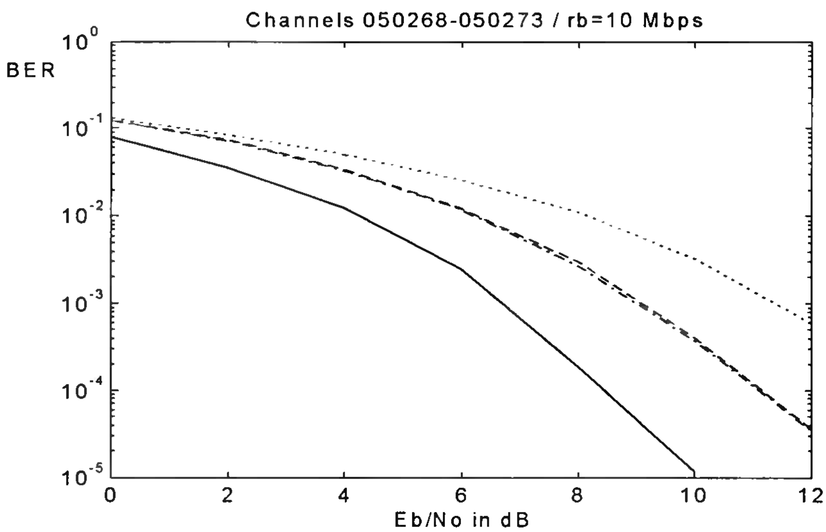

Figure 6-7 Reduction of ISI effects by triangular and sinusoidal pulse shapes

This figure gives evidence again of the performance enhancement achieved by pulse shaping for certain channels and bit rates. It is confirmed that the BER can be decreased for low noise levels more than an order of magnitude, and that the percentage of saved energy for a relatively low required BER, might be almost a 50%. Finally, the result of the comparison between triangular and sinusoidal pulse shapes is that their performance is almost the same, and according to this plot, the sinusoidal pulse probably performs better. As the optimum pulse shape depends on every channel, the purpose of this comparison is to give an idea of the best pulse shapes but not to determine the optimum with high accuracy. Therefore no further simulations where done. Besides, spectral characteristics of the sinusoidal pulse shape are better than the ones of the triangular pulse shape, according to the analysis of the last chapter, so it can be already stated that the sinusoidal pulse shape would be better for this conditions.

Figure 6-8 compares four different Gaussian pulse shapes. The simulations were done for the same conditions described above. The values of the parameter λ corresponding to each line style are listed below:

················λ=0.7 —— ——λ=0.9 — – —λ=1

··O·······O· λ=1.1

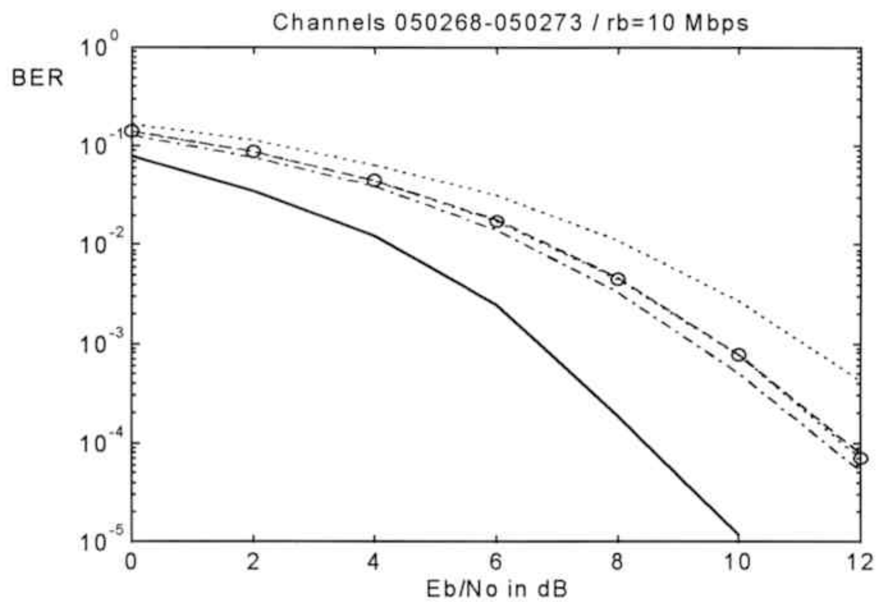

Figure 6-8 Reduction of ISI effects by Gaussian pulse shapes

From this figure, it seems that narrowing the pulse shape improves the performance of the system, but when the shape is too narrow, the BERs increase again. In Figure 6-8 this phenomenon is reflected in the better performance achieved by the Gaussian pulse shape with $\lambda = 1$ compared to the performances of the shapes corresponding to $\lambda = 1.1$ (a wider shape) and $\lambda = 0.9$ (a narrower shape). The case of $\lambda = 0.7$ shows how the BER can rise by decreasing the pulse time domain width. The other extreme would be the rectangular or non shaped pulse, that has already been commented above. Further simulations could determine the exact optimum value of λ, but as explained before, it is not the purpose of this section.

Figure 6-9 shows the BERs curves for three different raised cosine main lobes pulse shape for the conditions of the previous two figures. The values of the simulated roll-off factor are:

ρ = 0 (sinc) ρ = 0.6 ρ = 0.9

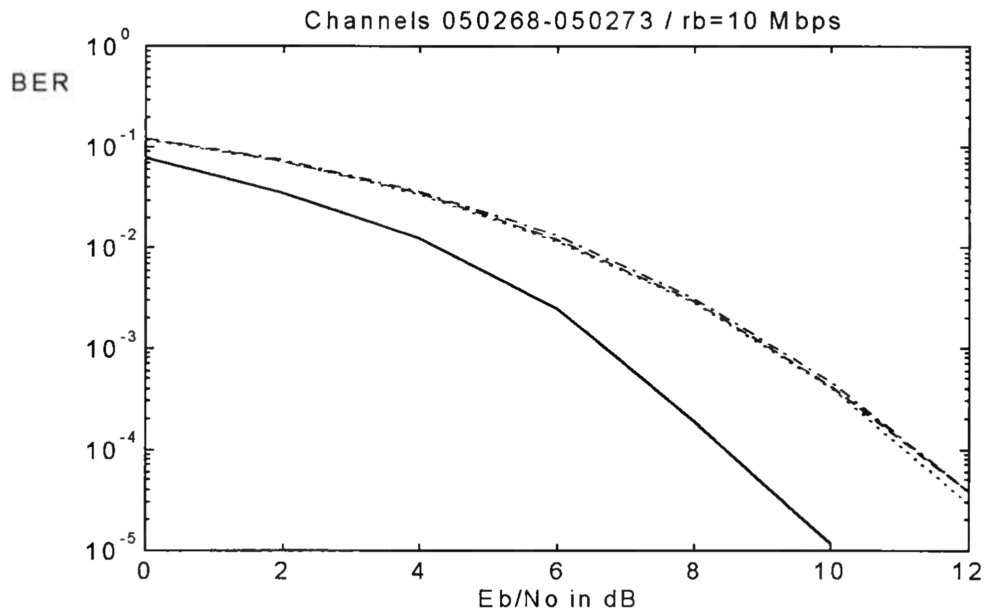

Figure 6-9 Reduction of ISI effects by raised cosine pulse shapes

Due to the similarities observed in the last chapter between all the raised cosine pulse shapes, their performances also resemble each other. It seems that the sine function achieves lower BERs and when the roll-off factor is increased the performance is slightly made worse. Their spectrums do not show important differences either so any of the shapes could be selected. However, maybe the sinc function would be the best choice as it has a lower amplitude as shown in Figure 5-15. High amplitude peaks require amplifiers with a larger linear range.

In Figure 6-10 three windowed or pulse shape products are considered. The selection includes shapes that achieved low BERs in the previous three figures:

················Triangular x ·sinc —— ——sinc x ·sin — – — $\sin^2$

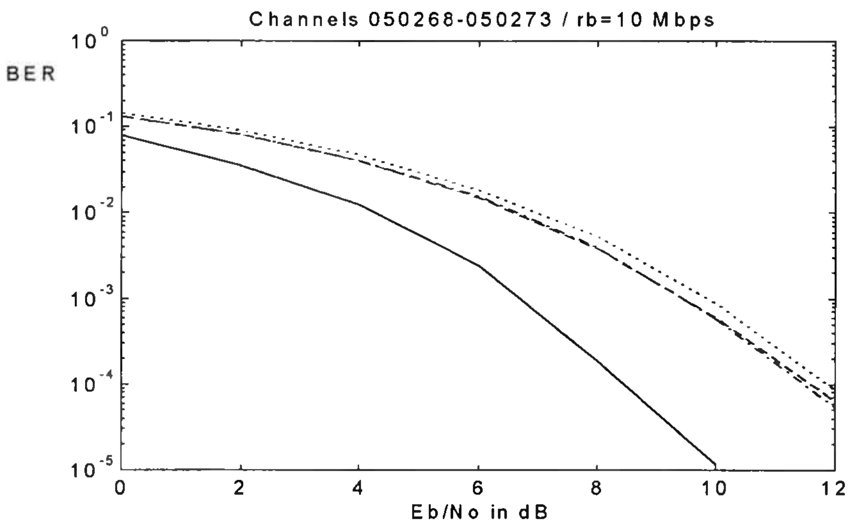

Figure 6-10 Reduction of ISI effects by windowed pulse shapes

The sinc function and the sinus function windowed by a sinusoidal half period, perform better than the sinc function windowed by a triangular pulse shape. However, between both functions windowed by the sinusoidal half period, the difference is not so clear. Maybe the sinusoidal pulse shape to the power of two, performs slightly better.

Finally, the best shapes of each group have been replotted together in Figure 6-11 to determine which kind of shape is the most suitable for this kind of channels.

················sinusoidal —— —— Gaussian (λ=1) — – — sinc

··O·······O· $\sin^2$

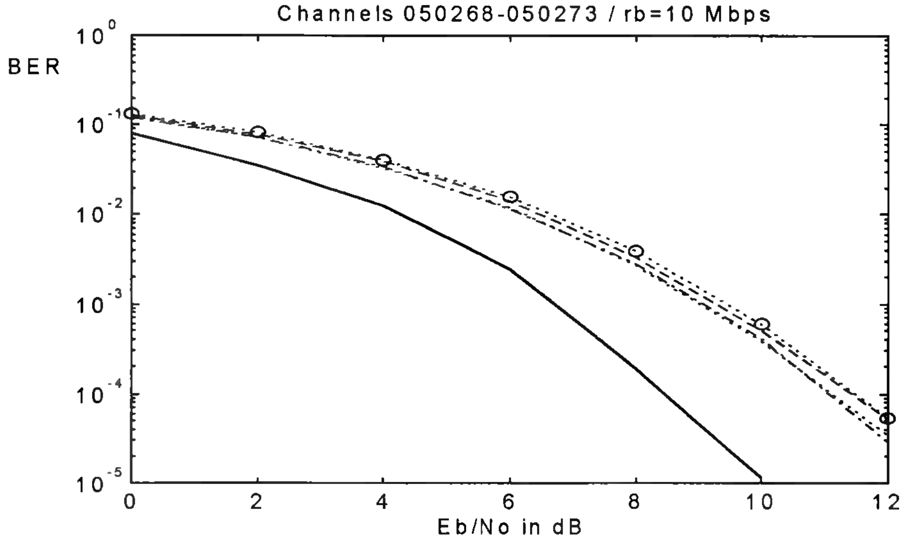

Figure 6-11 Reduction of ISI effects by the best pulse shapes

The most relevant aspect of Figure 6-11 is the similarity between all the curves. Even if their nature is completely different, the performance of the four shapes is almost the same. The sinc and sinusoidal functions are the ones achieving lower BER, with a small advantage for the sinc function. The example given for the Gaussian shape performs slightly worse but better than the sinusoidal pulse to the power two.

Completing the discussion with a comparison in the frequency domain, the sinusoidal and sinc function pulses would still be one of the best choices. On the other hand, the Gaussian shape with $\lambda=1$ does not have such a good frequency response as shown in Figure 5-14. For this reason in third place when spectral criteria is added, the best decision would be the windowed sinusoidal function.

After this comparison it can be concluded that all the pulses with shapes similar to the sinusoidal half period, can reduce the BER by at least one order of magnitude for low noise levels. In this group are included all the raised cosine shapes, and with less resemblance but also relatively good performances, the triangular pulse shape, Gaussian pulse shapes with its parameter around 1 and some windowed pulse shapes.

6.1.3 The effect of pulse shaping in OK-QPSK

In section 6.1.1 it was shown and explained that OK-QPSK performs better than QPSK in channels having phase shifts distributed in the interval [-90°,90°]. Besides, pulse shaping can reduce considerably the BER according to equation (6-3c). In this section this last point is going to be studied in more detail and the optimum shapes will be exposed as in the last section.

The study is going to be based on another group of profiles. The channels corresponding to locations 10 to 15 of the same local area. These profiles where selected because their phase shifts are not constrained to the interval [-90°,90°] but take, in most of the paths, low values.

This comparison could be not extrapolated to most of the real channels as their phases are uniformly distributed in the interval [-180°,180°] according to most of the models considered in the literature. However, when some kind of phase lock device is used, the receiver behaviour is equivalent to that of a receiver without phase tracking (as the one modelled in this project) but with virtual phase shifts. This virtual paths phase shifts equal to the subtraction of the real phase shifts and the estimated phases by the phase lock device. Therefore the virtual phase shifts will probably have an absolute value smaller than 90°. For this reason, this section can be meaningful for OK-QPSK receivers having relatively high phase lock error but always within the interval [-90°,90°].

First, a general comparison between the pulse shaped modulation schemes is done again but for the specific case of the considered group of channels. Then the pulse shape is optimized for the case of OK-QPSK.

The meaning of the line styles for Figure 6-12 is described below:

Modulation Methods:

.... BPSK —— —— OK-QPSK — – — QPSK

Pulse shape:

oooo Rectangular pulse shape **** Sinc main lobe pulse shape

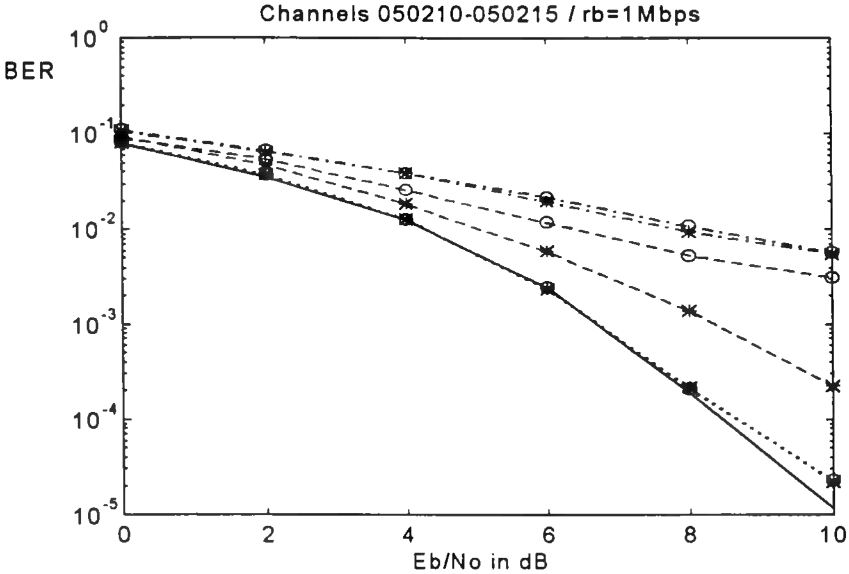

Figure 6-12 Performance of several modulation schemes in channels having low phase shifts

This figure confirms that BPSK performs better than QPSK in low phase shift channels, and that pulse shaping only improves slightly the performance due to the reduction of the ISI effects. Offset Keying reduces the BER of QPSK and pulse shaping can achieve extremely good performances as will be concluded at the end of this section.

In order to determine the width of the pulses achieving better performances, several Gaussian pulse shapes were first tested. The results are plotted in Figure 6-13 and the line styles are matched with the correspondent parameters below:

·················λ=1.1 —— ——λ=0.9 — – —λ=0.3

·o···o····o··λ=0.1

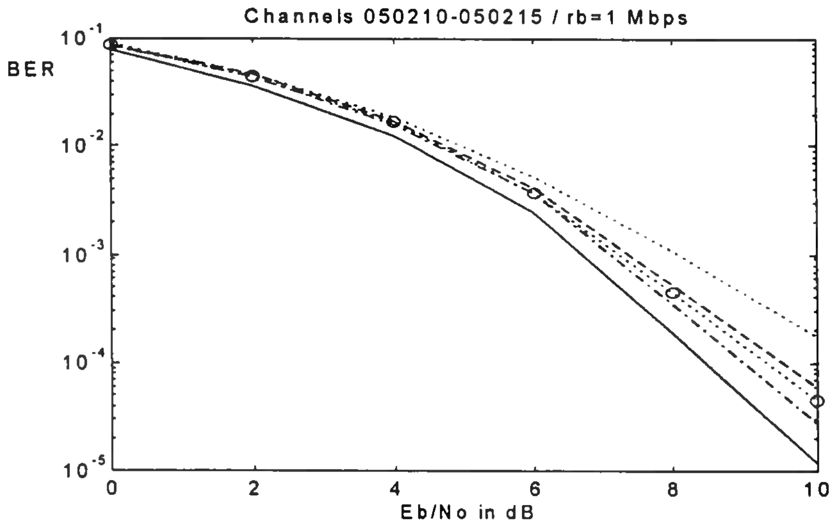

Figure 6-13 Performance of Gaussian pulse shapes in channels having low phase shifts

It is clearly observed in this figure that the narrower the pulse width (from λ=1.1 to λ=0.3), the lower the obtained BERs. However, when the pulse width is less than 50% of the symbol period, like the case of λ=0.1 (see Figure 5-11), the performance is not so enhanced.

The reasons can be found in the already given arguments. The initial reduction is due to the minimization of the integration of $g(t)g(t-T_b)$ during a symbol period. As was explained in section 6.1.1, for a rectangular pulse shape of only one bit duration, the result of this integration is zero. The Gaussian pulse shape with λ=0.3, has approximately a time width of one T_b (see Figure 5-11) while for λ=0.1 the width is less than $T_b/2$. For time widths less than one T_b, the integral obviously also equals zero but less signals carrying the demodulated bit are being correlated before the integration. Therefore the power of the filtered signal decreases degrading the performance.

For completeness, the BERs obtained for some other pulse shapes are compared in Figure 6-14.

··················sin	—— ——sinc	— – —triangular
o····o····o·sin^2	-+--+--+ sinc(4.5t)	-o—o—o- rectangular

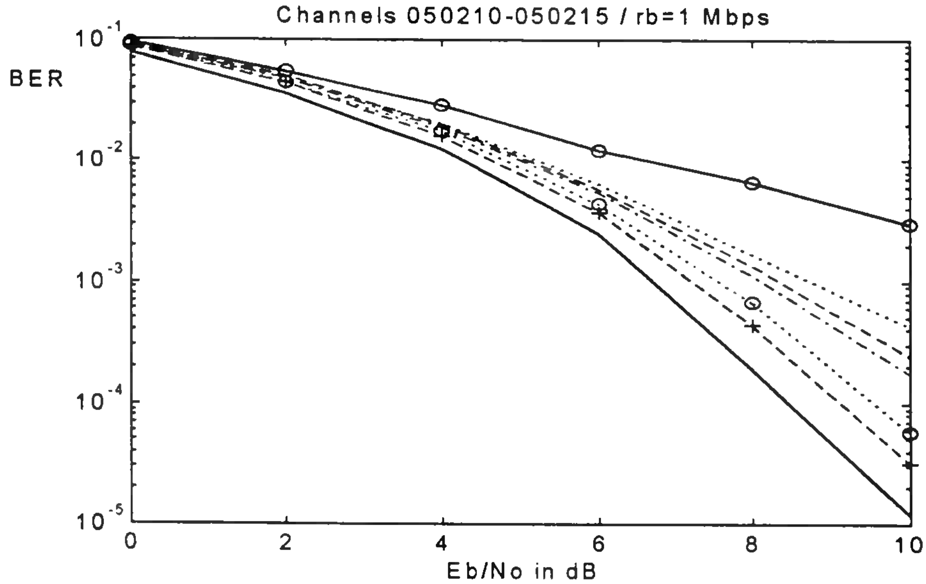

Figure 6-14 Performance of several pulse shapes in channels having low phase shifts

Again, the shapes having their energy more concentrated in a short period, perform better than shapes with their energy more uniformly distributed in the whole period, as the non shaped case. Therefore the lowest BERs are obtained for the sinc(4.5t) pulse shape. Ordered from the best to the worst performance, the tested pulse shapes would be sinc(4.5t), $\sin^2$, triangular, sinc, sin and rectangular. This results are in accordance with the results obtained by reducing the CDMA multi-user interference with chip shaping in [Cha].

It should be remarked that the best shapes of the two last figures achieve BER two orders of magnitude below the BER obtained by a rectangular pulse shape in some low noise levels. Comparing the sinc(4.5t) pulse shape and the best Gaussian pulse shape, the Gaussian shape performs better. Nevertheless, this result is not reliable as the scaling parameter in the first case and λ in the second case were not really optimized. Besides, the bandwidths of all these shapes should be calculated in order to select the best pulse shape.

It should be noted that OK-QPSK is actually MSK as was explained in chapter 2. And as the sinusoidal pulse shape is not optimum, some extra shaping could be added to improve the performance. However, the MODEM would not be anymore MSK in the strict sense.

In fact, the sinusoidal pulse shape has the property of conserving the constant envelope of the non shaped case, making MSK even more suitable for transmission using non linear amplifiers. Consequently, in some applications where the phase lock error is not as important as a constant envelope, sinusoidal pulse shaping might be a recommendable solution.

6.2 Multi-User Simulations

The main goal of this report is to discuss the effects of pulse shaping in a DS-CDMA system. The key to this issue is found in chapter 4, chapter 5 and in the last section. One of the conclusions of chapter 4 is that the capacity of DS-CDMA is limited by the multi-user interference, and that this interference is proportional to the cross-correlation between the generated codes. In chapter 5 was mentioned that pulse shaping CDMA could also be viewed as spreading the signal with a multi-level code (see Figure 5-2). Finally, in the last section, one of the effects of ISI was justified by stating that the result of:

$$\frac{\int_0^{T_s} g(t)g(t-T_b)dt}{\int_0^{T_s}[g(t)]^2 dt}$$

can be made zero by pulse shaping.

This expression is actually very similar to the definition of the auto-correlation in equation (5-1). If the pulse shape function is made discrete by sampling it every T_c and instead of both functions being shifted T_b they are shifted by wT_c, this expression becomes the definition of the auto-correlation of function g(t), which is denoted by R(w).

If instead of g(t), the auto-correlation is calculated for g(t)c(t) (where c(t) is the code sequence), the expression will be exactly the auto-correlation of the pulse shaped code sequence. And finally:

$$R(\tau) = \frac{\int_0^{T_s} g(t)c^1(t)g(t-\tau)c^2(t-\tau)dt}{\int_0^{T_s} [g(t)]^2 dt}, \qquad (6\text{-}5)$$

where $R(\tau)$ is the cross-correlation function for a delay τ (which unlike w can take any real value, instead of only integers) and $c^1(t)$ and $c^2(t)$ are two different codes. If both codes are equal, the ross-correlation function is in fact the auto-correlation function.

Therefore, it can be already stated, that the main effect of pulse shaping in a DS-CDMA system will be the reduction of the spreading code correlation properties. It can also be foreseen, that the reduction will be more important for those delays near the half symbol duration.

The interference between two users is highly related to the cross-correlation of their codes given by equation (6-5) with τ being the time shift between their bit streams. In consequence, if pulse shaping reduces the values corresponding to some delays of the cross-correlation function, the performance of a DS-CDMA system will be probably enhanced. Another fact derived from this reasoning is that the pulse shape effect will depend on the delay between the users. In real DS-CDMA systems the users' signals are not synchronized, so their delays are random. However, all the simulations have been carried out synchronizing the users in the optimum way to achieve interference reduction by pulse shaping[2]. The plotted BERs intend to show the maximum performance that could be obtained by pulse shaping and not the average performance in a real system. Besides, to give the average performances, the simulations would take much longer, and the differences between the effects of several pulse shapes would not be so clearly distinguished.

All the previous arguments do not depend on the nature of the system channel. Hence, the pulse shaping effects will be first analysed in an ideal channel and finally some results will be given for a multipath fading channel. As was mentioned in the last chapter, all the simulations have been done considering a code length of 100 chips. It should be noted that due to the variations of the cross-correlation function of the random generated codes, the performance might change slightly depending on the generated spreading code.

[2] For this purpose the users' time references should be uniformly distributed in a symbol period

6.2.1 Interference reduction in an ideal channel

In order to confirm the theory discussed above, BPSK has been simulated first for several number of users and with rectangular and sinc main lobe pulse shapes, and afterwards for 12 users and for several pulse shapes. Other modulation schemes were not simulated as in chapter 2 it was made clear that their BERs are identical in ideal channels.

Figure 6-15 shows how the multi-user interference degrades the performance of a DS-CDMA system. It can be appreciated that for 12 users a high level of power is required to achieve BERs below 10^{-3}. For this study, the most important aspect of this figure, is that in all the three cases, a significant BER reduction is observed when the pulses are shaped. This effect is more evident for the system with 8 users. The reason might be that for 4 users the BERs take already relatively low values, and for 12 users the effect is not so important because the separation time between the users' references is shorter.

Number of users:

.... 4 users —— ——8 users — – — 12 users

Pulse shape:

oooo Rectangular pulse shape **** Sinc main lobe pulse shape

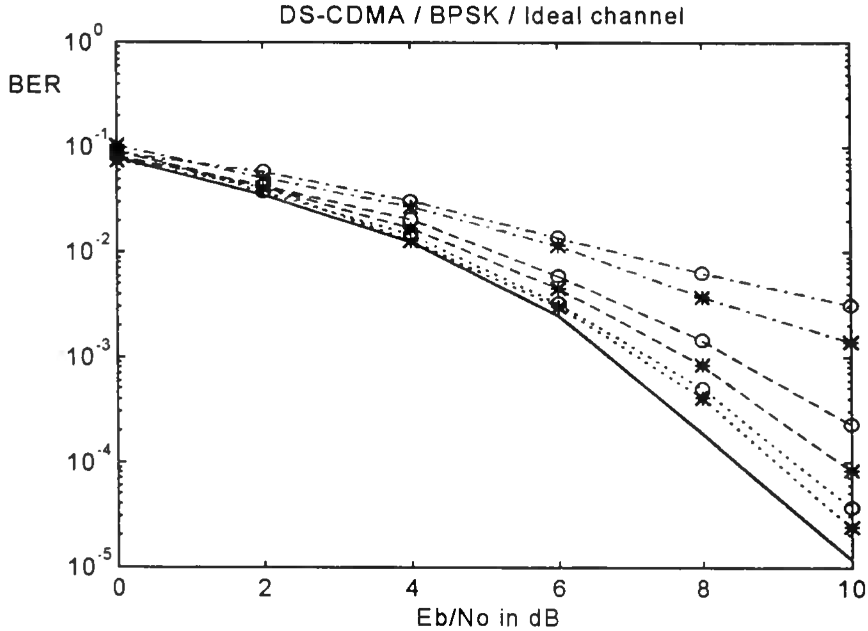

Figure 6-15 Maximum performance enhancement of DS-CDMA in an ideal channel by a sinc main lobe pulse shape

According to the conclusions derived before, pulses having their energy concentrated in a short period of time should perform better, so the shapes that present this property have been simulated[3]. The number of users chosen for this simulation is 12 as the improvement margin is very wide.

The line styles of Figure 6-16 are indicated below:

················ Gauss (λ=0.5) —— ——Gauss (λ=0.3) — — —Gauss (λ=0.1)

·o···o····o··sinc(4.5t) -o—o—o- rectangular

[3] The widths of the simulated pulses are compared in figures 5-11 and 5-17.

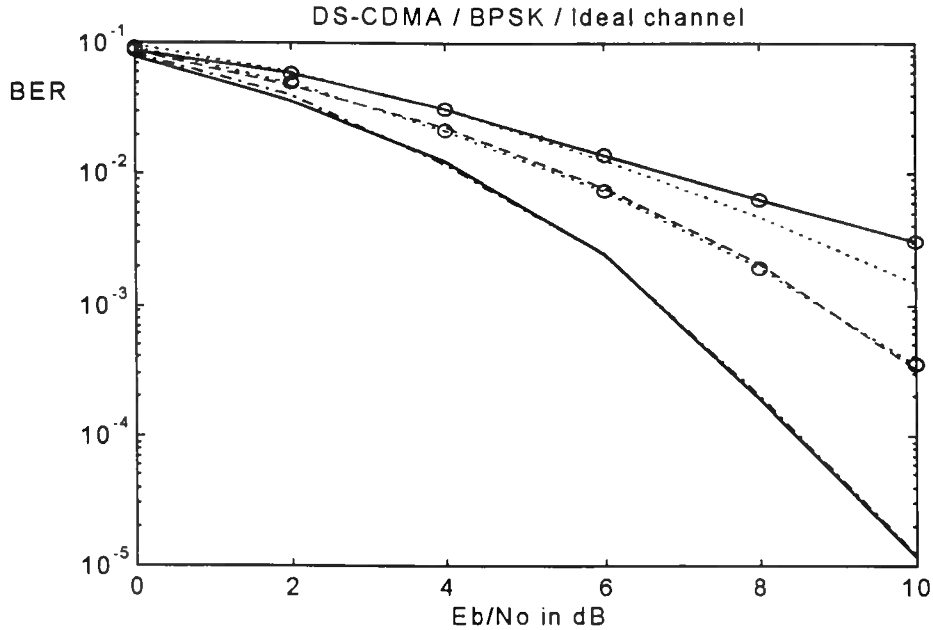

Figure 6-16 Maximum performance enhancement of a DS-CDMA system with 12 users in and ideal channel by different pulse shapes

The previous theoretical reasoning is confirmed by this figure. The narrower the pulse width the better the obtained performance. Unlike the case of OK-QPSK in multipath channels discussed in section 6.1.3, when the pulse lasts for a low percentage of the total symbol period, the BER does not rise again. The reason is that ideal channels have no delay and the received signal is always perfectly correlated.

It should be remarked that this promising results can only be achieved with a perfect synchronization between all the users. The problem is that while the cross-correlation functions achieves extreme low values for values around half of the code length, it takes higher values for low or very high delays.

This can be understood with the help of a simple example. Considering that the pulse width is limited to one chip, the cross-correlation function would equal always zero except for the value corresponding to zero delay, which would equal one.

Two main characteristics of the cross-correlation function should be taken into account in order to compare them: the maximum peak value and the average value. It is clear that the peak value rises when the pulse is narrowed. However, it is not so easy to predict the value of the average cross-correlation.

To compare better the performance of every pulse, the peak values observed out of 10^5 different codes, and the calculated average values are shown in the table below. The data has been obtained by executing the cross-correlation program mentioned in the last chapter and listed in appendix A.1.

Table 6-1 Cross-correlation peak and average values of different shaped codes

Pulse shape	Peak value	Average value
Rectangular	0.48	0.080
Triangular	0.54	0.077
$\sin^2(t)$	0.58	0.075
Gaussian (λ=0.5)	0.79	0.056
sinc(4.5t)	0.83	0.060
Gaussian (λ=0.3)	0.89	0.044
Gaussian (λ=0.1)	0.99	0.026

This table confirms the fact that pulse shaping increases the cross-correlation peak values, however, it shows that due to the reduction of the function for middle delays, the mean value is still reduced, which is a very important conclusion. It should be noted that sinc(4.5t) pulse shape increases the peak value up to 0.79 but does not reduce the average value as Gaussian (λ=0.5), therefore Gaussian shapes are more suitable for pulse shaping in DS-CDMA systems.

The following figures will help understand the previous reasoning:

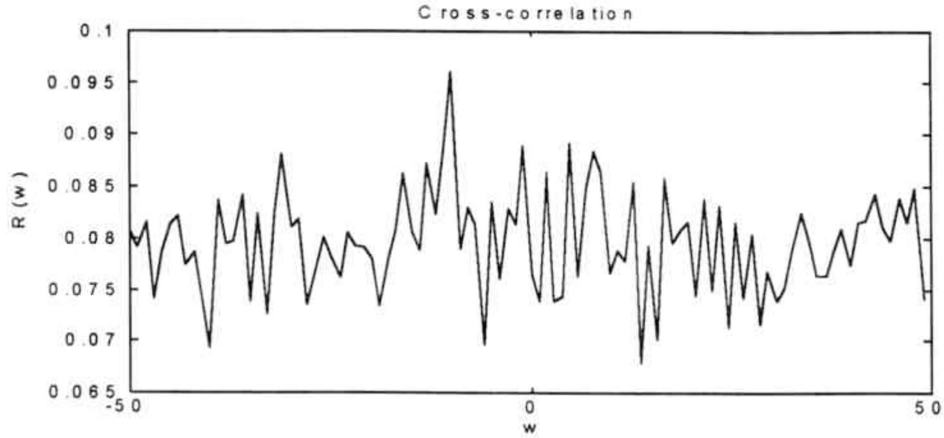

Figure 6-17 Average cross-correlation function of non-shaped random codes

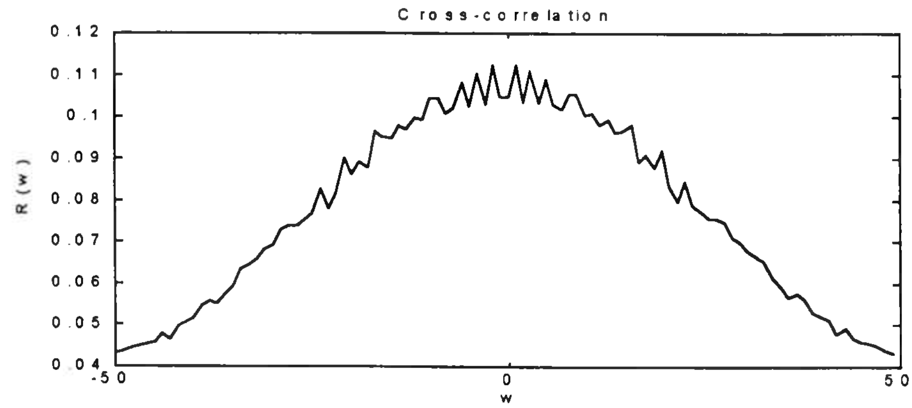

Figure 6-18 Average cross-correlation function of triangular shaped random codes

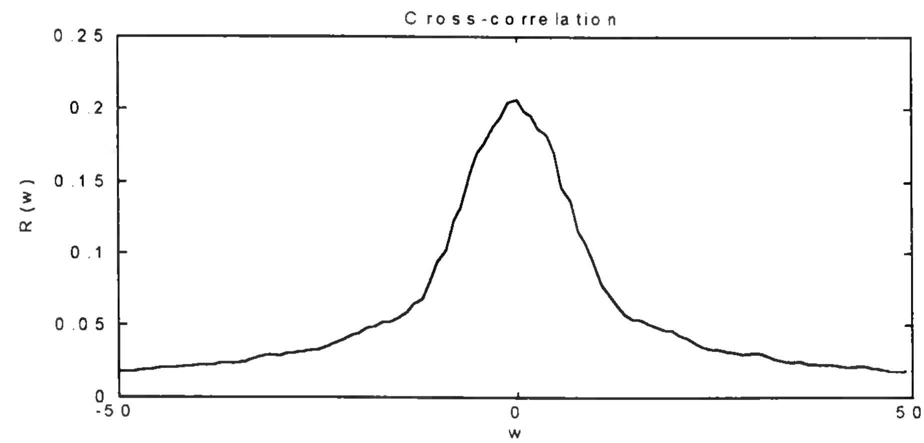

Figure 6-19 Average cross-correlation function of sinc(4.5t) shaped random codes

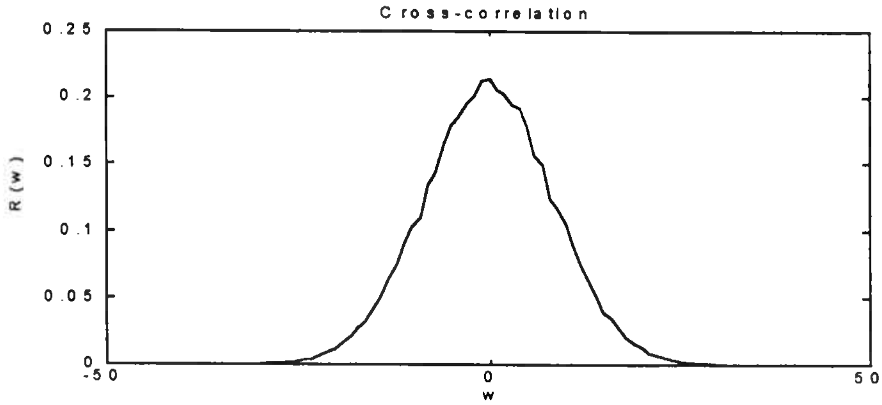

Figure 6-20 Average cross-correlation function of Gaussian (λ=0.3) shaped random codes

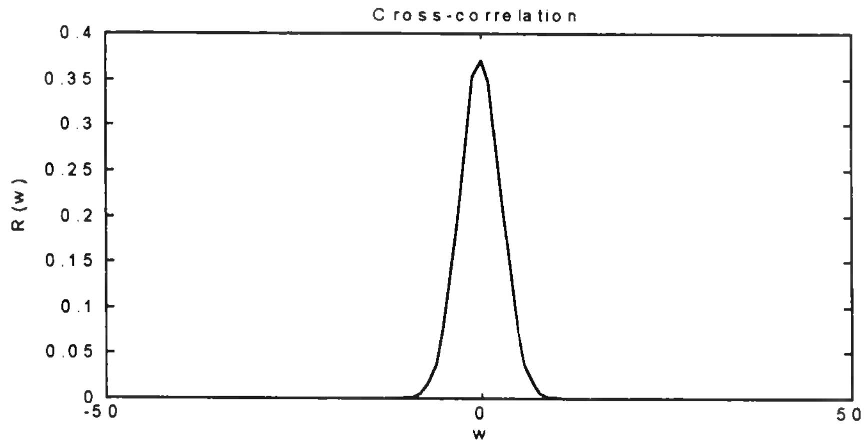

Figure 6-21 Average cross-correlation function of Gaussian (λ=0.1) shaped random codes

It has been confirmed by Table 6-1 and the figures above that pulse shaping can decrease the average cross-correlation at the expense of increasing the peak values of this function. In a DS-CDMA system with a few users, this would be reflected in a reduction of the interference for most of the users, but for those pairs of users with small delays between their time references, the performance would be considerably degraded by pulse shaping.

For a real system with many users, further research using codes with lower cross-correlation values should be carried out to determine the effect of pulse shaping on the general performance. Besides, for pulses with widths compared to a few chip periods, the bandwidth enlargement of the spread signal should be taken into account.

6.2.2 Effect of pulse shaping on the performance of DS-CDMA in a multipath channel

As was explained in the last chapter, because of simulation time constrains, only a common channel for all the users has been simulated. Due to the process by which this channel has been obtained (see section 3.4), its phase shifts are not uniformly distributed in the interval [-180°,180°]. They are more concentrated around zero, so an acceptable BER is achieved by receivers without any phase locking device.

Besides, BPSK has been the simulated modulation method as it was shown to be the scheme that achieved better performances in low phase shifts channels.

On the other hand, the time delay spread of the average channel is also rather small, 4.5 ns. The bit rate chosen for this simulation is 100 Kbps, so the chip rate is 10 Mcps. Hence, the chip duration is about 20 times longer than T_m, and no severe ISI is expected. For much higher bit rates, ISI would be dominant, and the multi-user interference reduction would not be appreciated. For more complex receivers higher bit rates could be simulated achieving still acceptable performances.

As in Figure 6-15, the simulations were carried out for several number of users and for a rectangular and a sinc main lobe pulse shape:

Number of users:

.... 4 users —— ——8 users — – — 12 users

Pulse shape:

oooo Rectangular pulse shape **** Sinc main lobe pulse shape

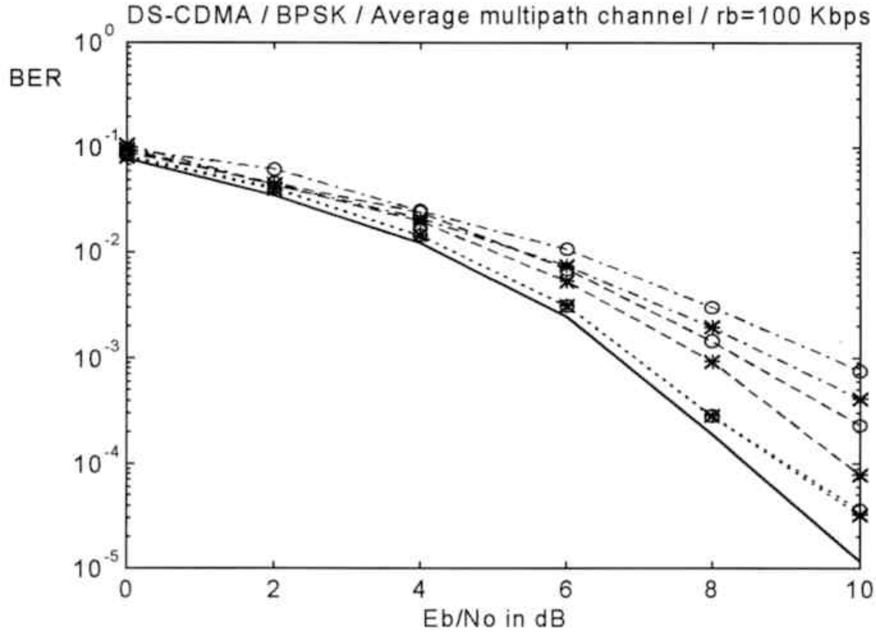

Figure 6-22 Maximum performance enhancement of DS-CDMA in a multipath fading channel by a sinc main lobe pulse shape

It is observed in this last figure that, as was expected, the BERs for the same number of users is higher in a multipath fading channel than in an ideal channel. Besides, the performance improvement achieved by pulse shaping is similar to the one obtained in Figure 6-15. It should be noted that for the case of only one user, the performance is exactly the same for any pulse shape. The reason is that, as it was explained before, the effect of pulse shaping in DS-CDMA systems is due to a reduction in the multi-user interference.

The performance of QPSK should be further studied in CDMA systems, as the I and Q bit streams are spread with independent codes and their interference could be considerably reduced. Besides, the advantage shown for pulse shaped OK-QPSK in section 6.1.3 would certainly be experienced in a multi-user system because the two bit streams of each user are still synchronized and shifted one bit period. The cross-correlation of two codes for a delay half of their lengths has been proved to be minimum.

Finally, it should be mentioned that bit shaping in DS-CDMA systems does not achieve any ISI reduction when the time delay spread is comparable with a chip period. An effective ISI counter measure could be chip shaping instead of bit shaping. When the time delay spread is in the order of several chips, the effect of pulse shaping is similar to the already discussed effect of the multi-user interference reduction. However, in this case the auto-correlation function would play the main role, and the delays between the users' time references would simply be the delay differences between the paths.

The performance of chip shaping in [Cha] has only been studied for an ideal channel, so the improvement achieved is also due to a reduction on the multi-user interference and not on ISI. Therefore an extra improvement might be achieved in multipath fading channels.

The advantage of chip shaping compared to pulse shaping is not only an ISI reduction but a higher multi-user interference reduction. The reason is that for certain delays the cross-correlation could be significantly reduced, but for other delays the cross-correlation could never be higher than without pulse shaping. This statement can be understood considering the I and Q carrier interference of section 6.1.3 as the multi-user interference in DS-CDMA.

Nevertheless, chip shaping presents a clear disadvantage compared to pulse shaping. The bandwidth of the spread signal is almost proportional to the chip shape bandwidth. It was shown in [Cha] that the optimum shape considering the interference reduction and a bandwidth constrain was the sinc(4.5t) pulse shape, but it not be optimum in a multipath fading channel. Besides, the complexity involved with chip shaping would be probably higher than with bit shaping, as the relation between the duration of both pulses is approximately the processing gain.

6.3 Concluding Remarks

This chapter has analysed first the effect of pulse shaping on a single-user system, and afterwards the effect on a DS-CDMA system. It has been explained that the effects on both cases are related but they show important differences. For instance, the bandwidth in a single-user system is more sensitive to the pulse shape than in a SS signal. To finish this chapter a brief summary about the effects of pulse shaping on the reduction of three different kinds of interference is given:

* **ISI**. Section 6.1 showed that quadrature methods experienced less degradation due to ISI because of their lower symbol rate. Besides, in single-user systems, some pulse shapes could reduce significantly the ISI caused by multipath propagation. For the simulated channels a sinc main lobe shape achieved a BER reduction of one order of magnitude for low noise levels. Even if the optimum shape will depend on the specific channel, a sinc main lobe, other raised cosine shapes, or a half-period sinusoidal shape seem to be good candidates. The reason is that they can reduce ISI because their extremes take lower values, but they are wide enough to allow the receiver correlate most of the same bit delayed signals. Besides, their spectral features are relatively good compared to other shapes. To achieve the same effect in a multi-user system, considering that the time delay spread of the channel is of the same order as the chip duration, the shaping should be applied to the chips. For time delay spreads longer than several chip periods, the auto-correlation function of the shaped codes will determine the ISI.

* **Carriers interference**. In quadrature modulation schemes, the information is transmitted also by two carrier waves shifted 90 degrees. In a multipath environment, unless a very complex receiver is used, the path phase shifts introduce some interference between the I and Q carrier waves. It was discussed in section 6.1 that this interference degraded more the performance of quadrature shemes than the one of BPSK and between both quadrature methods, it degrade more QPSK than OK-QPSK. Besides, the performance of OK-QPSK can be considerably enhanced by pulse shaping. The optimum pulse shapes for this purpose are narrower than the ones optimum to reduce ISI. The Gaussian pulse shape with λ=0.3 or the sinc(4.5t) pulse shape achieved a BER reduction of two orders of magnitude for low noise levels. However, in order to select a final shape the spectrums of several shapes should be compared and their performances calculated for each kind of channel and receiver. In a DS-CDMA system, this kind of interference should be lower if the I and the Q bit streams are spread with different code sequences. Even if non-shaped OK-QPSK would have no advantage compared to QPSK, pulse shaping could still improve considerably the performance of OK-QPSK whereas it would be useless for QPSK.

* **Multi-user interference**. Bit shaping on a DS-CDMA system can decrease the average multi-user interference, but the Signal to Interference Ratio (SIR) will be probably increased for those users having their time reference near to another user time reference. This is understood

considering that pulse shaping is like shaping the code sequences and therefore, like shaping their cross-correlation function. A significant reduction of the multi-user interference could also be achieved by means of chip shaping without increasing the peak values of the cross-correlation function. However, this would be at the expense of increasing the spread signal bandwidth.

7. CONCLUSIONS AND RECOMMENDATIONS

The first part of this last chapter gives the main conclusions on the efficiency of pulse shaping in increasing the capacity of a DS-CDMA system. Some other conclusions derived from this work have been already presented at the end of each chapter. Those of the last chapter are specially important to understand the effect of pulse shaping. However, it is not the main goal of this section to review them.

After the conclusions, some recommendations for future research will be listed. Some of them are directly related with this project and are mainly points that were not developed due to time constraints, whereas other recommendations may open new fields of study.

7.1 Conclusions

On a DS-CDMA system, pulse shaping can be considered as code shaping. The shaped codes present a different cross-correlation function. The new shape of this function looks like the pulse shape itself. The consequence on the DS-CDMA performance is that the signal-to-interference ratio achieved by some users will be significantly increased whereas for other users it will be decreased. On the average, this ratio is expected to be increased and therefore a performance enhancement should be expected. However, the service degradation experienced by some users can suppose a serious limitation on the application of pulse shaping in a real system. To solve this problem, some options are exposed in the next section. Besides, some further evaluation of the quality-of-service should be considered in order to determine the optimum pulse shape. This first and main conclusion does not depend on the nature of the channel.

The most important effect of multipath propagation on a spread spectrum signal has been shown to be ISI. Pulse shaping is a technique often used to reduce the channel distortion. It has been proved that pulse shaping can reduce the probability of error of single-user systems in the presence of ISI. Nevertheless, the effect of ISI in a DS-CDMA system is not significantly influenced by pulse shaping. For this purpose chip shaping could achieve better results.

The path phase shifts of a multipath channel might degrade considerably the system performance, specially for non-complex receivers and quadrature modulation schemes. When the transmitted signal is modulated by OK-QPSK, the BER can be reduced by means of pulse shaping.

The main disadvantage of pulse shaping is that in order to transmit the same energy per bit, the maximum amplitude has to be increased. As the envelope of a pulse shaped signal will not be constant in most of the cases, for those applications having a power amplifier with a short linear range, high amplitude values could limit the transmitted power.

Other minor disadvantages are the need of an impulse generator and a pulse shape filter, and for some shapes, an increase of the signal bandwidth. However, a digital pulse shape filter and an impulse generator can be easily implemented and the bandwidth of a spread signal is not very sensitive to the pulse shape, unless the shape width is comparable to the chip duration.

Therefore, if it is finally proved by further research, that pulse shaping can reduce the average multi-user interference without degrading significantly some of the users' transmission quality, this technique could increase the capacity of DS-CDMA systems.

7.2 Recommendations

1.- As has just been concluded, even if pulse shaping seems to decrease the average multi-user interference, the BER of some users could be increased. In order to reduce this last effect, several techniques could be applied and evaluated. For instance, some kind of synchronization between the users could be introduced. This might lead to a CDMA-TDMA hybrid MA protocol. Another solution could be modify CDMA to the opposite direction, towards contention protocols. For example, a repeated random access method could be implemented for the poorest transmissions. Finally, some diversity techniques might lead to a significant performance enhancement.

2.- The results of this first study have been obtained spreading the signal with random codes. The code sequences generated in real systems, as Gold codes, usually present lower cross-correlation values, and should also be tested to observe the influence of pulse shaping on their correlation properties.

3.- The BER is the main measure of the system performance in this work. However, other variables can be used. For instance, the signal to interference ratio can also be a good measure for DS-CDMA systems. The global quality-of-service of a multiple access system is not always well described by the average signal-to-interference ratio or the BER. Therefore, for a deeper study of pulse shaping on DS-CDMA systems, other performance metrics should also be considered.

4.- As mentioned in the conclusions, chip shaping is more efficient in reducing the ISI caused by multipath propagation. Besides, it also decreases the multi-user interference. Nevertheless, it should be taken into account that the spread signal bandwidth might be considerably higher for some narrow chip shapes. As the features of bit and chip shaping seem to complement each other well, a system combining both techniques could achieve very good results, specially in multipath environments.

5.- Another way to improve the performance in multipath fading channels would be increasing the receiver complexity. The correlation receiver implemented in this project is optimum for ideal channels, but its detection capabilities are severely degraded in multipath environments. A more suitable receiver for these channels is the so-called RAKE receiver. Some diversity techniques are also especially effective to reduce the multipath effects. Another method could be adding an adaptive equalizer or some kind of channel estimation technique.

6.- The expected effects of pulse shaping on DS-CDMA systems are basically the same for the three simulated modulation schemes. However, OK-QPSK should experience some extra performance enhancement in multipath environments and more simulations could be carried out to determine the exact improvement. Besides, the effects with some other modern (GMSK or $\pi/4$ QPSK) modulation methods could be also studied.

7.- In further research, other bit rates, code lengths and pulse shapes could be also simulated. The spectral features of pulse shapes should be studied in more detail when considering chip shaping.

8.- Finally, in order to determine more accurately the behaviour of pulse shaped real systems, simulations including a transmitter band pass filter[1], or the influence of non-linear amplifiers could be carried out. On these simulations, pulse shapes presenting a more constant envelope would probably achieve better results.

[1] A common device in real transmitters is a band pass filter at their output. The spectrum of a modulated signal often contains frequency components outside the assigned bandwidth. The purpose of this filter is to reduce the power of these components which could cause ACI to other signals.

REFERENCES

[Agh] A.H. Aghvami,
"Digital modulation techniques for mobile and personal communication systems",
Electronics & Communication Engineering Journal, pp 125-132, June 1993.

[Bel1] P.A. Bello, B.D. Nelin,
"The influence of Fading Spectrum on the Binary Error Probabilities of Incoherent and Differentially Coherent Matched Filter Receivers",
IRE Trans. on Commun. Systems, Vol. CS-10, pp. 160-168, June 1962.

[Bel2] P.A. Bello, B.D. Nelin,
"The Effect of Frequency Selective Spectrum on the Binary Error Probabilities of Incoherent and Differentially Coherent Matched Filter Receivers",
IEEE Trans. on Commun. Systems, Vol. CS-11, pp. 170-186, June 1963.

[Bra] R. Braham,
"Prolog to the Indoor Radio Propagation Channel",
Proceedings of the IEEE, Vol. 81, no. 7, pp 941-942, July 1993.

[Car] A. B. Carlson,
Communication Systems, third edition,
Singapore: McGraw-Hill, 1986.

[Cha] J.P. Chaib and H. Leib,
"Chip Shaping and Channel Coding",
European Trans. on Telecomunications. Vol. 7, No. 2, pp 133-143, March-April 1996.

[Coo] G.R. Cooper and C. D. Mc. Gillem,
Modern Communications and Spread Spectrum,
New York: Mc.Graw-Hill, 1986.

[Dix] R.C. Dixon,
Spread Spectrum Systems,
New York: John Whiley & Sons, 1984.

[Fat] O. Fatah,
"Performance analysis of a Pico-Cellular CDMA network based on Hybrid DS/SFH, DS and SFH, DS and SFH in a Shadowed Rician Fading channel",
Delft University of Technology, Telecommunication and Traffic-control Systems Group,
Graduation Thesis, May 1995.

[Feh] K. Feher,
"MODEMS for Emerging Digital Celllular-Mobile Radio System",
IEEE Trans. on Veh. Technol., Vol. 40, no. 2, pp 355-365, May 1991.

[Har] F.J. Harris,
"On the Use of Windows for Harmonic Analysis with the Discrete Fourier Transform"
Procedings of the IEEE, Vol. 66, no. 1, pp 51-78, January 1978.

[Has1] H. Hashemi,
"Impulse Response Modeling of Indoor Radio Propagation Channels",
IEEE Journal on Select. Areas in Commun., Vol. 11, pp 967-977, September 1993.

[Has2] H. Hashemi,
"The Indoor Radio Propagation Channel",
Proceedings of the IEEE, Vol. 81, no. 7, pp 943-967, July 1993.

[Hay] S.Haykin,
Communication Systems, first edition,
New York: John Wiley & Sons, 1978.

[How] S.J. Howard and D. Pahlavan,
"Measurement and Analysis of the Indoor Radio Channel in the Frequency Domain",
IEEE Trans. on Instrum. and Measurem., Vol. 39, no. 5, pp 751-755, October 1990.

[Jak] W.C. Jakes,
Microwave Mobile Communications,
New York: John Whiley & Sons, 1974.

[Jan] M.G. Jansen,
"Design considerations for specifying, modelling and performance trade-offs of wireless communications systems based on DS-CDMA",
Delft University of Technology, Telecommunication and Traffic-control Systems Group,
Twaio Thesis, June 1994.

[Lee] E. A. Lee, D.G Messerschmith
Digital Communication, second edition,
Boston: Kluwer, 1994.

[Mur] K. Murota and K. Hirade,
"GMSK Modulation for Digital Mobile Radio Telephony",
IEEE Trans. Commun, Vol. COM 29, pp 1044-1050, July 1981.

[Oet] J.D. Oetting,
"A comparison of Modulation Techniques for Digital Radio",
IEEE Trans. Commun.,Vol. COM 27, pp 1752-1762, December 1979.

[Opp] A. V. Oppenheim and R.W. Schafer,
Digital Signal Processing,
Englewood Cliffs: Prentice-Hall, 1975.

[Pas] S. Pasupathy,
"Minimum Shift Keying: A spectrally efficient modulation",
IEEE Commun. Mag.,pp. 14-22, July 1979.

[Pra1] R. Prasad,
"Netwerken voor Persoonlijke Communicatie",
Delft University of Technology, Telecommunication and Traffic-control Systems Group,
Lecture notes, April 1996.

[Pra2] R. Prasad,
CDMA for Wireless Personal Communications,
Boston: Artech House, 1996.

[Pre] W. H. Press, B.P. Flannery, S. A. Teukolsky and W. T. Vetterling,
Numerical Recipes,
Cambridge: Cambridge University Press, 1990.

[Pro] J. G. Proakis,
Digital Communications, second edition,
New York: McGraw-Hill, 1989.

[Sal] A.A.M. Saleh and R.A. Valenzuela,
"A Statistical Model for Indoor Multipath Propagation",
IEEE Journal on Select. Areas in Commun., Vol. 5, no. 2, pp 128-137, February 1987.

[Sha] K. S. Shanmugam,
Digital and Analog Communication Systems,
New York: John Wiley & Sons, 1979.

[Spi] J.J. Spilker (Jr.),
Digital Communications by Satellite,
Englewood Cliffs: Prentice-Hall, 1977.

[Sri] S. Srivastava,
"Performance Analysis of a DS-CDMA system using measured delay profiles",
Delft University of Technology, Telecommunication and Traffic-control Systems Group,
Graduation Thesis, May 1994.

[Ste] S. Stein,
"Fading Channel Issues in System Engineering",
IEEE Journal on Select. Areas in Commun., Vol. 5, no. 2, pp 68-89, February 1987.

[Tur1] G.L. Turin,
"Communication through noisy, random-multipath channels",
IRE Conven. Rec., pt. 4, pp. 154-166, 1956.

[Tur2] G.L. Turin, F.D. Clapp, T.L. Johnston, S.B. Fine and D. Lavry,
"A Statistical Model of Urban Multipath Propagation",
IEEE Trans. on Veh. Technol., Vol. 21, no. 2, pp 1-9, February 1972.

[Tur3] G.L. Turin,
"Introduction to Spread-Spectrum Antimultipath Techniques and their Application to Urban Digital Radio",
Procedings of the IEEE, Vol. 68, no. 3, pp 328-363, March 1980.

[Wib] J.E. Wibowo,
"Performance Analysis of DS, SFH and Hybrid DS/SFH, in a Micro - and Macro cellular Environment with Fading and Shadowing",
Delft University of Technology, Telecommunication and Traffic-control Systems Group,
Task Report, December 1995.

APPENDIX A: SOURCE CODES OF COMPUTER PROGRAMS

A.1 Codes Correlation Analysis Program

This program has been implemmented in Borland Turbo C++ version 4.5. It can calculate the absolute valued cross-correlation function of "code1" and "code2" or the auto-correlation of "code1", which consist of "N" chips. The code generator is described in section A.1.2. The codes can be shaped with several pulse shapes, "g(t)". The pulse shape initialization function is listed in section A.1.3. The average is done taking "IT" different codes. The program also gives the maximum value calculated of the correlation function "MAX", denoted in Table 6-1 as peak value, and the average value "TOTAL".

A.1.1 Main Program

```
#include <iostream.h>   // for input
#include <stdio.h>      // and output
#include <conio.h>      // functions
#include <math.h>       // for pow function

#define pi 3.141592654

const int N=100;
double g[N];
void ini_codegen();
int generate_code();
void ini_g (int ps);

void main (void)
{
 const int CL=100;
 const int PS=1;
 const long int IT=100000;
 long int l;
 int i,j;
 double code1[CL],code2[CL];
 double corr[CL],av[CL],MAX,TOTAL;
 FILE *cross;

 ini_codegen();
 // clrscr();

 MAX=0;
 for(i=0;i<CL;i++) av[i]=0;

 cross=fopen("CROSS011.DAT","wb");

 ini_g(PS);

for (l=0;l<IT;l++)
{
 for (i=0;i<CL;i++)
 {
   code1[i]=generate_code()*g[i];
   code2[i]=generate_code()*g[i];
   //code2[i]=code1[i];
 }

 for (i=0;i<CL;i++)
 //for (i=1;i<CL;i++)
 {
   corr[i]=0;
   for (j=0;j<CL;j++)
   {
     if (i+j<CL)
        corr[i]=corr[i]+(double)code1[j]*code2[i+j];
     else
        corr[i]=corr[i]+(double)code1[j]*code2[i+j-
                                               CL];
   }
   av[i]=av[i]+fabs(corr[i]);
   if (fabs(corr[i])>MAX) MAX=fabs(corr[i]);
 }
 if (l%100==0) cout << "\niteracio no: " << (long
                                             int) l;
```

```
}
 TOTAL=0;
 for (i=0;i<CL;i++)
 //for (i=1;i<CL;i++)
 {
   fprintf(cross,"%e \n",av[i]/IT);
   TOTAL=TOTAL+av[i];
 }
```

```
  cout << "\nThe maximum is: " << MAX;
  cout << "\nThe average is: " << TOTAL/(IT*CL);

  fclose(cross);

  getche();
}
```

A.1.2 Code generator functions

As was explained in chapter 5, the code generator is a random generator that generates “1” and “-1” with the same probability. It consists of an initialization function and a function that randomly returns a “1” or a “-1”.

```
#include <stdlib.h>  // for the random
#include <time.h>    //   functions

const unsigned long length = 2147483646; // 2^31 - 1.
const unsigned long multiplier = 16807;  // 7^5.

unsigned long nextvaluec = 1;


void ini_codegen()
{
        randomize();
        nextvaluec = (multiplier * random(10000)) % length;
}


int generate_code()
{
        nextvaluec = (multiplier * nextvaluec) % length;
        if (( (double) nextvaluec/ (double) length)< 0.5 ) return (-1);
        else return (1);
}
```

A.1.3 Pulse Shape Initialization Function

```
void ini_g (int ps)
{
  double ro,t,tau;  // rolloff factor
  int i;
  double a,EN;
  EN=0;
  switch (ps)
  {
    case 1:            // rectangular
        for (i=0;i<N;i++)
        {
          g[i]=1;
          EN=EN+g[i]*g[i];
        }
        break;

    case 2:            // triangular
        for (i=0;i<N;i++)
        {
          if (i<=N/2) g[i]=i;
          else g[i]=N-i;
          EN=EN+g[i]*g[i];
        }
        break;

    case 3:            // sinc function main lobe
        ro=0;
        for (i=0;i<N;i++)
        {
          a=pi*(-1+2*(double)i/N);
          if (a==0) g[i]=1;
          else g[i]=(sin(a)/a)*(cos(ro*a)/(1-
                    pow(2*ro*a/pi,2)));
          EN=EN+g[i]*g[i];
        }
        break;

   case 4:            // sinc(4.5t)
        for (i=0;i<N;i++)
        {
          ro=0;
          t=-1+2*(double)i/N;
          a=4.5*pi*t;
          if (a==0) g[i]=1;
          else g[i]=sin(a)/a;
          EN=EN+g[i]*g[i];
        }
        break;

    case 5:            // raised cosine with ro=0.9
        ro=0.9;
        for (i=0;i<N;i++)
        {
          a=pi*(-1+2*(double)i/N);
          if (a==0) g[i]=1;
          else g[i]=(sin(a)/a)*(cos(ro*a)/(1-
                    pow(2*ro*a/pi,2)));
        }
        break;

    case 6:            // Gaussian with lambda=0.1
        tau=0.1;
        for (i=0;i<N;i++)
        {
          t=-1+2*(double)i/(N-1);
          g[i]=exp(-pi*t*t/(tau*tau))/tau;
          EN=EN+g[i]*g[i];
        }
        break;

    case 7:            // half sinusoidal period
        for (i=0;i<N;i++)
        {
          t=-1+2*(double)i/(N-1);
          g[i]=cos(pi*t/2);
          EN=EN+g[i]*g[i];
        }
        break;
    case 8:            // sin^2
        for (i=0;i<N;i++)
        {
          t=-1+2*(double)i/(N-1);
          g[i]=cos(pi*t/2);
          g[i]=g[i]*g[i];
          EN=EN+g[i]*g[i];
        }
        break;

    default: cout << "error in pulse shape selection";
  }
  for (i=0;i<N;i++)
    g[i]=g[i]/sqrt(EN);
}
```

A.2 Pulse Shapes Analysis Program

To plot and calculate the discrete Fourier transform of the different pulse shapes tested in the simulations, a Matlab program has been implemented. The results are shown and discussed in chapter 5.

A.2.1 Non-Coded Pulse Shapes Program

In order to calculate the discrete Fourier transform "N" samples of each pulse shape "g(t)" are taken, and zero padded up to 1000 samples "gzp(l)".

```
clear
N=100;
GR=0;
GTR=0;
GRC0=0;
GRC6=0;
GRC9=0;
GRC45=0;
GG1=0;
GG3=0;
GG5=0;
GG11=0;
GCOS=0;
GRC9TR=0;
for i=1:N
 t=-1+2*i/N;
 a=pi*t;
% rectangular
  gr(i)=1;
  GR=GR+gr(i)*gr(i)/N;
%triangular
 if (i<=N/2)
  gtr(i)=i;
 else
  gtr(i)=N-i;
 end
 GTR=GTR+gtr(i)*gtr(i)/N;
%sinc
 ro=0;
 if (a==0)
  grc0(i)=1;
 else
  grc0(i)=(sin(a)/a)*(cos(ro*a)/(1-(2*ro*a/pi)^2));
 end
 GRC0=GRC0+grc0(i)*grc0(i)/N;
%sinc45
 if (a==0)
  grc45(i)=1;
 else
  grc45(i)=sin(4.5*a)/(4.5*a);
 end
 GRC45=GRC45+grc45(i)*grc45(i)/N;
%gaussian with tau 0.1
 tau=0.1;
 gg1(i)=exp(-a*t/(tau*tau))/tau;
 GG1=GG1+gg1(i)*gg1(i)/N;
%gaussian with tau 0.3
 tau=0.3;
 gg3(i)=exp(-a*t/(tau*tau))/tau;
 GG3=GG3+gg3(i)*gg3(i)/N;
%gaussian with tau 0.5
 tau=0.5;
 gg5(i)=exp(-a*t/(tau*tau))/tau;
 GG5=GG5+gg5(i)*gg5(i)/N;
%gaussian with tau 1.1
 tau=1.1;
 gg11(i)=exp(-a*t/(tau*tau))/tau;
 GG11=GG11+gg11(i)*gg11(i)/N;
%cosinus
 gcos(i)=cos(a/2);
 GCOS=GCOS+gcos(i)*gcos(i)/N;
%raised cosine with ro=0.6
 ro=0.6;
 if (a==0)
  grc6(i)=1;
 else
  grc6(i)=(sin(a)/a)*(cos(ro*a)/(1-(2*ro*a/pi)^2));
 end
 GRC6=GRC6+grc6(i)*grc6(i)/N;
%raised cosine with ro=0.9
 ro=0.9;
 if (a==0)
  grc9(i)=1;
 else
```

```
 grc9(i)=(sin(a)/a)*(cos(ro*a)/(1-(2*ro*a/pi)^2));
 end
 GRC9=GRC9+grc9(i)*grc9(i)/N;
%raised cosine ro=0.9 windowed by triangular
 grc9tr(i)=grc9(i)*gtr(i);
 GRC9TR=GRC9TR+grc9tr(i)*grc9tr(i)/N;
end
g1=grc9tr/sqrt(GRC9TR);
for l=1:100
 X1(l)=l/100;
end
figure(1)
plot(X1,g1,'w-')
title('Triangular windowed raised cosine pulse
shape')
xlabel('time (t) in seconds')
ylabel('g(t)')
print -dmeta
for l=1:N
 gzp(l)=g1(l);
end
for l=N+1:1000
 gzp(l)=0;
end
F=fft(gzp);
AB=10*log10(abs(F));
for l=-500:-1
 X(l+501)=l;
 Y(l+501)=AB(1001+l);
end
for l=0:499
 X(l+501)=l;
 Y(l+501)=AB(l+1);
end
X=X/10;
figure(2)
plot(X,Y,'w-')
title('Triangular windowed raised cosine pulse
shape')
xlabel('frequency (f) in Hz')
ylabel('mod(G(f)) in dB')
```

A.2.2 Coded Pulse Shapes Program

The following program only analyses a rectangular coded pulse shape, with a code length of 100 chips and taking 1000 samples (10 per chip). To analysed other coded pulse shapes, the pulse shapes implemented in the program of section A.2.1, could be simply multiplied with the generated code "co(i)".

```
clear
N=1000;
auxi=1;
%code
 if (auxi==1)
  rv=rand;
  if(rv>0.5)
   chip=1.000000001;
  else
   chip=-1.000000001;
  end
  auxi=10;
 else
  auxi=auxi-1;
 end
 co(i)=chip;
end
g1=co;
for l=1:1000
 X1(l)=l/1000;
end
figure(1)
plot(X1,g1,'w-')
title('Spreading code pulse shape')
xlabel('time (t) in seconds')
ylabel('g(t)')
print -dmeta
for l=1:N
 gzp(l)=g1(l);
end
F=fft(gzp);
AB=10*log10(abs(F));
for l=-500:-1
 X(l+501)=l;
 Y(l+501)=AB(1001+l);
end
for l=0:499
 X(l+501)=l;
 Y(l+501)=AB(l+1);
end
figure(2)
plot(X,Y,'w-')
title('Spreading code pulse shape')
xlabel('frequency (f) in Hz')
ylabel('mod(G(f)) in dB')
```

A.3 Simulation Program

Several Turbo C++ source codes have been ran to obtain the results shown in chapter 6. For instance a different program was used for the single-user simulations and the multi-user simulations, or for each modulation method. As these programs do not present many differences between them, only the two more representative source codes will be given in this section.

The purpose of the simulation programs is to write in a file the BERs corresponding to diffferent E_b/N_o, for a determined pulse shape. Some variables and steps are commented to make the program easier to understand. It should be noted that the pulse shape initialization function was already listed in section A.1.

A.3.1 Single-user OK-QPSK

```
#include <iostream.h>   //  for input
#include <stdio.h>      //  and output
#include <conio.h>      // functions
#include <math.h>       // for pow function

#define pi 3.141592654

// subrutines declaration

int generate_bit();
void ini_bitgen();
double generate_noise();
void ini_noisegen(double nvar);
void ini_g(int ps);
void ini_h(int ch);

// Global variables
// DETERMINATION OF N and NS: N=ISI*Ts/Tisi     Where Ts=2/Rb(bit rate)
// and Tisi is the time that lasts the channels impulse time response
// In the channel files Tisi=500 ns and ISI=NS*FCS so N/NS=FCS*Ts/Tisi
// EXAMPLE1: If Rb=100Mbps then Ts=20 ns and Ts/Tisi=0.04.
            // N/NS has to be 100*0.04=4 if N=40 NS has to be 10
// EXAMPLE2: If Rb=20Mbps then Tb=50 ns, Ts=100 ns and Ts/Tisi=0.2.
            // N/NS has to be 100*0.2=20
// EXAMPLE3: If Rb=5Mbps then Tb=200 ns, Ts=400 ns and Ts/Tisi=0.8.
            // N/NS has to be 100*0.8=80
// EXAMPLE4: If Rb=1Mbps then Tb=1000 ns, Ts=2000 ns and Ts/Tisi=4.
            // N/NS has to be 100*4=400

const int N=400;     // number of samples in one Ts
const int NS=1;      // number of program samples in one channel
                                     // file sample
const int FCS=100;       // number of file channel samples
const int ISI=FCS*NS;        // Number of program samples in the time that
                                     // lasts h(c) (Tisi)
double g[N];          // pulse shape discretisation in Volts
double h[ISI][2];     // discreet time impulse channel response.

// program start
```

```
void main(void)
{
  // constants declaration
  const double maxbenpdr=10,minbenpdr=0,incbenpdr=2;
                                          // limits and increment of benpdr
  const double Tb=1;    // duration of a bit period in seconds, this
          // this value has no influence on the performance and its in the
          // program to make it more understandable. However N should be
          // chosen according to the real value of Tb in the simulated model
  const unsigned long GB=10000000;   // total number of generated bits
  const unsigned int MAXGBEC=1000;  // total number of generated periods to
                                   // to calculate the average received energy
  const int FCH=1, LCH=75; // first and last channels averaged
  const int PSMAX=2;        // pulse shapes considered
  const int XMAX=20; // maximum of diferent benpdr to be simulated
  const int MNPB=50+1;     // maximum number of previous bits

  // variables declaration
  int bi[MNPB+1][2], bo[2];  // input and previous input bits, output bits
  int i,b,th,j;          // auxiliar variables
  int ps,ch,x;              // kind of pulse shape, number of channel,
                                   // order of the benpdr considered
  int npb;       // number of previous bits that must be considered
  unsigned long n1, n2, gb, eb;  // order of a sample, number of generated
                                          // bits, number of error bits

  double benpdr;            // bit-energy to noise-power-density ratio
                                   // which is (Eb/No) in dBs
  double bep[XMAX][PSMAX+1];   // bit error probabilties matrix
  double z[ISI][2];              // modulator output
  double s[2];    // channel output without noise
  double so[MNPB+1][2];  // integrators outputs without noise
  double vo[2];     // demodulators outputs with noise
  double P,RP;    // pulse power, equivalent to A^2 and recived power
  double BE,RBE;      // Bit transmited Energy, and Recived Bit Energy
  // FILE *benpdrfile;
  FILE *bepfile;     // pointer to output file

  // clear screen
  clrscr();

 // Eb/No limits asking
// do
// {
//    cout << "Enter the energy per bit to one-sided power spectral
\n density of noise ratio (Eb/No) limits and increment in dB(MAX,MIN,INC):\n ";
//    cin >> maxbenpdr>>minbenpdr>>incbenpdr;
//    if (maxbenpdr<=minbenpdr) cout << "\nNot valid limits";
// }while (maxbenpdr<=minbenpdr);

 // file input oppening
 // benpdrfile = fopen("BENPDIN2.DAT","wb");

 // inicializations
 for(x=0;x<XMAX;x++)
   for(ps=0;ps<=PSMAX;ps++)
          bep[x][ps]=0;

 ini_bitgen();

 for (ch=FCH;ch<=LCH;ch++)
 {
   ini_h(ch);
   //h[0][0]=1;
   //h[0][1]=0;

   for (ps=1;ps<=PSMAX;ps++)
   {
          ini_g(ps);

          //for (i=0;i<N;i++) cout << "\ng[" << i << "]= " << g[i];
          //for (i=0;i<ISI;i++) cout << "\nh[" << i << "]=
                   (" << h[i][0] << ", " <<h[i][1] << ")";

          // TRANSMITED BIT ENERGY CALCULATION
          P=0;
          for (i=0;i<N;i++) P=P+g[i]*g[i];
          P=P/N;
          BE=P*Tb;  // the 0.5 due to int(cosWc*t) is canceled with the 2
                    // due to 2*Tb (the total time). The real power is 2P
                    // as the two bits are transmitted simulatanuously

          //cout << "\nThe average transmited bit enrergy (BE) is: "<< BE;
```

```
// NUMBER OF PREVIOUS BITS CALCULATION

if (ISI%N!=0) npb=((int)(ISI/N))+2;
else npb=(int) (ISI/N) +1;

// CONTRIBUTION OF EVERY BIT TO THE FILTER OUTPUT CALCULATION\
for (b=0;b<npb;b++)   // b indicates what previous bit is calculated
{
  so[b][0]=0;
  for (n1=0;n1<N;n1++)
  {
    s[0]=0;
    for(n2=0;n2<N;n2++)
    {
          th=b*N+n1-n2;     // calculates which term of h should
                            // multiplied with each term of g[n2]
          if (th>=0 && th<ISI) s[0]=s[0]+g[n2]*h[th][0];
    }
    // integrator (real part of the complex product)
    so[b][0]=so[b][0]+s[0]*Tb*g[n1]/N;
          // the 0.5 for the integration of cos(Wc*t) is
          // canceled with the 2 of the 2*Tb integrating time
  }
}
so[npb][0]=0;

for (b=0;b<=npb;b++)
{
  so[b][1]=0;
  for (n1=0;n1<N;n1++)
  {
    s[0]=0;
    for(n2=0;n2<N;n2++)
    {
          th=b*N+n1-n2-N/2;
          if (th>=0 && th<ISI) s[0]=s[0]+g[n2]*h[th][1];
    }
    // integrator (real part of the complex product)
    so[b][1]=so[b][1]+s[0]*Tb*g[n1]/N;
          // the 0.5 for the integration of cos(Wc*t) is
          // canceled with the 2 of the 2*Tb integrating time
  }
}

// RECIVED BIT ENERGY CALCULATION
RP=0;
for (i=0;i<ISI;i++)
{
  z[i][0]=0;
  z[i][1]=0;
}
for (b=0;b<=npb;b++)
{
  bi[0][0]=generate_bit();
  bi[0][1]=generate_bit();
  for (n1=0;n1<N;n1++)
  {
    for (i=0;i<ISI-1;i++)
    {
          z[i][0]=z[i+1][0];
          z[i][1]=z[i+1][1];
    }
    z[ISI-1][0]=bi[0][0]*g[n1];
    z[ISI-1][1]=bi[0][1]*g[n1];
  }
}
bi[0][0]=generate_bit();
bi[0][1]=generate_bit();
for (n2=0;n2<N/2;n2++)
{
  for (i=0;i<ISI-1;i++)
    z[i][1]=z[i+1][1];
  z[ISI-1][1]=bi[0][1]*g[n2];
}
gb=0;
n1=0;
n2=N/2;

while (gb<=MAXGBEC)
{
  // modulation
  for (i=0;i<ISI-1;i++)
  {
    z[i][0]=z[i+1][0];
```

```
    z[i][1]=z[i+1][1];
  }
  z[ISI-1][0]=bi[0][0]*g[n1];
  z[ISI-1][1]=bi[0][1]*g[n2];

  // channel
  s[0]=0;
  s[1]=0;
  for (i=0;i<ISI;i++)
  {
    s[0]=s[0]+z[i][0]*h[ISI-i-1][0]-z[i][1]*h[ISI-i-1][1];
    s[1]=s[1]+z[i][0]*h[ISI-i-1][1]+z[i][1]*h[ISI-i-1][0];
  }

  // power calculation
  RP=RP+(s[0]*s[0]+s[1]*s[1])/N;

  // next sample
  n1++;
  n2++;

  if (n1==N)  // every 2 Tb
  {
    // next bit generation
    bi[0][0]=generate_bit();
    gb++;       // gb indicates only the generated bits in
    n1=0;       // the in-phase channel
  }

  if (n2==N)  // every 2 Tb
  {
    // next bit generation
    bi[0][1]=generate_bit();
    n2=0;
  }

}
RP=RP/gb;
RBE=0.5*RP*Tb;  // 0.5 due to int(cosWc*t), the 2 of 2Tb is canceled
                // with 1/2 to get the energy of every bit, as the
                // signal contains 2 bits at the same time
```

```
// outputs the results in the user's screen and in the i/o files
cout << "\nchannel: " << int (ch);
cout << "  pulse shape: " << int (ps);
cout << "\nThe average recived bit enrergy (RBE) is: "<< RBE;
for (b=0;b<=npb;b++)
{
  for (j=0;j<2;j++)
  {
    cout << "\nFor the previous bit:" << int (b);
    if (j==0) cout << "  the in-phase filter output equals = " << double (so[b][j]);
    else cout << "  the quadrature filter output equals = " << double (so[b][j]);
  }
}

// SIMULATION START

for(benpdr=minbenpdr;benpdr<=maxbenpdr;benpdr=benpdr+incbenpdr)
{
  ini_noisegen(0.5*BE*RBE*pow(10,(-benpdr/10))); // The terms are:
                   // RBE to get No from the benpr input: RBE*(No/RBE)=No
                   // 0.5*BE because of the power of noise after filtering
                   // it with a coherent demodulator that uses the
                   // original signal as the match signal
  gb=0;
  eb=0;
  for (b=0;b<=npb;b++)
  {
    bi[b][0]=generate_bit();
    bi[b][1]=generate_bit();
  }
  vo[0]=0;
  vo[1]=0;
  while (gb<=GB && eb<100)
  {
    // total filter output
    for (b=0;b<=npb;b++)
          vo[0]=vo[0]+so[b][0]*bi[b][0]-so[b][1]*bi[b][1];

    // AWGN
    vo[0]=vo[0]+generate_noise();

    // Threshold device (A/D)
```

```
   if (vo[0]>0) bo[0]=1;
   else bo[0]=-1;

   // bit comparison
   if (bi[0][0]!=bo[0]) eb++;

   // next symbol generation
   for (b=1;b<=npb;b++)
         bi[b][0]=bi[b-1][0];
   bi[0][0]=generate_bit();
   gb++;
   vo[0]=0;

   //Total filter output
   for (b=0;b<=npb;b++)
         vo[1]=vo[1]+so[b][0]*bi[b][1]+so[b][1]*bi[b][0];

   // AWGN
   vo[1]=vo[1]+generate_noise();

   // Threshold device (A/D)
   if (vo[1]>0) bo[1]=1;
   else bo[1]=-1;

   // bit comparison
   if (bi[0][1]!=bo[1]) eb++;

   // next symbol generation
   for (b=1;b<=npb;b++)
         bi[b][1]=bi[b-1][1];
   bi[0][1]=generate_bit();
   gb++;
   vo[1]=0;
 }

 // outputs the results in the user's screen
 cout << "\nchannel: " << int (ch);
 cout << "  pulse shape: " << int (ps);
 cout << "\nFor benpdr= " << double (benpdr);
 cout << "  The bit error probability is:" << (double) eb/(gb-2) ;
 x=(benpdr-minbenpdr)/incbenpdr;
 bep[x][ps]=bep[x][ps]+ (eb/(double) gb)/(LCH-FCH+1);
```

```
        }
    }
}

// writtes the results in the output files
for(ps=1;ps<=PSMAX;ps++)
{
  switch (ps)
  {
        case 1:         // rectangle / gaussian tau=0.1
          bepfile = fopen("A913V6P1.DAT","wb");
          break;

        case 2:         // triangle / gaussian tau=0.3
          fclose(bepfile);
          bepfile
          = fopen("A913V6P2.DAT","wb");
          break;

        case 3:          // sinc function / gaussian tau=0.5
          fclose(bepfile);
          bepfile = fopen("A563V6P3.DAT","wb");
          break;

        case 4:          // gaussian tau=0.7 / gaussian tau=0.7
          fclose(bepfile);
          bepfile = fopen("A563V6P4.DAT","wb");
          break;
        case 5:          // gaussian tau=0.9
          fclose(bepfile);
          bepfile = fopen("A563V6P5.DAT","wb");
          break;
        case 6:          // cosine
          fclose(bepfile);
          bepfile = fopen("A563V6P6.DAT","wb");
          break;
        case 7:          // raised cosine with ro=0.9
          fclose(bepfile);
          bepfile = fopen("A563V6P7.DAT","wb");
          break;
        default: cout << "error in pulse shape selection";
  }
```

```
    for(x=0;x<=(maxbenpdr-minbenpdr)/incbenpdr;x++)
                    fprintf(bepfile,"%e\n", bep[x][ps]);
  }
   // writes the inputs used or 'x'
   //for(benpdr=minbenpdr;benpdr<=maxbenpdr;benpdr=benpdr+incbenpdr)
        // fprintf(benpdrfile,"%e\n",benpdr);
  fclose(bepfile);
  cout << "\n \n";
  // waits for the user to press a key
  getche();

  // closes file
  //fclose(benpdrfile);

}



void ini_h(int ch)
{
  int i,j;
  double dB,ph,t;
  FILE *afile, *pfile, *tfile;

  #include "opench2.cpp"

  if (afile && pfile && tfile)
  {
   for (i=0;i<FCS;i++)
   {
        fscanf(afile,"%le",&dB);
        fscanf(pfile,"%le \n",&ph);
        fscanf(tfile,"%le \n",&t);
        if (t==0)
          for (j=NS*i;j<NS*(i+1);j++)
          {
            h[j][0]=0;
            h[j][1]=0;
          }
         else
           for (j=NS*i;j<NS*(i+1);j++)
           {
                h[j][0]=pow(10,(dB/10))*cos(2*ph);
                h[j][1]=pow(10,(dB/10))*sin(2*ph);
           }
   }
  }
  else cout << "Doesn't exist such a file";
  fclose(afile);
  fclose(pfile);
  fclose(tfile);

}
```

A.3.2 Multi-user BPSK

The next program analyses the performance of BPSK in a DS-CDMA system for an ideal channel.

```
// FILE CONTAINING THE BASK MODULATION METHOD AND CDMA PROTOCOL

#include <iostream.h>   //  for input
#include <stdio.h>      //  and output
#include <conio.h>      // functions
#include <math.h>       // for pow function

#define pi 3.141592654

// subrutines declaration

int generate_bit();
void ini_bitgen();
double generate_noise();
void ini_noisegen(double nvar);
void ini_g(int ps);
void ini_h(int ch);
void ini_codegen();
int generate_code();

// Global variables
// DETERMINATION OF N: N=ISI*Tb/Tisi Where Tb=1/Rb(bit rate)
// and Tisi is the time that lasts the channels impulse time response
// In the channel files Tisi=500 ns and ISI=100
// EXAMPLE1: If Rb=1Mbps then Tb=1000 ns, and Tb/Tisi=2. N=100*2=200
// EXAMPLE2: If Rb=5Mbps then Tb=200 ns, and Tb/Tisi=0.4. N=100*0.4=40

const int N=200;    // number of samples in one Tb
const int ISI=1;    // Number of channel impulse response samples
double g[N];  // pulse shape discretisation in Volts
double h[ISI];  // discreet time impulse channel response

// program start
void main(void)
{
  // constants declaration
  const double maxbenpdr=10,minbenpdr=0,incbenpdr=2;
                                              // limits and increment of benpdr
  const double Tb=1;     // duration of a bit period in seconds, this
          // this value has no influence on the performance and its in the
          // program to make it more understandable. However it should be
          // 5 ns multiplied by N as 5 ns is the time between samples.
  const unsigned long GB=10000000;   // total number of generated bits
  const unsigned int MAXGBEC=1000;  // total number of generated periods to
                                     // to calculate the average received energy
  const int FCH=57,LCH=63; // first and last channels averaged
  const int PSMAX=6;         // pulse shapes considered
  const int XMAX=20; // maximum of diferent benpdr to be simulated
  const int USERS=12;  // number of users of the channel
  const int CL=100;    // code length or nunmber of chips in one Tb
  const int NSC=N/CL;  //Number of samples in one chip
               // WATCH OUT! IT HAS TO BE AN INTEGER!
  // variables declaration
  int bi[USERS],bo,i,j;    // bit input, bit output, auxiliar variables
  int ps,ch,x;             // kind of pulse shape, number of channel,
                                     // order of the benpdr considered
  int codes[CL][USERS];       //  codes matrix
  unsigned long n[USERS],gb,eb;  // number of samples, number of generated
                                              // bits, number of error bits
  double benpdr, z[ISI];  // bit-energy to noise-power-density ratio, modulator output
  double bep[XMAX][PSMAX+1];  //bit error probabilties matrix
  double s;          // channel output without noise
  double so[USERS];        // integrator output without noise
  double vo;         // demodulator output with noise
  double P,RP;   // pulse power, equivalent to A^2 and recived power
  double BE,RBE;       // Bit Energy and recived Bit Energy
  FILE *bepfile;     // pointer to the output file

  // clear screen
```

```
clrscr();

// bit-energy to noise-power-density ratio limits asking
//do
//{
//   cout << "Enter the bit-energy to noise-power-density ratio (Eb/eta) \n limits and increment
in dB(MAX,MIN,INC):\n ";
//   cin >> maxbenpdr>>minbenpdr>>incbenpdr;
//   if (maxbenpdr<=minbenpdr) cout << "Not valid limits\n";
//}while (maxbenpdr<=minbenpdr);

// file input and output oppenings
//benpdrfile = fopen("BENPDI11.DAT","wb");

// inicializations
for(x=0;x<XMAX;x++)
  for(ps=0;ps<=PSMAX;ps++)
        bep[x][ps]=0;

ini_bitgen();
ini_codegen();
for(i=0;i<USERS;i++)
  for(j=0;j<CL;j++)
        codes[j][i]=generate_code();
        //codes[j][i]=1;

for (ch=FCH;ch<=LCH;ch++)
{
  //ini_h(ch);
  h[0]=1;

  for (ps=1;ps<=PSMAX;ps++)
  {
        ini_g(ps);
        //getche();
        for (i=0;i<N;i++) cout << "\ng[" << i << "]= " << g[i];
        //for (i=0;i<ISI;i++) cout << "\nh[" << i << "]= " << h[i];

        // TRANSMITED BIT ENERGY CALCULATION
        P=0;
        for (i=0;i<N;i++) P=P+g[i]*g[i];
        P=P/N;
BE=0.5*P*Tb;          // 0.5 due to int(cosWc*t)

// RECIVED BIT ENERGY CALCULATION
RP=0;
for (i=0;i<ISI;i++)
  z[i]=0;
gb=0;
n[0]=0;
bi[0]=generate_bit();
while (gb<=MAXGBEC)
{
  // modulation
  for (i=0;i<ISI-1;i++)
    z[i]=z[i+1];
  z[ISI-1]=bi[0]*g[n[0]]*codes[(int) n[0]/NSC][0];

  // channel
  s=0;
  for (i=0;i<ISI;i++)
    s=s+z[i]*h[ISI-i-1];

  // recived power calculation
   RP=RP+s*s/N;

  // next sample
  n[0]++;

  if (n[0]==N)  // every Tb
  {
    // next bit generation
    bi[0]=generate_bit();
    gb++;
    n[0]=0;
  }
}
RP=RP/gb;
RBE=0.5*RP*Tb;   // 0.5 due to int(cosWc*t)

// outputs the results in the user's screen and in the i/o files
cout << "\nchannel: " << int (ch);
cout << "  pulse shape: " << int (ps);
cout << "\nThe average recived bit enrergy (RBE) is: "<< RBE;
```

```
// SIMULATION START

for(benpdr=minbenpdr;benpdr<=maxbenpdr;benpdr=benpdr+incbenpdr)
{
  ini_noisegen(2*BE*RBE*pow(10,(-benpdr/10))); // The terms are:
                    // RBE to get No from the benpr input: RBE*(No/RBE)=No
                    // 0.5*BE because of the power of noise after filtering
                    // it with a coherent demodulator that uses the
                    // original signal as the match signal

  for (i=0;i<ISI;i++)
    z[i]=0;
  for (i=0;i<USERS;i++)
  {
    bi[i]=generate_bit();
    n[i]=(int) i*N/USERS;
    so[i]=0;
  }
  gb=0;
  eb=0;
  while (eb<100 && gb<=GB)
  {
    // modulation
    for (i=0;i<ISI-1;i++)
          z[i]=z[i+1];
    z[ISI-1]=0;
    for (i=0;i<USERS;i++)
          z[ISI-1]=z[ISI-1]+bi[i]*g[n[i]]*codes[(int) n[i]/NSC][i];

    // channel
    s=0;
    for (i=0;i<ISI;i++)
          s=s+z[i]*h[ISI-i-1];

    for (i=0;i<USERS;i++)
    {
          // integrator
          so[i]=so[i]+Tb*s*g[n[i]]*codes[(int) n[i]/NSC][i]/N; // the *2 for the second
integrator is simplified
                    // with the /2 for the integration of cos(Wc*t)

          // next sample                    n[i]++;

          if (n[i]==N)  // every Tb
          {
            // additive gaussian filtered noise
            vo=so[i]+generate_noise();

            // Threshold device (A/D)
            if (vo>0) bo=1;
            else bo=-1;

            // bit comparison
            if (gb>USERS && bi[i]!=bo) eb++;

            // next bit generation
            bi[i]=generate_bit();
            gb=gb++;
            so[i]=0;
            n[i]=0;
          }
    }
  }

  // outputs the results in the user's screen and in the i/o files
  cout << "\nchannel: " << int (ch);
  cout << "  pulse shape: " << int (ps);
  cout << "\nFor benpdr (REb/eta)= " << double (benpdr);
  cout << "   The bit error probability is:" << (double) eb/(gb-USERS);
  x=(benpdr-minbenpdr)/incbenpdr;
  bep[x][ps]=bep[x][ps]+ (eb/(double) (gb-USERS))/(LCH-FCH+1);
 }
 }
}

// writtes the results in the output files
for(ps=1;ps<=PSMAX;ps++)
{
  switch (ps)
  {
        case 1:
          bepfile = fopen("C043V2P1.DAT","wb");
          break;
```

```
            case 2:
              fclose(bepfile);
              bepfile = fopen("C043V2P2.DAT","wb");
              break;
            case 3:
              fclose(bepfile);
              bepfile = fopen("C043V2P3.DAT","wb");
              break;
            case 4:
              bepfile = fopen("C043V2P4.DAT","wb");
              break;
            case 5:
              fclose(bepfile);
              bepfile = fopen("C043V2P5.DAT","wb");
              break;
            case 6:
              fclose(bepfile);
              bepfile = fopen("C043V2P6.DAT","wb");
              break;
            case 7:
              fclose(bepfile);
              bepfile = fopen("C043V2P7.DAT","wb");
              break;
            case 8:
              fclose(bepfile);
              bepfile = fopen("C033V2P8.DAT","wb");
              break;

            default: cout << "error in pulse shape selection";
      }
      for(x=0;x<=(maxbenpdr-minbenpdr)/incbenpdr;x++)
                    fprintf(bepfile,"%e\n", bep[x][ps]);
  }

  // writes the inputs used or 'x'
  //for(benpdr=minbenpdr;benpdr<=maxbenpdr;benpdr=benpdr+incbenpdr)
  //   fprintf(benpdrfile,"%e\n",benpdr);

  cout << "\n \n";
  // waits for the user to press a key
    getche();

    // closes file
    fclose(bepfile);
  }
```

APPENDIX B: MAIN CHARACTERISTICS OF THE MEASURED CHANNELS

Most of the simulations in this project have been done using 75 measured impulse responses of real channels. For the multi-user simulations, an average channel of these 75 impulse responses was used. The method followed to obtain the average channel is described in section 3.4.

In Table B-1 the values of four parameters are shown to characterize each channel:

$E[\tau]$: average delay.

T_m : time delay spread.

$(\Delta f)_c$: coherence bandwidth.

$E[|\theta|]$: average phase shift.

The average phase has been calculated weighting the absolute values of the phase shifts by the corresponding gains to the power of two. The other variables were discussed in chapter 3.
It is important to note that the last channel, denoted by AV, does not correspond to the average of the parameters of the 75 measured channels, but to the parameters of the average channel.

Table B-1 Characteristics of the measured channels

Ch.	$E[\tau]$ (ns)	T_m (ns)	$(\Delta f)_c$ (MHZ)	$E[\|\theta\|]$ (rad)
1	3.254767e+01	1.450081e+01	6.896166e+01	4.826623e-01
2	2.949133e+01	1.216277e+01	8.221813e+01	8.222530e-01
3	4.120146e+01	5.547658e+00	1.802563e+02	8.749050e-01
4	4.080619e+01	4.851485e+00	2.061225e+02	8.932731e-01
5	4.075993e+01	4.841202e+00	2.065603e+02	8.390341e-01
6	4.084985e+01	5.310266e+00	1.883145e+02	7.485951e-01
7	4.132210e+01	6.510780e+00	1.535914e+02	6.479075e-01
8	4.273648e+01	8.497440e+00	1.176825e+02	5.491335e-01
9	9.752110e+00	6.436322e+00	1.553682e+02	1.373785e+00
10	7.704708e+00	5.439346e+00	1.838456e+02	5.710658e-01

11	6.515392e+00	4.384602e+00	2.280709e+02	2.573623e-01
12	5.718990e+00	2.983149e+00	3.352163e+02	2.304837e-01
13	5.695188e+00	2.905746e+00	3.441456e+02	4.218434e-01
14	5.780472e+00	3.085328e+00	3.241146e+02	6.837982e-01
15	5.897813e+00	3.291208e+00	3.038398e+02	8.504664e-01
16	5.965525e+00	3.362678e+00	2.973821e+02	1.062084e+00
17	6.062088e+00	3.433788e+00	2.912235e+02	1.184844e+00
18	6.231318e+00	3.863055e+00	2.588625e+02	1.341799e+00
19	6.305904e+00	3.740544e+00	2.673408e+02	1.465272e+00
20	6.518190e+00	4.334384e+00	2.307133e+02	1.618074e+00
21	6.429530e+00	4.491286e+00	2.226534e+02	1.739652e+00
22	6.150665e+00	4.412526e+00	2.266276e+02	1.918396e+00
23	6.231970e+00	4.661626e+00	2.145174e+02	2.091546e+00
24	5.795084e+00	3.967611e+00	2.520408e+02	2.242888e+00
25	5.625552e+00	3.686879e+00	2.712321e+02	2.303483e+00
26	5.484232e+00	3.137266e+00	3.187489e+02	2.341643e+00
27	5.441998e+00	2.834539e+00	3.527911e+02	2.347951e+00
28	5.483865e+00	2.771382e+00	3.608309e+02	2.347965e+00
29	5.967762e+00	3.359728e+00	2.976432e+02	2.299528e+00
30	6.922058e+00	4.291297e+00	2.330298e+02	2.302951e+00
31	7.970081e+00	4.862800e+00	2.056428e+02	2.330005e+00
32	1.599875e+01	4.268919e+00	2.342514e+02	2.681761e+00
33	1.671677e+01	5.388711e+00	1.855731e+02	2.571929e+00
34	1.908578e+01	7.096876e+00	1.409071e+02	2.338621e+00
35	1.745173e+01	1.071216e+01	9.335188e+01	2.051306e+00
36	1.780958e+01	1.124717e+01	8.891123e+01	1.571412e+00
37	2.475227e+01	8.723204e+00	1.146368e+02	1.260151e+00
38	6.863506e+00	5.881242e+00	1.700321e+02	2.016294e+00
39	6.370076e+00	4.942396e+00	2.023310e+02	2.127581e+00
40	5.988240e+00	4.051566e+00	2.468181e+02	2.325939e+00
41	5.740007e+00	3.549365e+00	2.817406e+02	2.526451e+00

42	5.616570e+00	3.186522e+00	3.138218e+02	2.794495e+00
43	5.607262e+00	3.188048e+00	3.136716e+02	2.941605e+00
44	5.645348e+00	3.283903e+00	3.045157e+02	3.048153e+00
45	5.647405e+00	3.326507e+00	3.006156e+02	2.935896e+00
46	5.654431e+00	3.460493e+00	2.889762e+02	2.836339e+00
47	5.629309e+00	3.461249e+00	2.889131e+02	2.777338e+00
48	5.708976e+00	3.790137e+00	2.638427e+02	2.697940e+00
49	5.853339e+00	4.223139e+00	2.367907e+02	2.620388e+00
50	5.921143e+00	4.525863e+00	2.209523e+02	2.514230e+00
51	5.754861e+00	4.276596e+00	2.338309e+02	2.433842e+00
52	5.793370e+00	4.427133e+00	2.258798e+02	2.226389e+00
53	5.724415e+00	4.029801e+00	2.481512e+02	1.985457e+00
54	5.699465e+00	3.702298e+00	2.701025e+02	1.644827e+00
55	5.609275e+00	3.004982e+00	3.327807e+02	1.322856e+00
56	5.508042e+00	2.706518e+00	3.694784e+02	8.981170e-01
57	5.407260e+00	2.387188e+00	4.189028e+02	5.620162e-01
58	5.410199e+00	2.310591e+00	4.327897e+02	2.354264e+00
59	5.359454e+00	2.230116e+00	4.484072e+02	1.935296e-01
60	5.233479e+00	1.850851e+00	5.402919e+02	4.623121e-01
61	5.305908e+00	2.141812e+00	4.668943e+02	6.482098e-01
62	5.403577e+00	2.579359e+00	3.876932e+02	8.144043e-01
63	5.480195e+00	2.938365e+00	3.403254e+02	9.320564e-01
64	5.524039e+00	3.177270e+00	3.147356e+02	1.052264e+00
65	5.639569e+00	3.578416e+00	2.794533e+02	1.153301e+00
66	5.765216e+00	3.994534e+00	2.503421e+02	1.257677e+00
67	5.883891e+00	4.422451e+00	2.261190e+02	1.349408e+00
68	2.604539e+01	7.174434e+00	1.393838e+02	2.174701e+00
69	2.488605e+01	7.160957e+00	1.396461e+02	2.020988e+00
70	2.057585e+01	6.836611e+00	1.462713e+02	1.649904e+00
71	2.143981e+01	8.359477e+00	1.196247e+02	1.179034e+00
72	1.907213e+01	8.664450e+00	1.154141e+02	9.644512e-01

73	1.761223e+01	9.663185e+00	1.034856e+02	1.019161e+00
74	1.579409e+01	7.679995e+00	1.302084e+02	8.519362e-01
75	1.698437e+01	7.795816e+00	1.282739e+02	5.320652e-01
AV	6.703937e+00	4.544417e+00	2.200502e+02	4.358701e-01